AD-A087 360 GENERAL DYNAMICS CORP FORT WORTH TX FORT WORTH DIV F/G 11/6
FATIGUE BEHAVIOR OF ADHESIVELY BONDED JOINTS. VOLUME II. APPEND--ETC(U)
APR 80 J ROMANKO, W G KNAUSS F33615-76-C-5220

UNCLASSIFIED AFWAL-TR-80-4037-VOL-2 NL

1 OF 1
AD A
087360

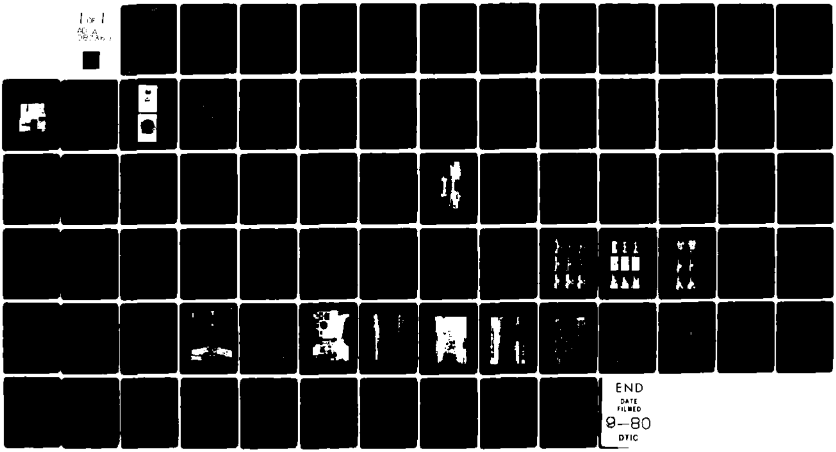

END
DATE
FILMED
9-80
DTIC

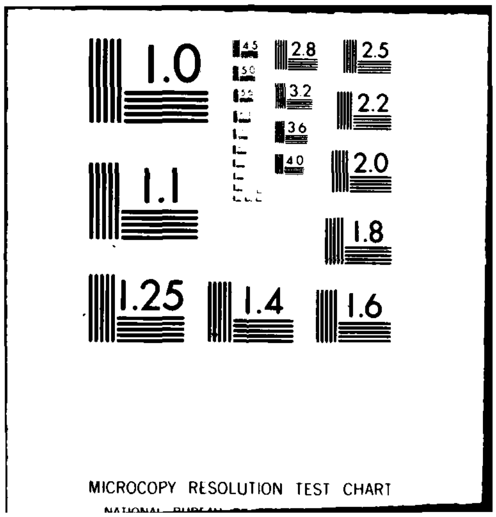
1.0
2.8
2.5
3.2
2.2
3.6
4.0
2.0
1.1
1.8
1.25
1.4
1.6
MICROCOPY RESOLUTION TEST CHART

AFWAL-TR-80-4037
Volume II

LEVEL III A087 280

ADA087360

FATIGUE BEHAVIOR OF ADHESIVELY BONDED JOINTS

Volume II: Appendices

JOHN ROMANKO
W. G. KNAUSS
GENERAL DYNAMICS, FORT WORTH DIVISION
PASADENA, CALIFORNIA

APRIL 1980

TECHNICAL REPORT AFWAL-TR-80-4037, Vol. II
Final Report for Period July 1976 — December 1979

Approved for public release; distribution unlimited.

MATERIALS LABORATORY
AIR FORCE WRIGHT AERONAUTICAL LABORATORIES
AIR FORCE SYSTEMS COMMAND
WRIGHT-PATTERSON AIR FORCE BASE, OHIO 45433

NOTICE

When Government drawings, specifications, or other data are used for any purpose other than in connection with a definitely related Government procurement operations, the United States Government thereby incurs no responsibility nor any obligation whatsoever; and the fact that the government may have formulated, furnished, or in any way supplied the said drawings, specifications, or other data, is not to be regarded by implication or otherwise as in any manner licensing the holder or any other person or corporation, or conveying any rights or permission to manufacture, use, or sell any patented invention that may in any way be related thereto.

This report has been reviewed by the Office of Public Affairs (ASD/PA) and is releasable to the National Technical Information Service (NTIS). At NTIS, it will be available to the general public, including foreign nations.

This technical report has been reviewed and is approved for publication.

William B. Jones Jr.
WILLIAM B. JONES, JR., PhD, Matls Rsch Engr.
Composites, Adhesives & Fibrous Matls Br
Nonmetallic Materials Division

Theodore J Reinhart Jr
THEODORE J. REINHART, JR., Chief
Composites, Adhesives & Fibrous Matls Br
Nonmetallic Materials Division

FOR THE COMMANDER

F D Cherry
FRANKLIN D. CHERRY, Chief
Nonmetallic Materials Division

"If your address has changed, if you wish to be removed from our mailing list, or if the addressee is no longer employed by your organization please notify AFWAL/MLBC, W-PAFB, OH 45433 to help us maintain a current mailing list".

Copies of this report should not be returned unless return is required by security considerations, contractual obligations, or notice on a specific document.

Final technical rept. Jul 76 - Apr 80

SECURITY CLASSIFICATION OF THIS PAGE (When Data Entered)

19

REPORT DOCUMENTATION PAGE

READ INSTRUCTIONS BEFORE COMPLETING FORM

1. REPORT NUMBER

18 AFWAL-TR-80-4037, Vol. [redacted] 2

2. GOVT ACCESSION NO.

AD-A087360

3. RECIPIENT'S CATALOG NUMBER

4. TITLE (and Subtitle)

6 Fatigue Behavior of Adhesively Bonded Joints. Volume II. Appendices.

5. TYPE OF REPORT & PERIOD COVERED

Technical - Final
July 1976 - April 1980

6. PERFORMING ORG. REPORT NUMBER

7. AUTHOR(s)

10 John Romanko
W. G. Knauss

8. CONTRACT OR GRANT NUMBER(s)

9. PERFORMING ORGANIZATION NAME AND ADDRESS

General Dynamics
Fort Worth Division
~~Pasadena~~, California

10. PROGRAM ELEMENT, PROJECT, TASK AREA & WORK UNIT NUMBERS

11

11. CONTROLLING OFFICE NAME AND ADDRESS

Materials Laboratory
Air Force Wright Aeronautical Laboratories
Wright-Patterson AFB, Ohio 45433

12. REPORT DATE

Apri[redacted]980

13. NUMBER OF PAGES

14. MONITORING AGENCY NAME & ADDRESS (if different from Controlling Office)

15 F3361[illegible]

15. SECURITY CLASS. (of this report)

Unclassified

15a. DECLASSIFICATION DOWNGRADING SCHEDULE

16. DISTRIBUTION STATEMENT (of this Report)

Approved for public release; distribution unlimited.

17. DISTRIBUTION STATEMENT (of the abstract entered in Block 20, if different from Report)

18. SUPPLEMENTARY NOTES

19. KEY WORDS (Continue on reverse side if necessary and identify by block number)

Adhesive Bonding, Structural Adhesives, Adhesive Material Characterization, Instrumented Fatigue Testing, Neat Materials, Bonded Joints, Stress Analysis, Finite Elements.

20. ABSTRACT (Continue on reverse side if necessary and identify by block number)

The fatigue behavior of adhesively bonded aluminum joints was investigated analytically and experimentally. Stress distributions in the adhesive interlayer were calculated to guide planning of the joint tests and the interpretation of the test results. Finite element stress analyses were conducted using a linear elastic, and a three-element linear viscoelastic model for (continued)

over

DD FORM 1 JAN 73 1473 EDITION OF 1 NOV 65 IS OBSOLETE

SECURITY CLASSIFICATION OF THIS PAGE (When Data Entered)

402109

JOB

the adhesive behavior. Thick adherend lap-shear specimens of the model joint configuration were fabricated and tested. These specimens were instrumented and subjected to sinusoidal fatigue tests at several frequencies, humidities and temperatures. Certain tests were interrupted at various stages and the specimens examined for fatigue damage. Damage was found to initiate in the (calculated) high stress regions, and to propagate with further load cycling. Observations and recommendations resulting from the investigation are included in this final report.

FOREWORD

This technical report describes the research conducted for the Air Force Wright Aeronautical Laboratory, Air Force Systems Command, Wright-Patterson Air Force Base, OH 45433, under Contract F33615-76-C-5220, with Dr. W. B. Jones, Jr., MLBC, as Project Engineer.

Dr. John Romanko, GD/FWD Program Manager, acknowledges the interest and guidance of Dr. Jones and consultant Dr. W. G. Knauss of California Institute of Technology in this program. Many scientists of Materials and Structures Technology, General Dynamics' Fort Worth Division, contributed to the efforts reported herein: Messrs. R. S. Chambers and L. R. Collins conducted the stress analysis task; Drs. P. L. Flynn and J. Romanko, and Messrs. R. H. McDaniel, F. C. Nordquist, M. A. Flanders and J. D. Reynolds were responsible for the materials characterization; Messrs. R. L. Jones and F. C. Nordquist conducted the cyclic fatigue testing; Ms. C. L. Amerson and Mr. M. E. Tohlen performed data evaluation, and Messrs. B. O. McCauley and E. W. Turns prepared the model joints and neat adhesive coupons, with assistance from Mr. W. L. Toothaker of the Quality Assurance Group.

This report is written in two volumes. Volume I contains the essential details of the program with Volume II contributing the supportive data and derivations in Appendix form.

TABLE OF CONTENTS

LIST OF ILLUSTRATIONS

LIST OF ILLUSTRATIONS (Continued)

LIST OF ILLUSTRATIONS (Continued)

LIST OF ILLUSTRATIONS (Continued)

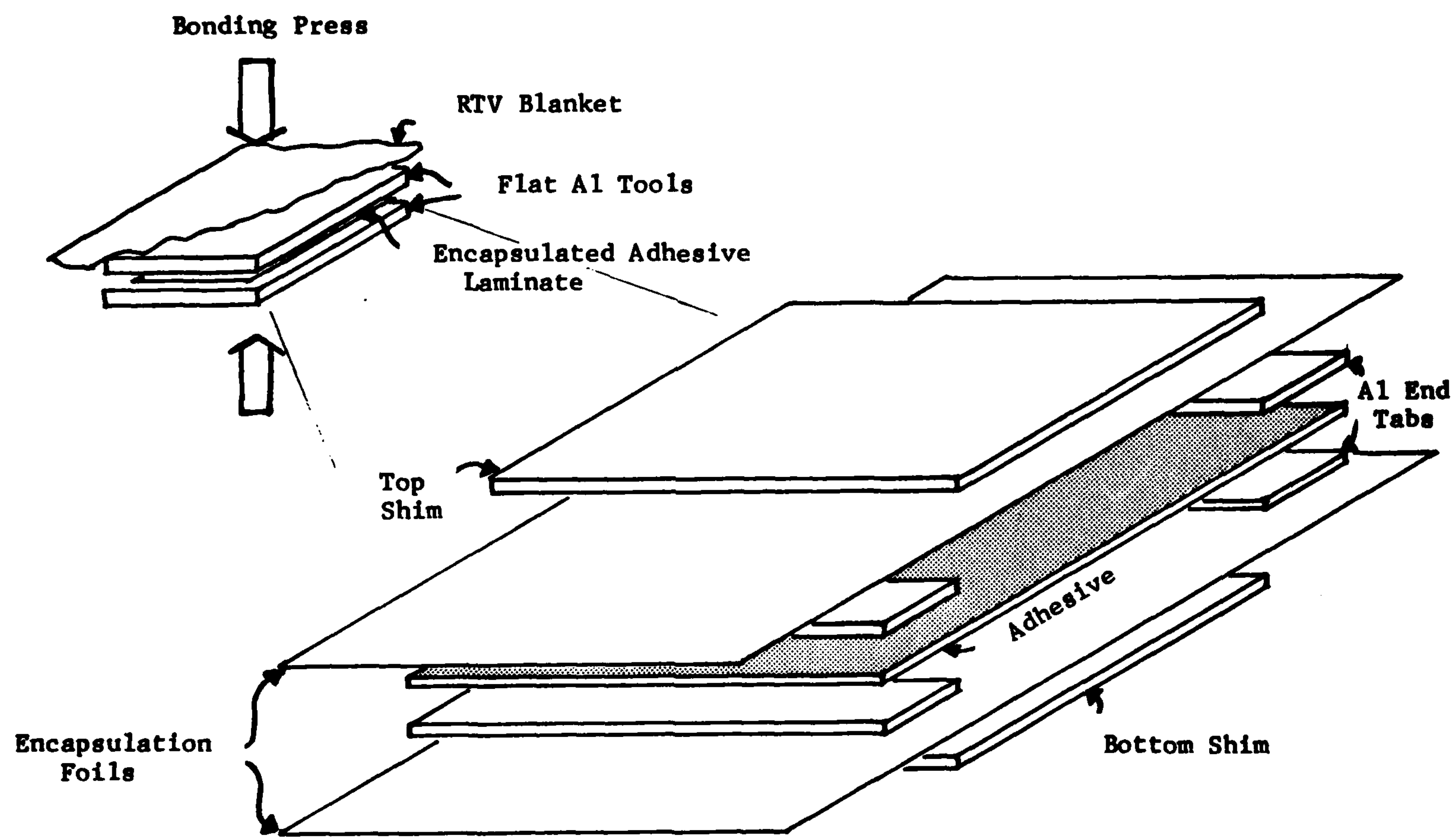

Figure A1 Cure Lay-Up for Adhesive Characterization Specimens

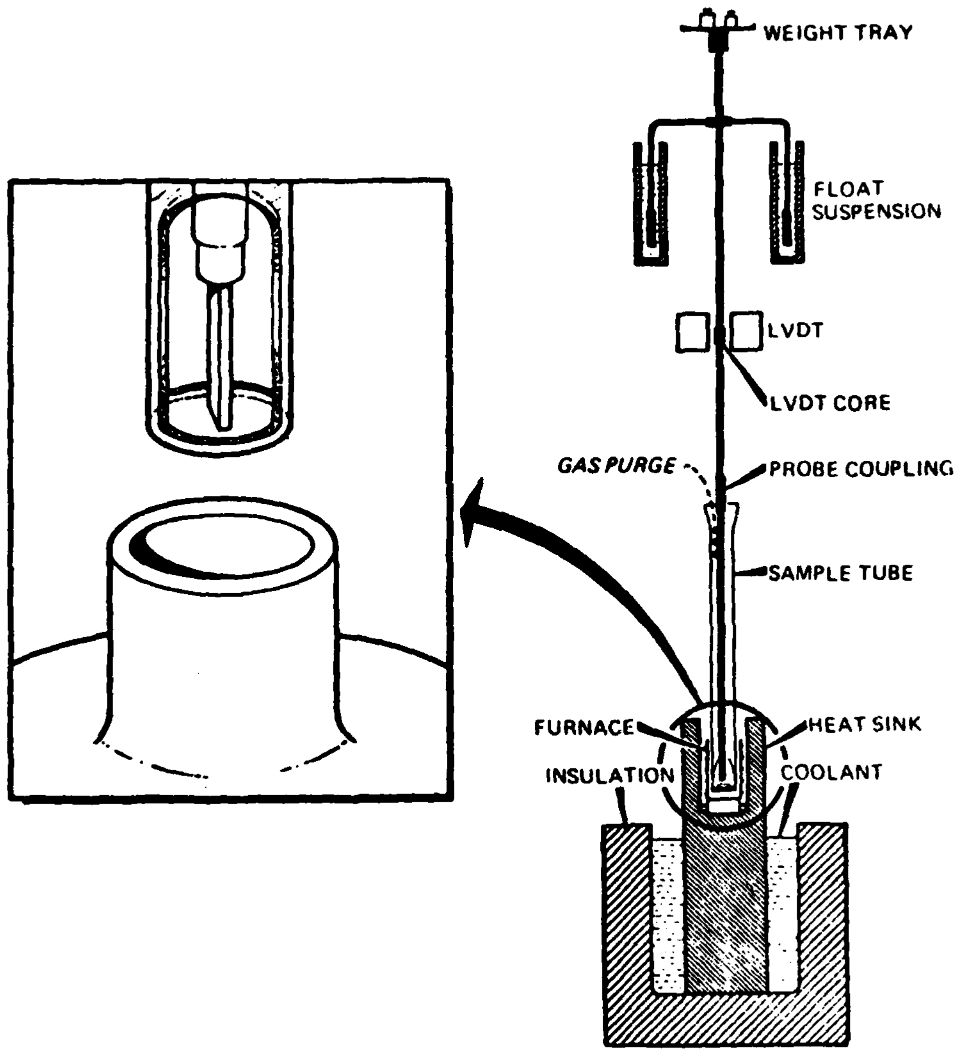

Figure A2 TMA Apparatus for Thermal Expansion Measurements (Schematic)

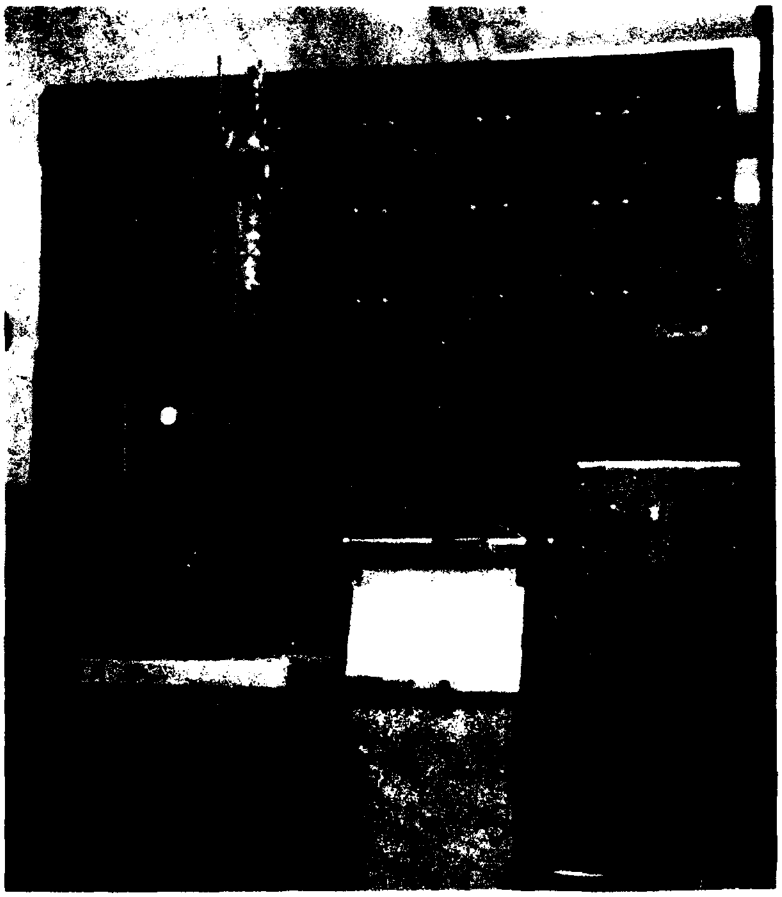

Figure A3 Adhesive Materials Characterization Creep Frame

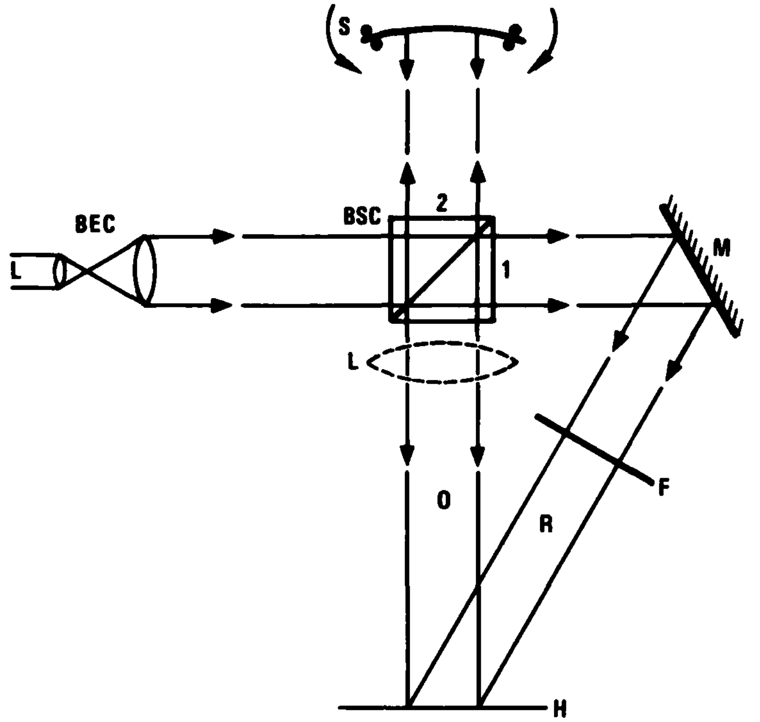

Figure A4 Laser/Optical Configuration for Measurement of Poisson's Ratio of Compliant Materials

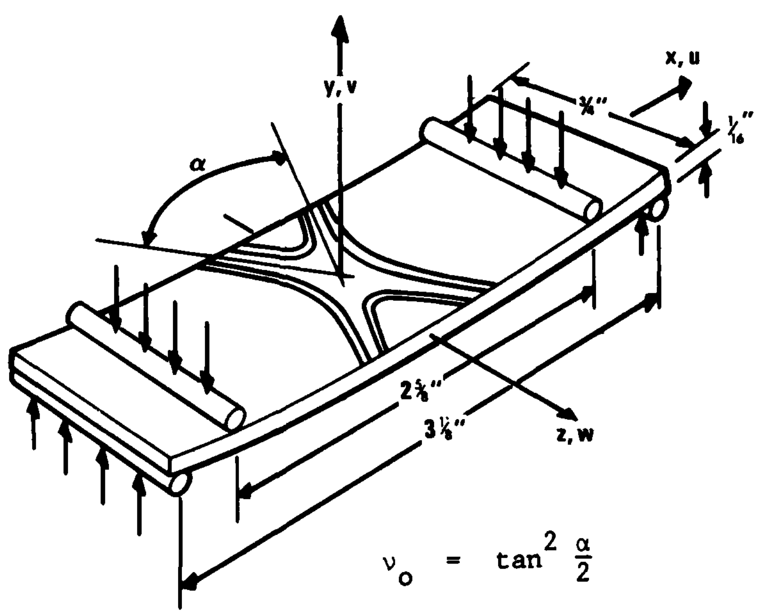

Figure A5 Test Geometry and Reference Frame

Poisson's Ratio $\nu_o = \tan^2 \frac{\alpha}{2}$

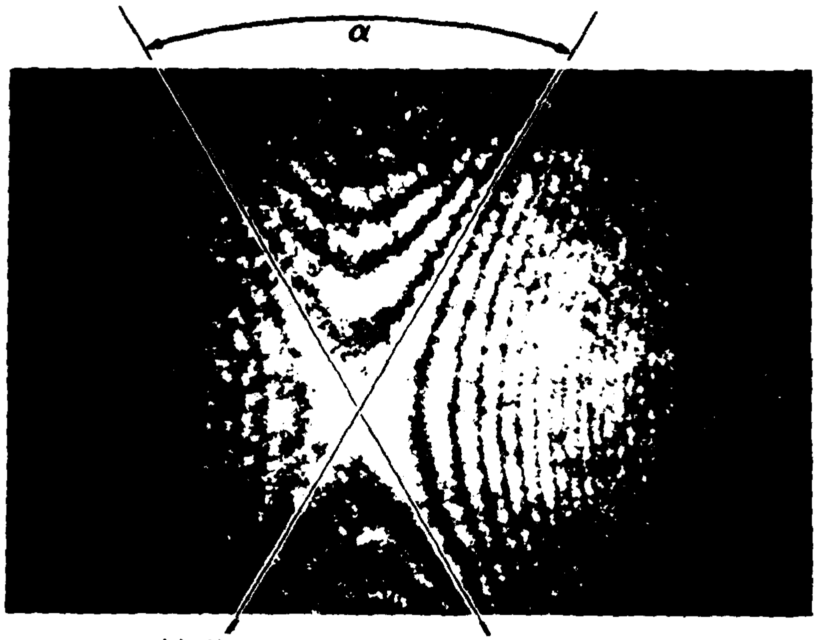

(a) Holographic Fringes for 2024 T6 Al with Asymptotic Tangent Construction

(b) Holographic Fringes for FM-73M (dry) with Calculated Fringe Fit Congugate Hyperbolae for $\nu = 0.320$

Figure A6 Poisson's Ratio Determination from Holographic Fringe Patterns

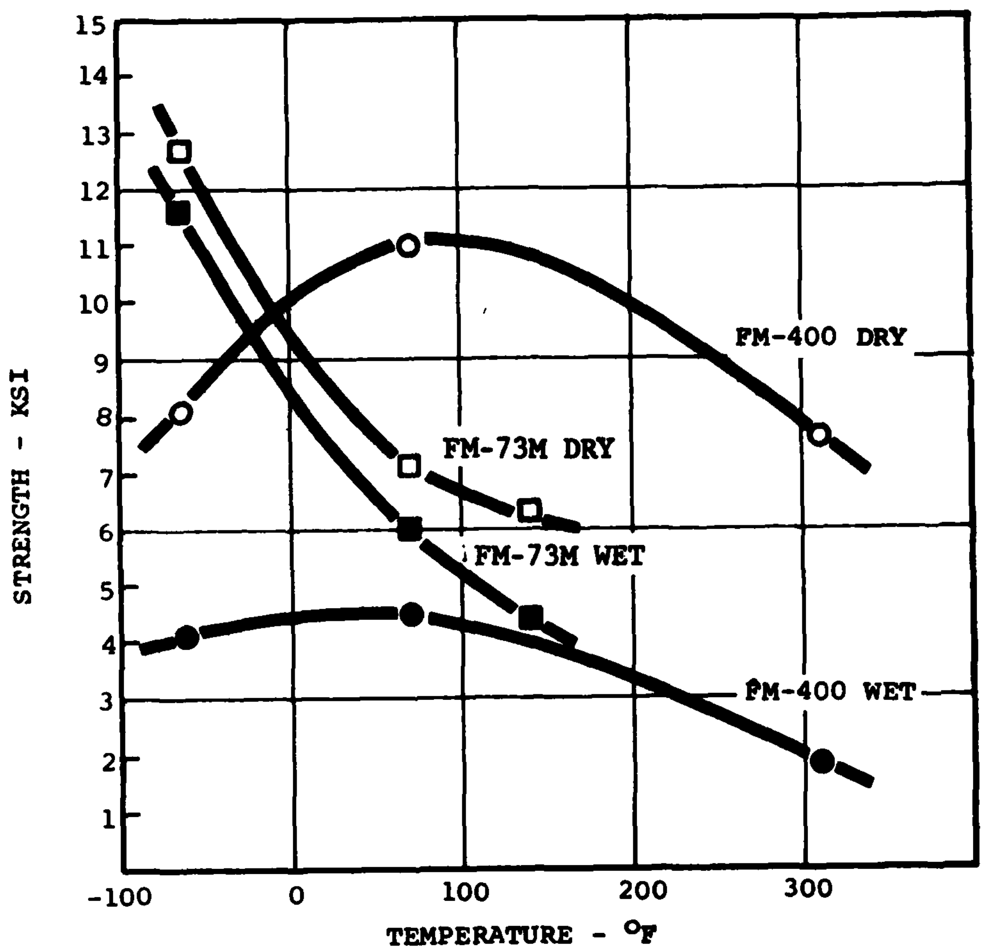

Figure A7 Strength-Temperature Histories for FM-73M and FM-400

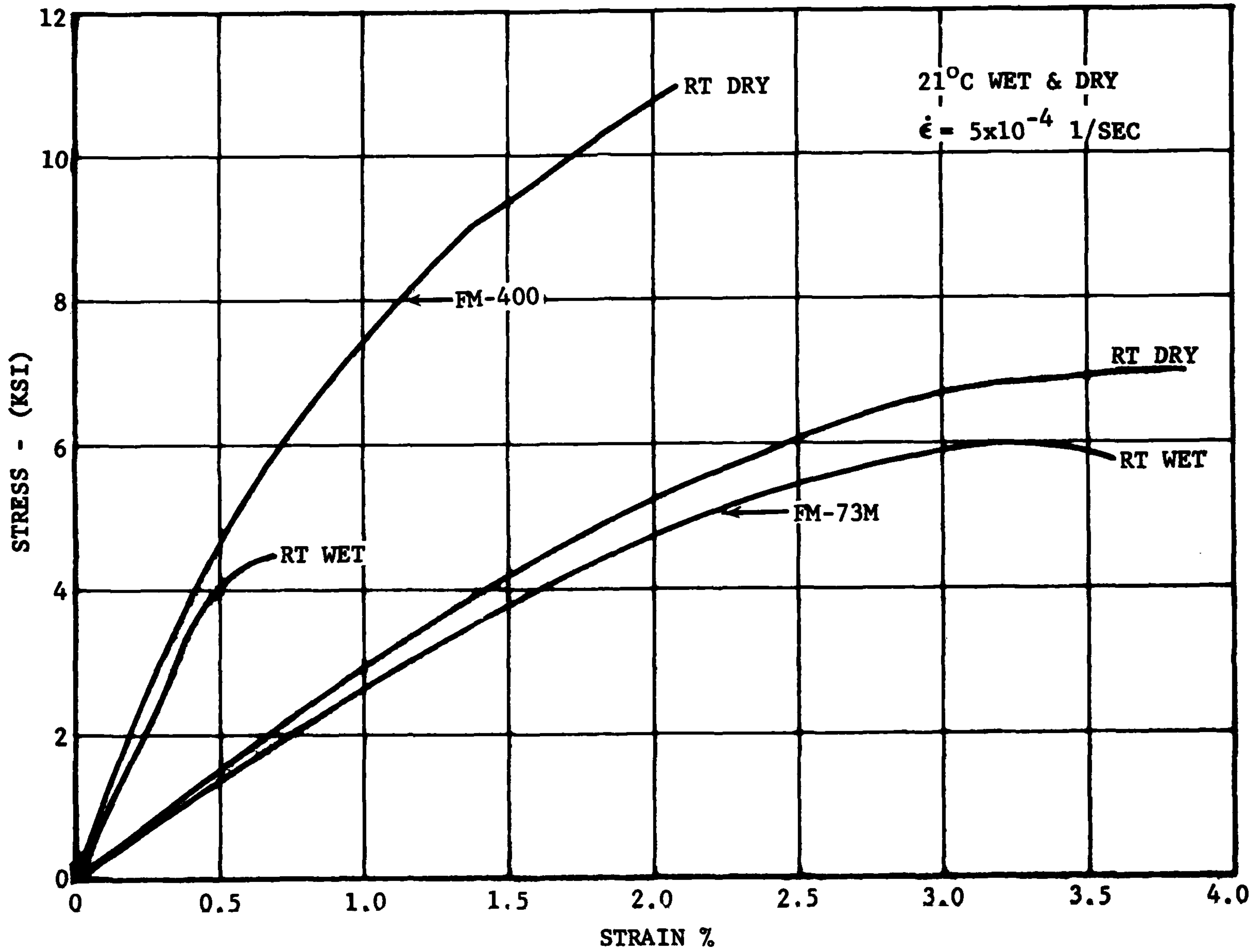

Figure A8 Stress-Strain History for FM-400

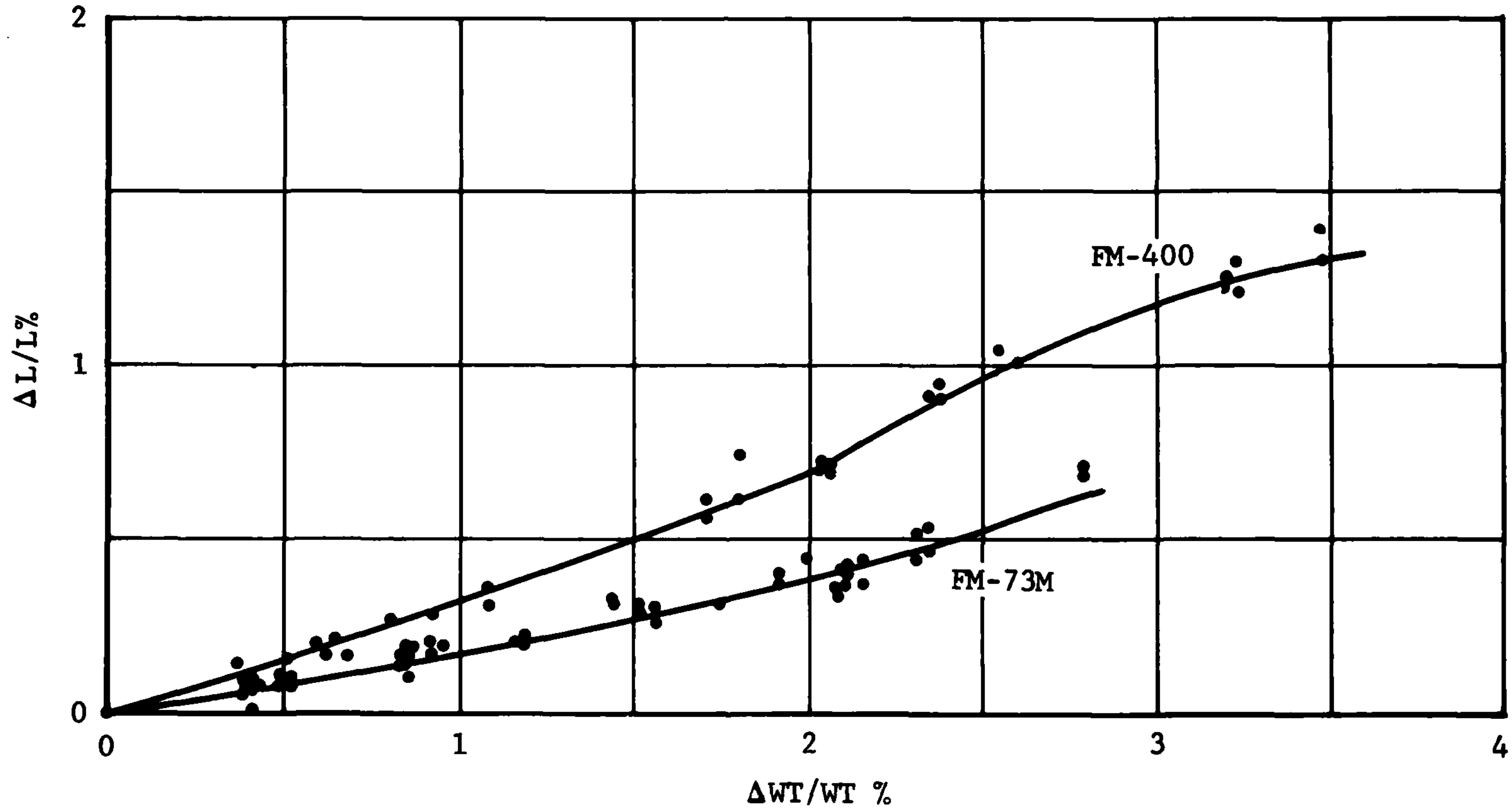

Figure A9 Moisture Expansion Curves for FM-73M and FM-400

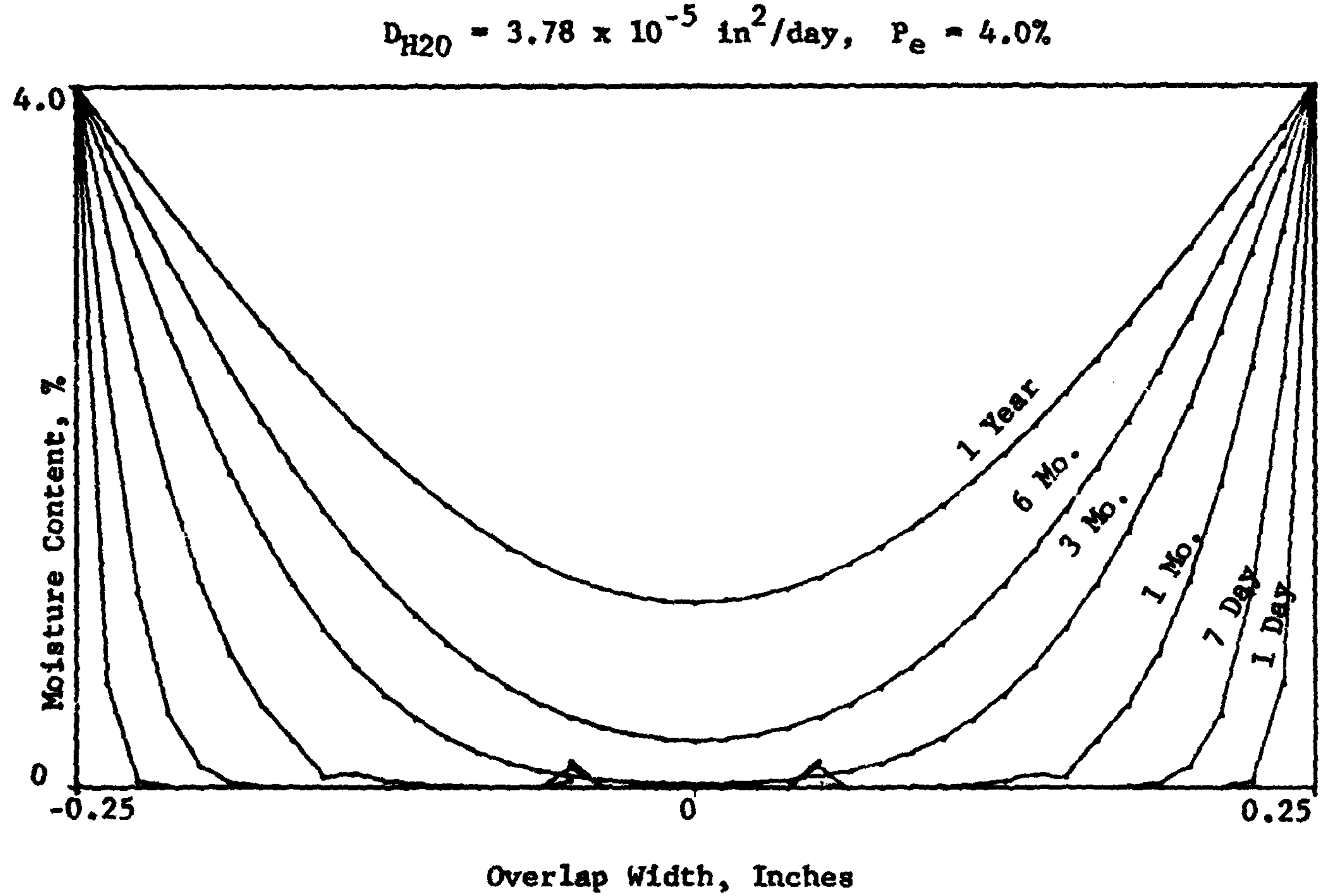

Figure A10 Moisture Distribution in a 0.5-inch Thick Slab of FM-400 Adhesive Exposed to 100% RH at 60°C

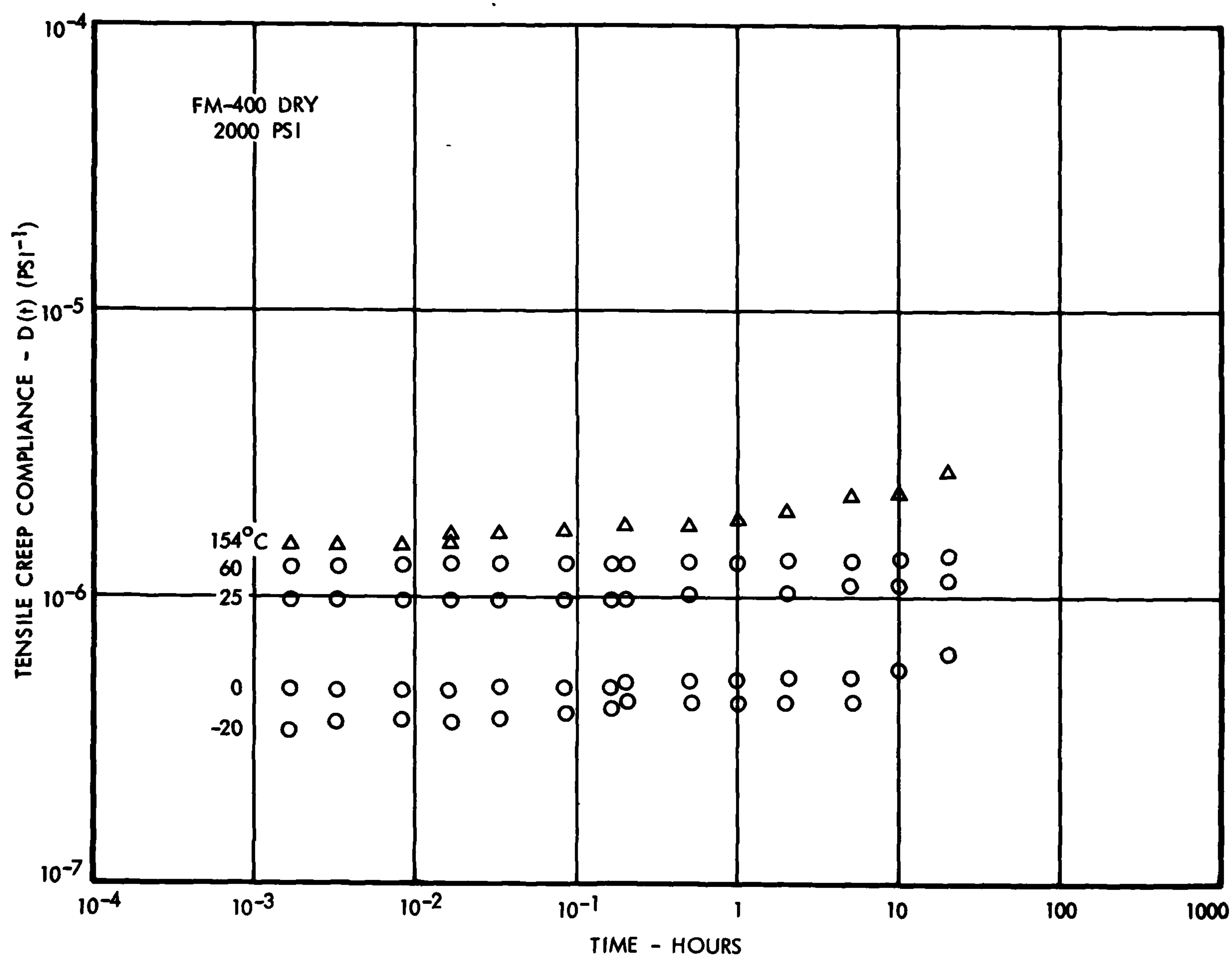

Figure A11 Tensile Creep Compliance Curves for FM-400 (dry) at Various Temperatures

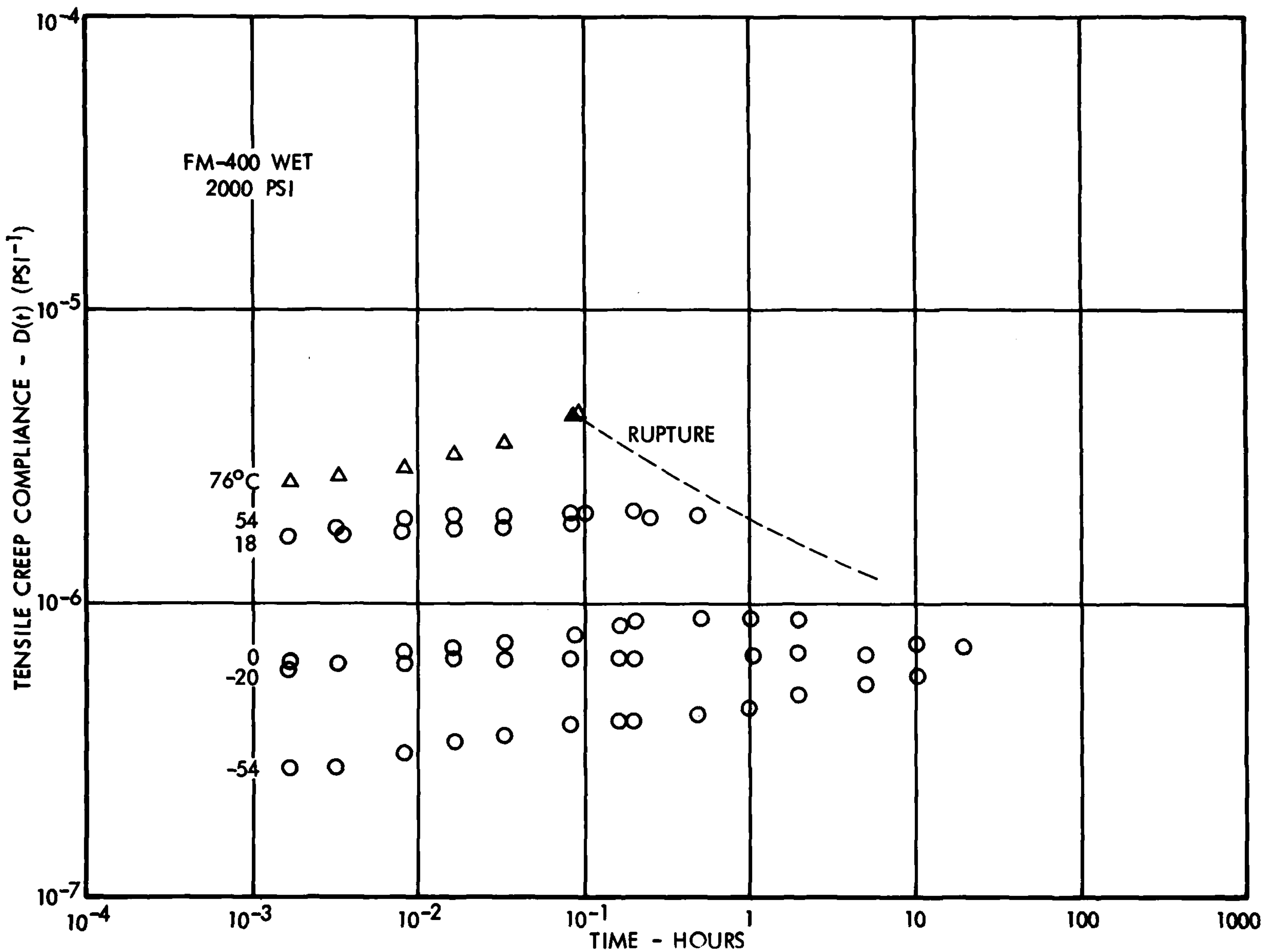

Figure A12 Tensile Creep Compliance Curves for FM-400 (wet) at Various Temperatures

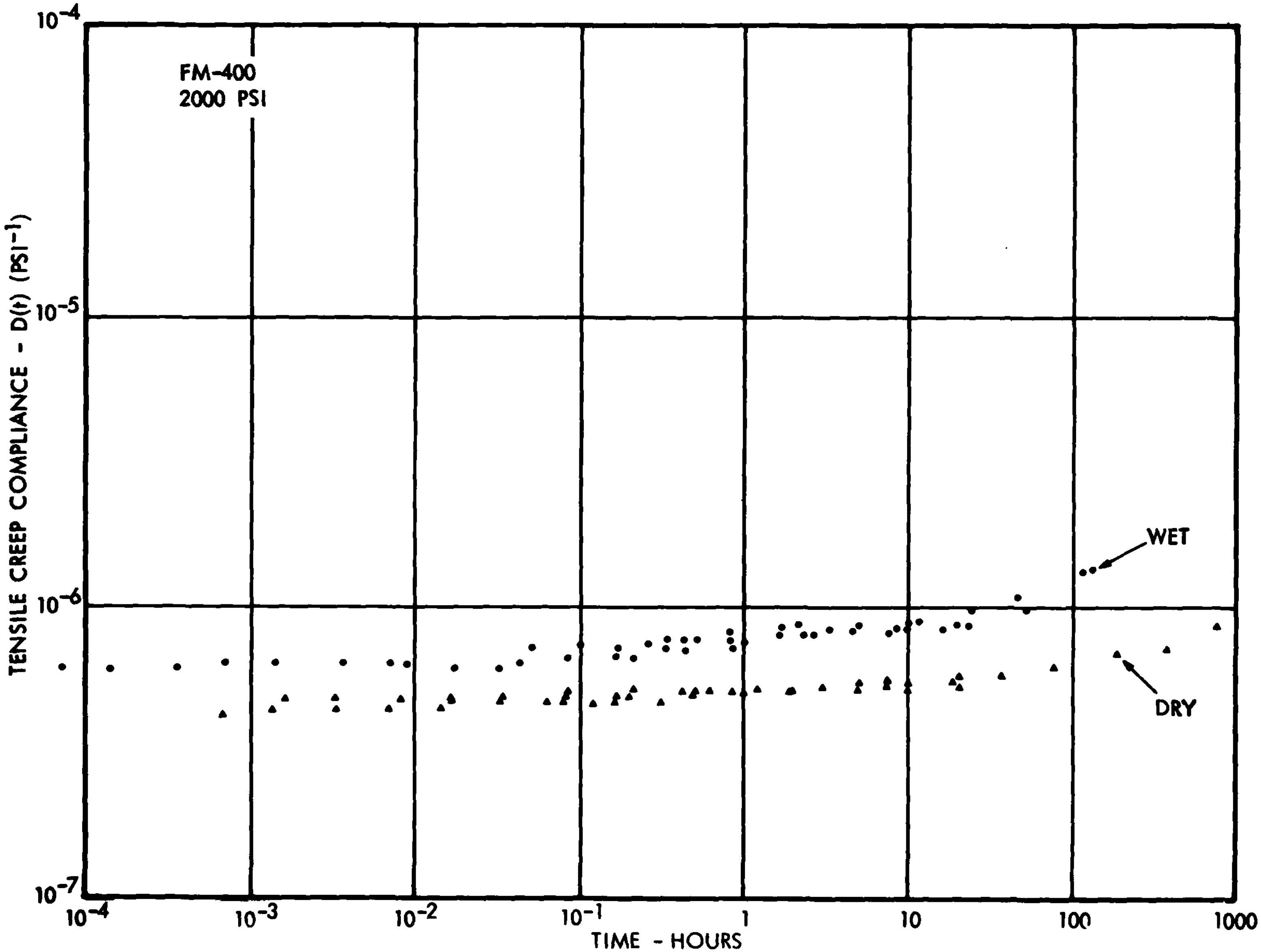

Figure A13 Tensile Creep Compliance Master Curves for FM-400 (Reduced to Reference Temperature 0°C)

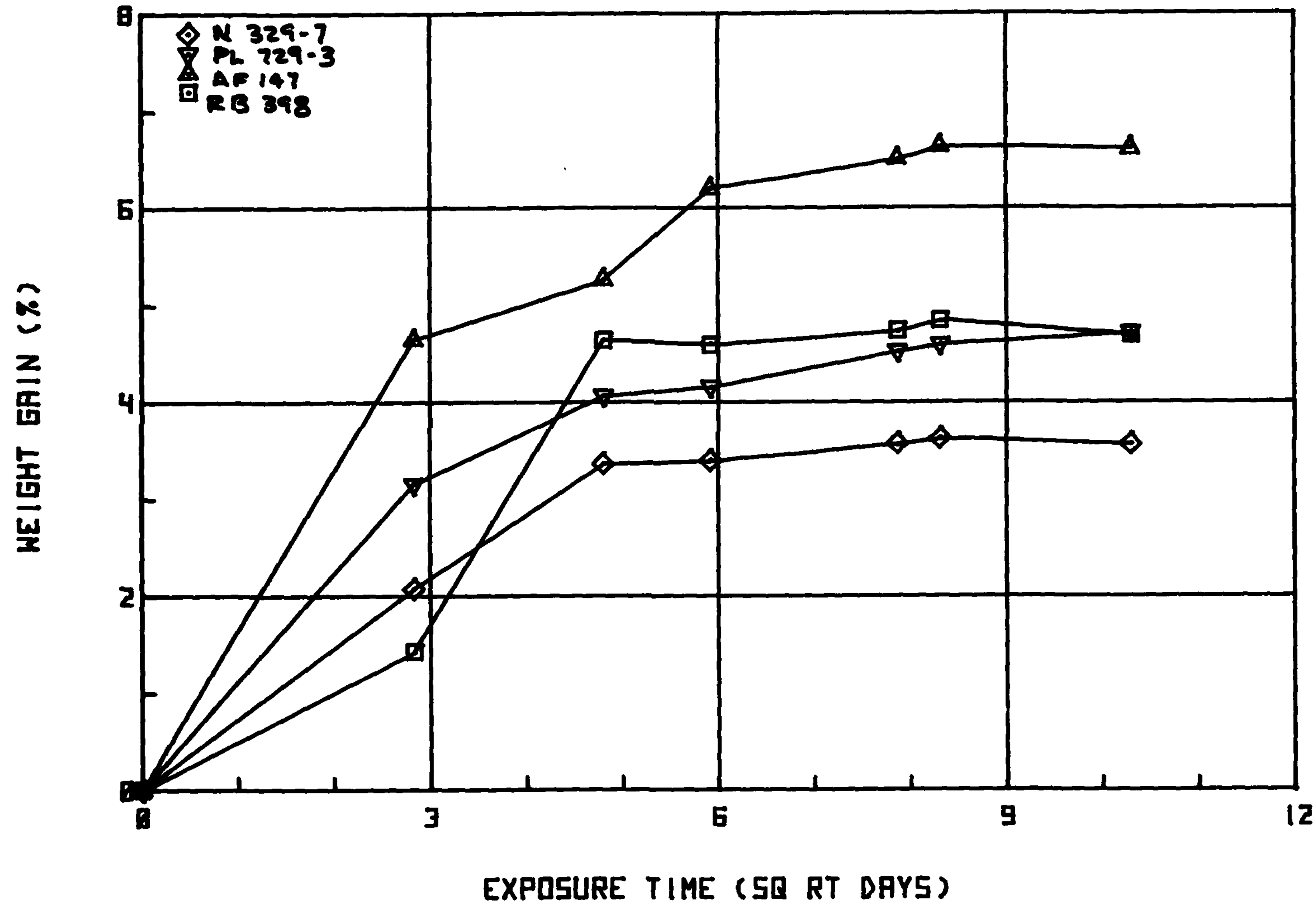

Figure A14 Weight Gain of 350°F Cured Adhesives in 150°F Water

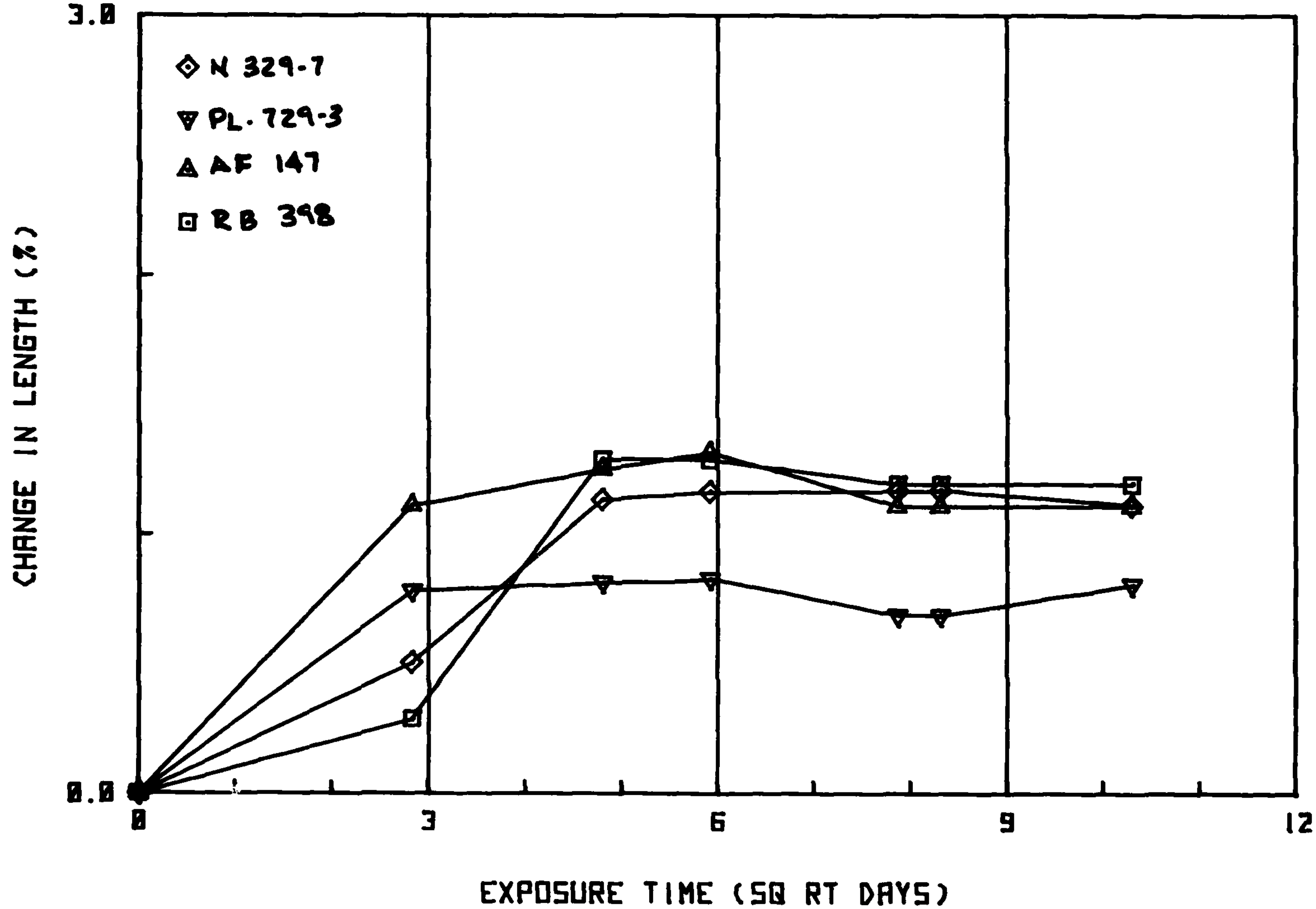

Figure A15 Length Change of 350°F Cured Adhesives in 150°F Water Vapor

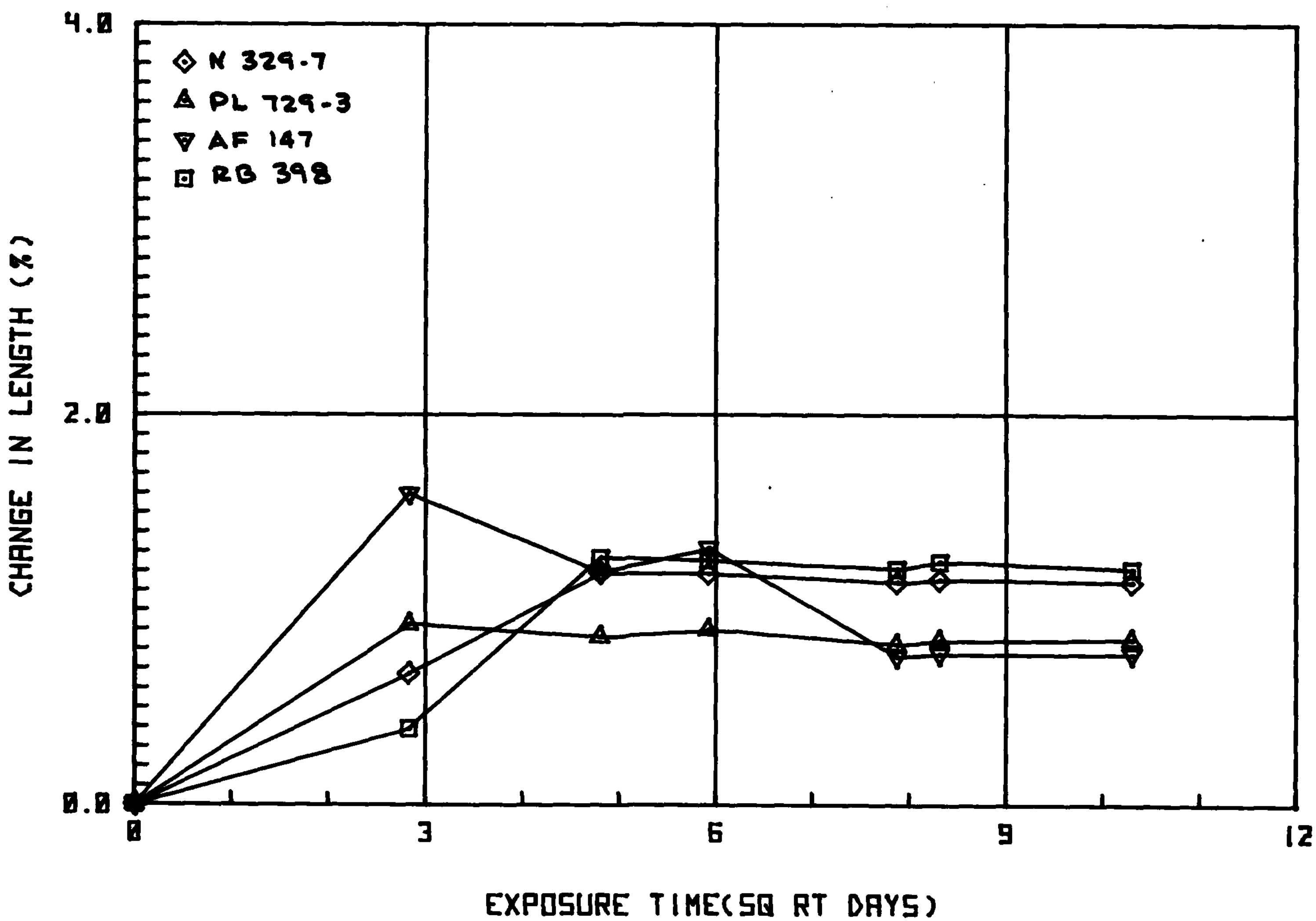

Figure A16 Length Change of 350°F Cured Adhesives in 150° Water

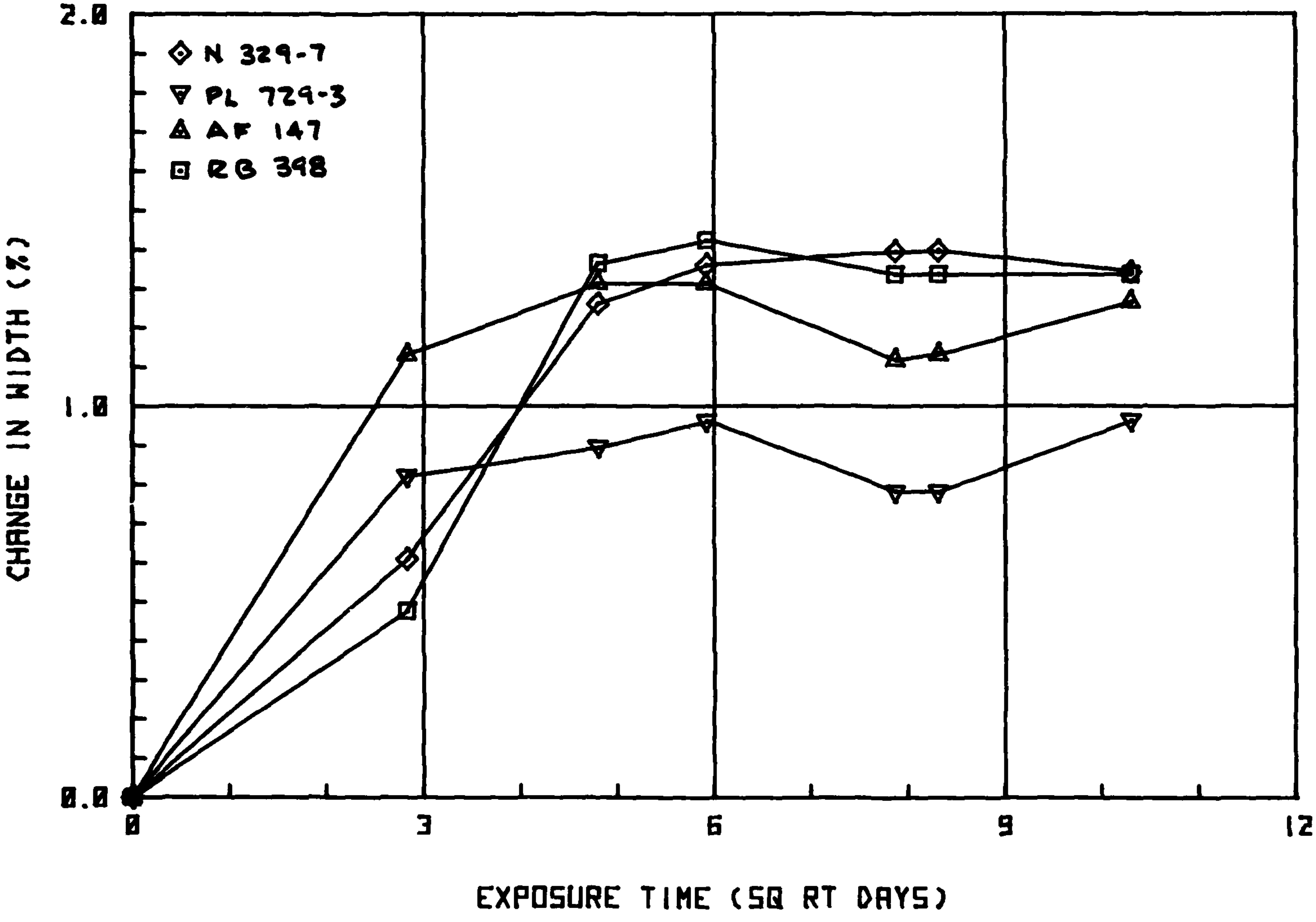

Figure A17 Width Change of 350°F Cured Adhesives in 150°F Water Vapor

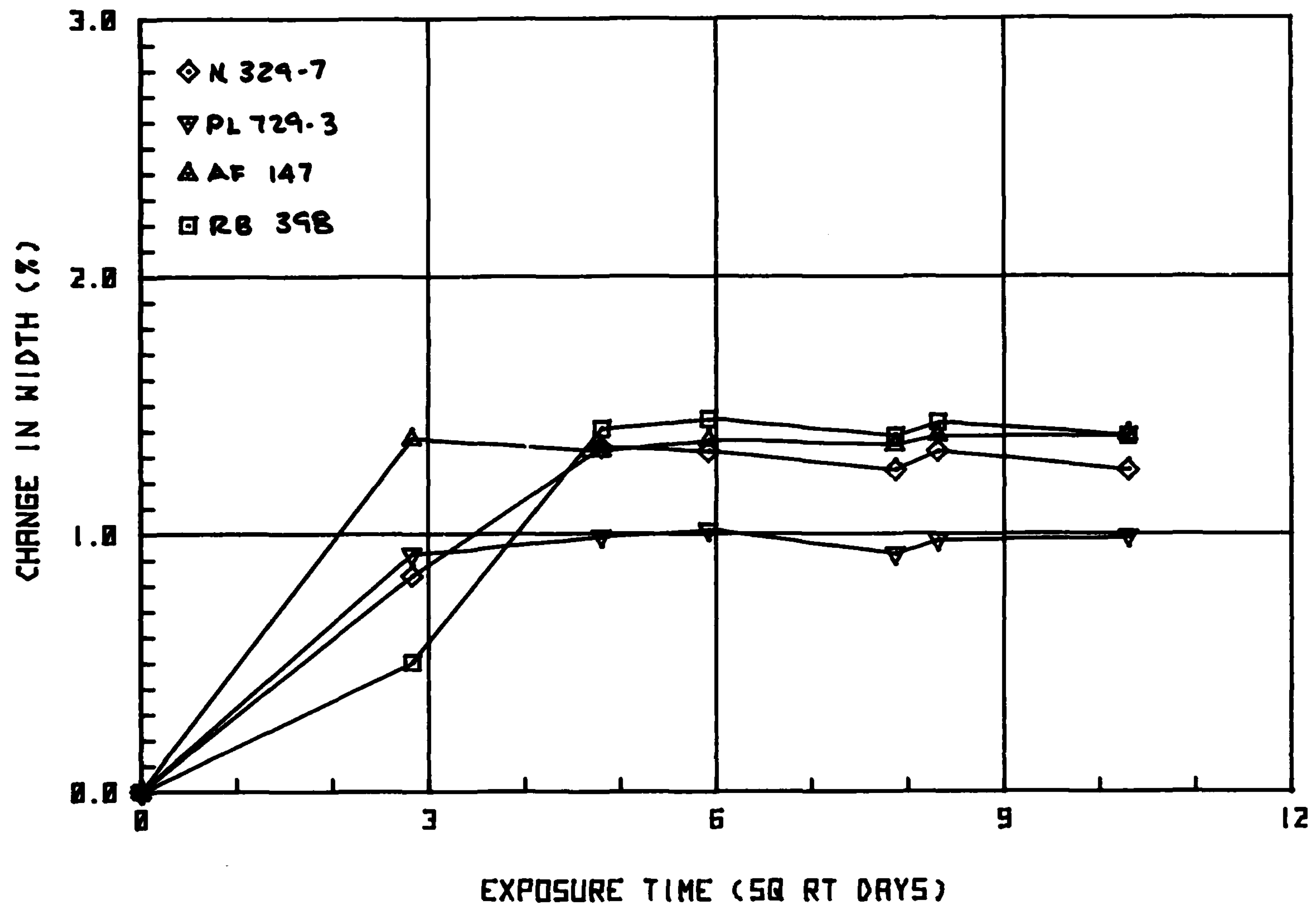

Figure A18 Width Change of 350°F Cured Adhesives in 150°F Water

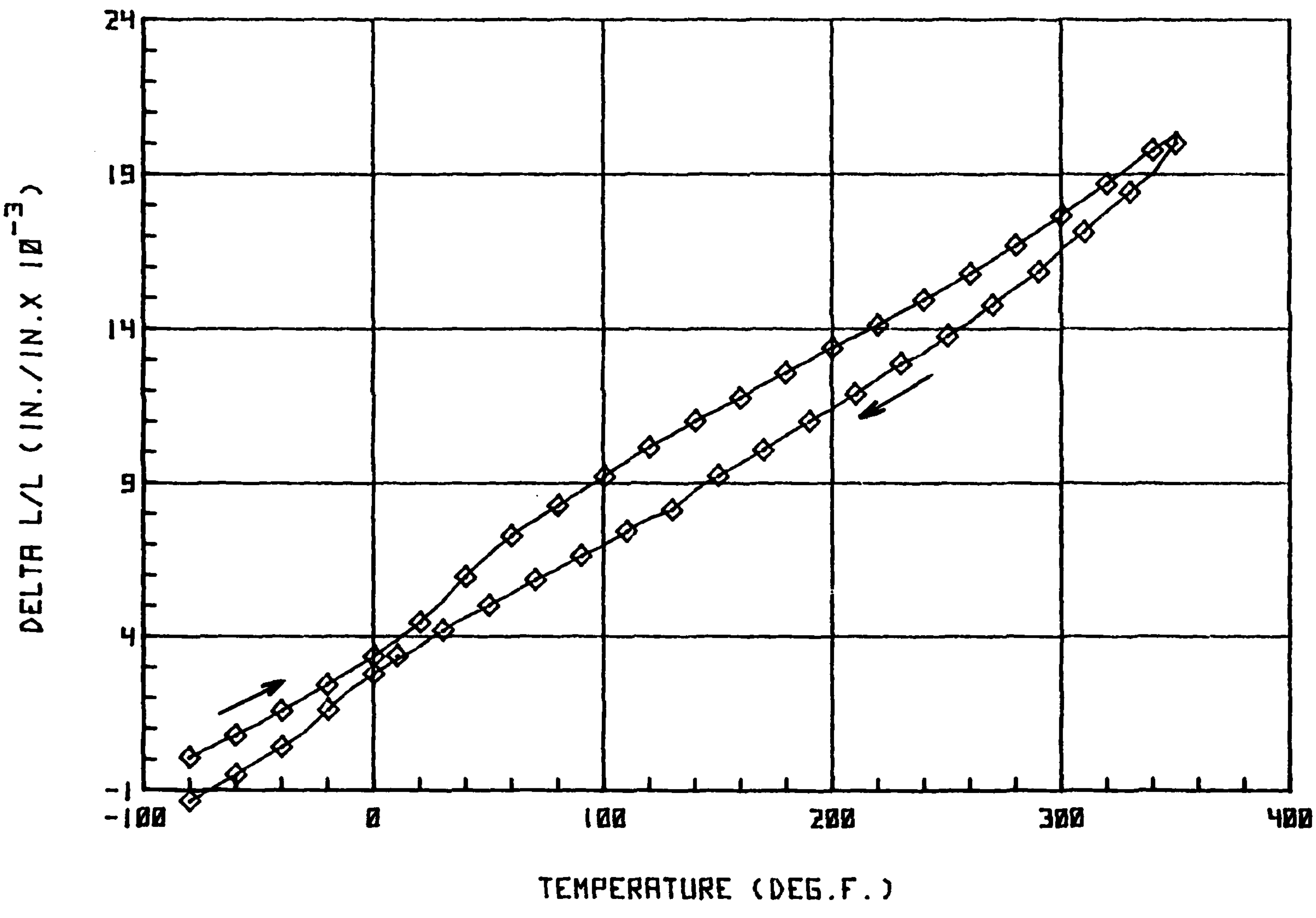

Figure A19 Thermal Expansion of Dry AF-147 Adhesive

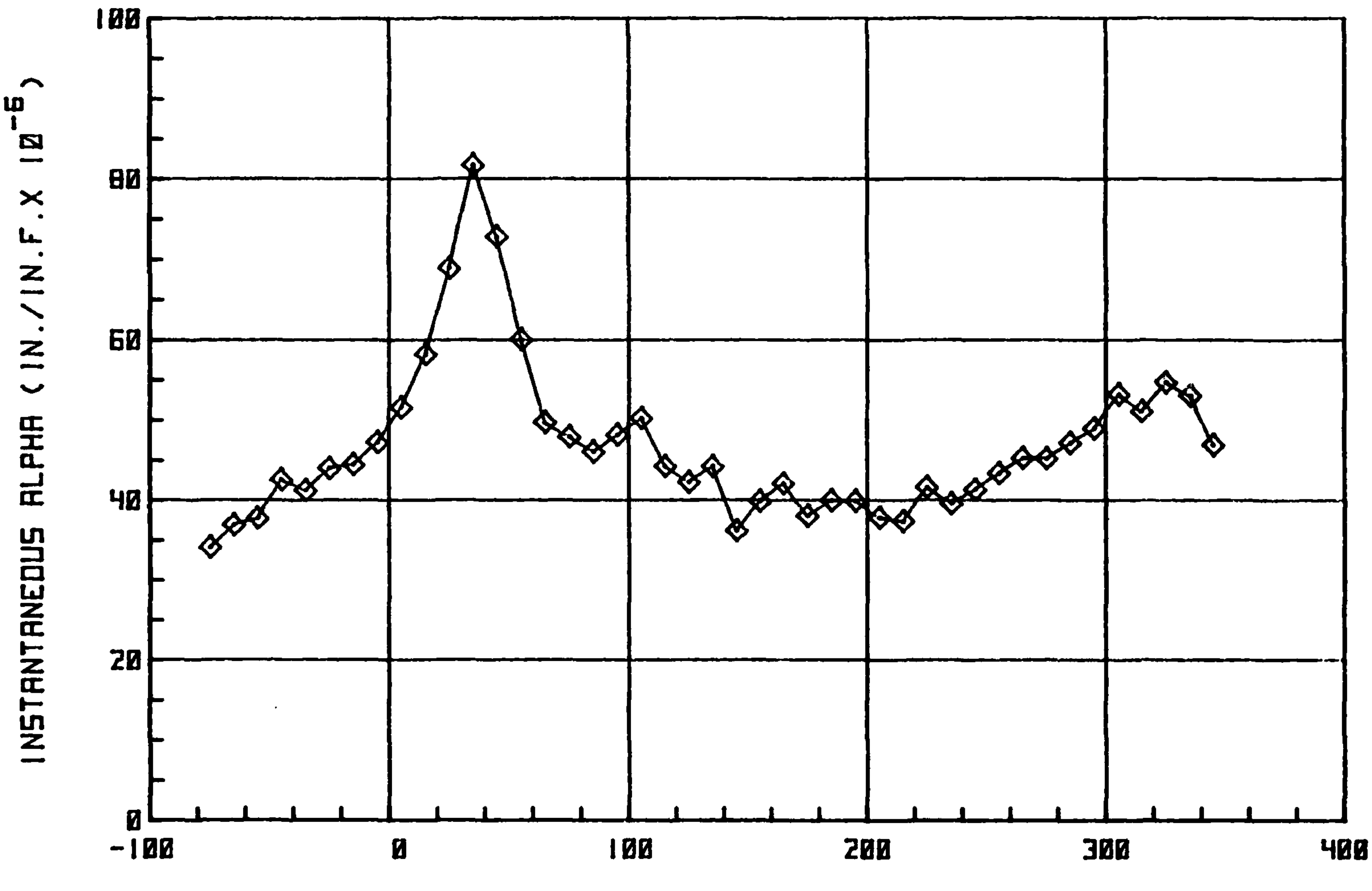

Figure A20 Thermal Expansion Coefficient of Dry AF-147

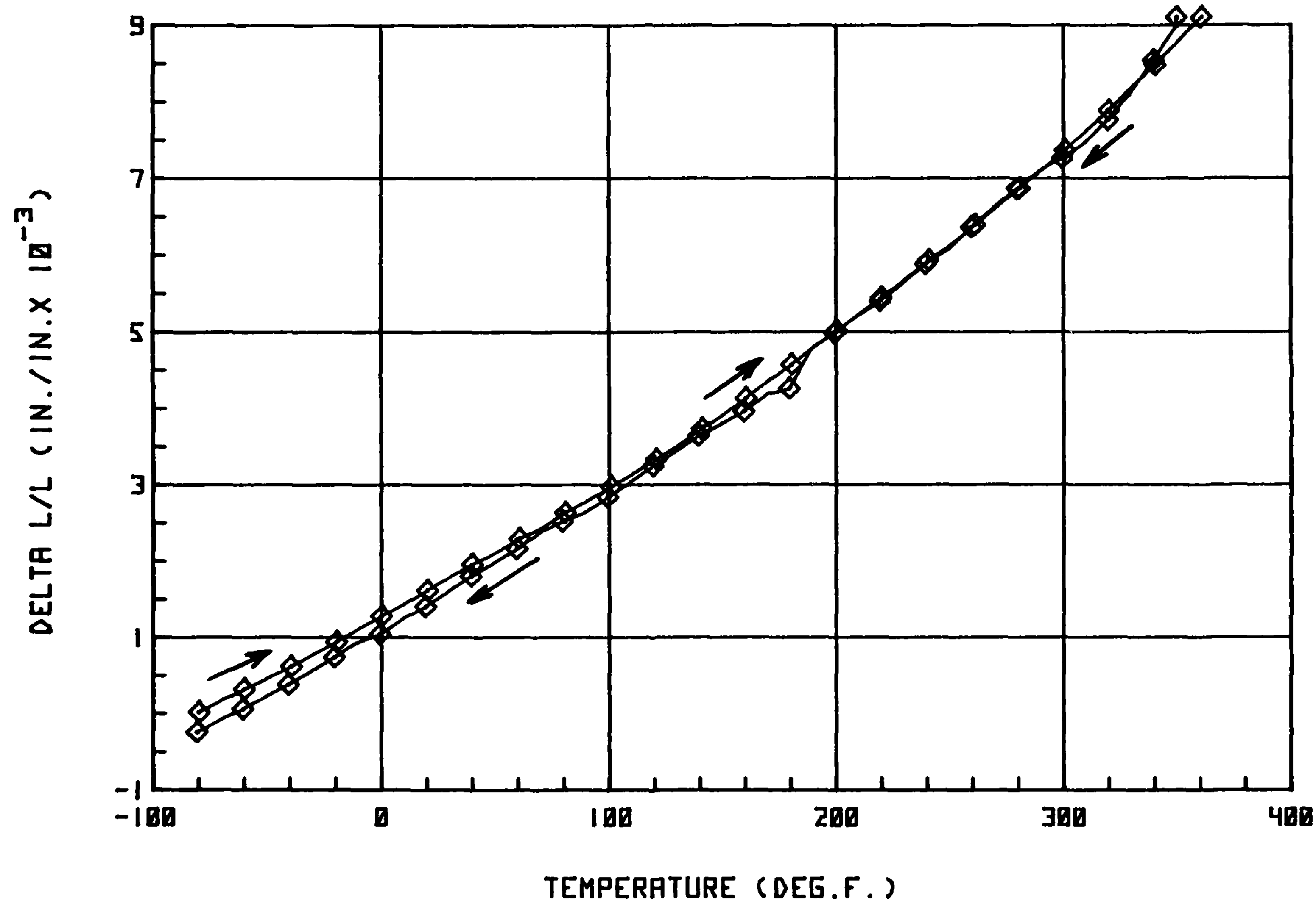

Figure A21 Thermal Expansion of Dry N329-7 Adhesive

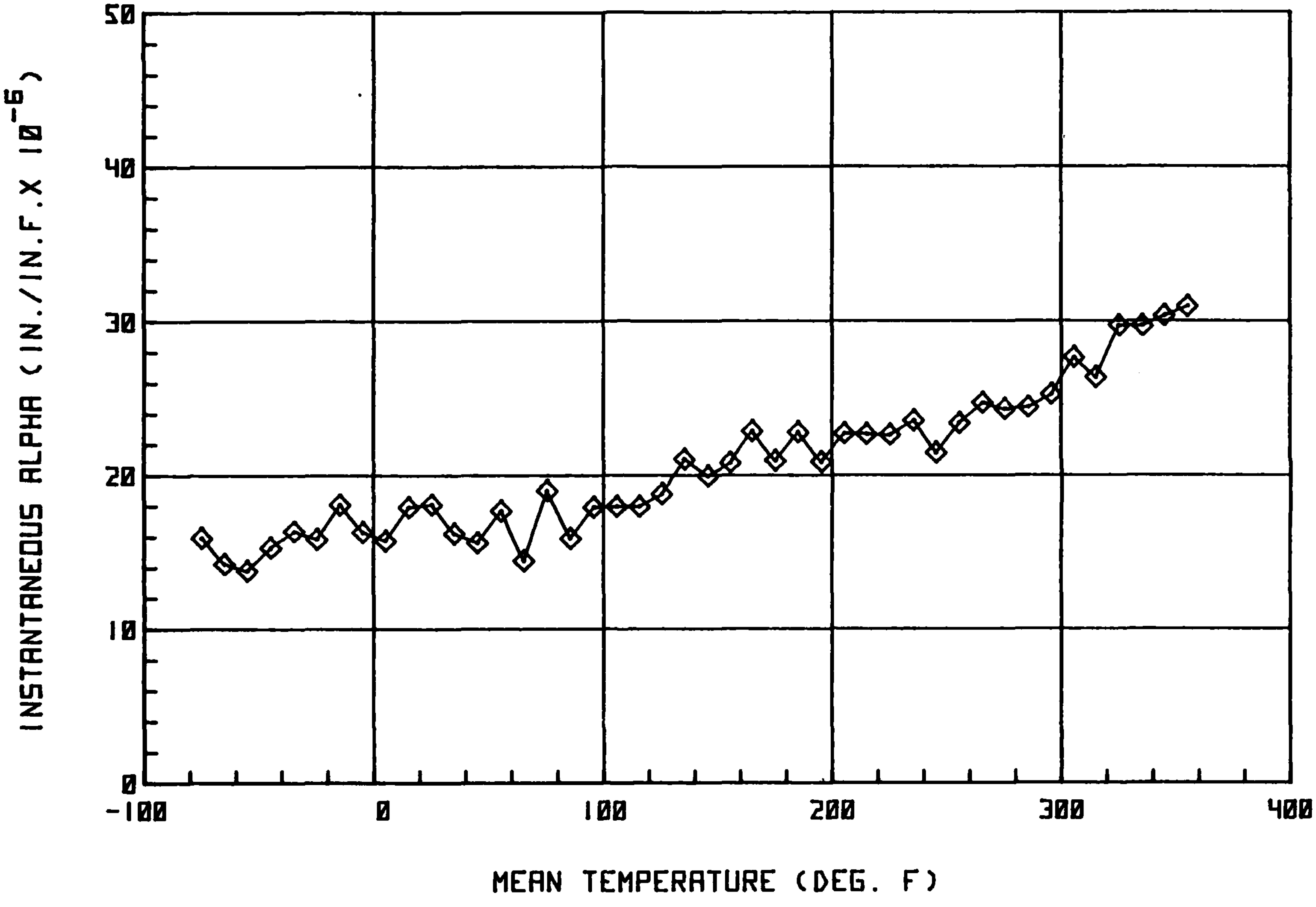

Figure A22 Thermal Expansion of Coefficient of Dry N329-7 Adhesive

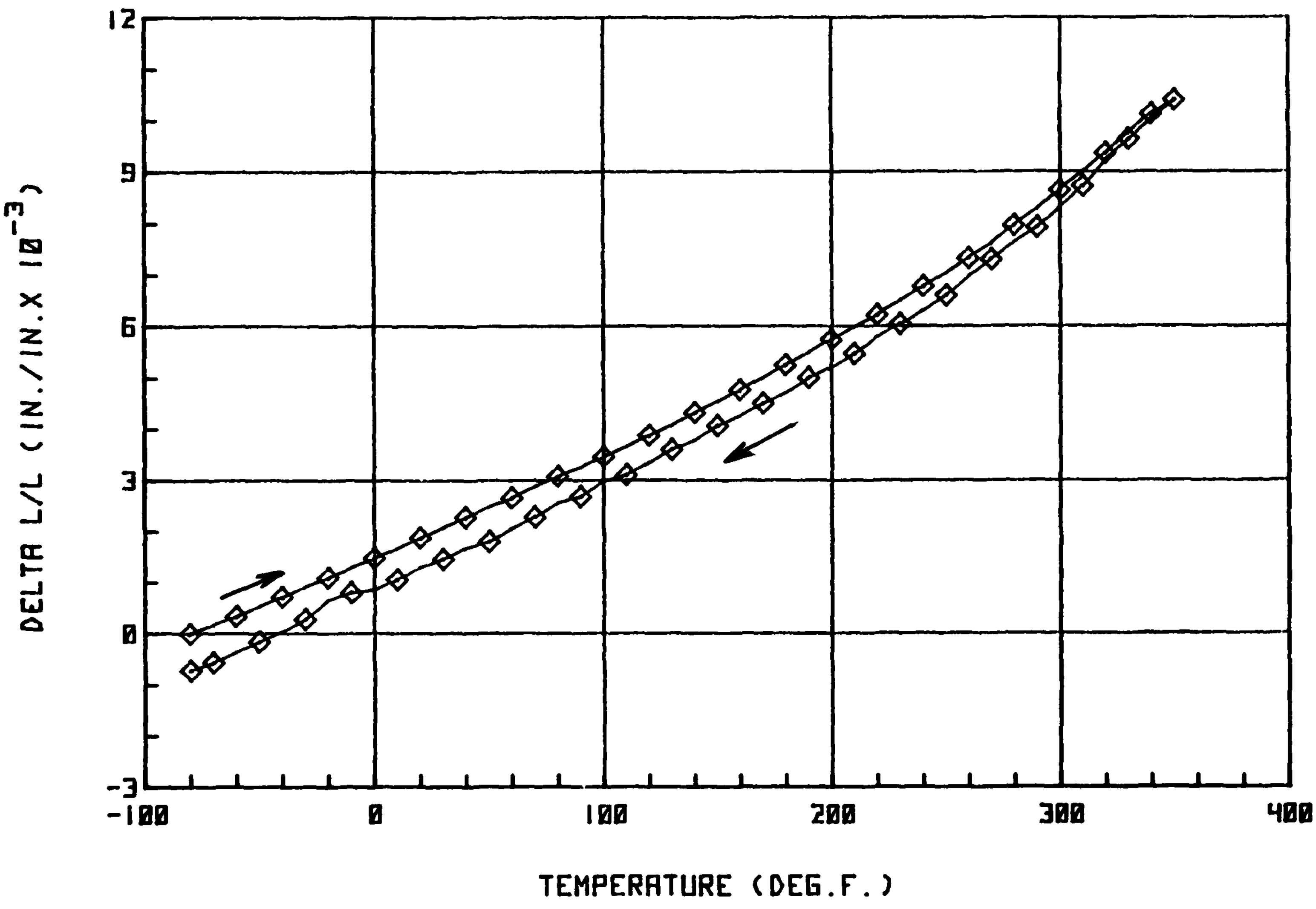

Figure A23 Thermal Expansion of Dry RB-398 Adhesive

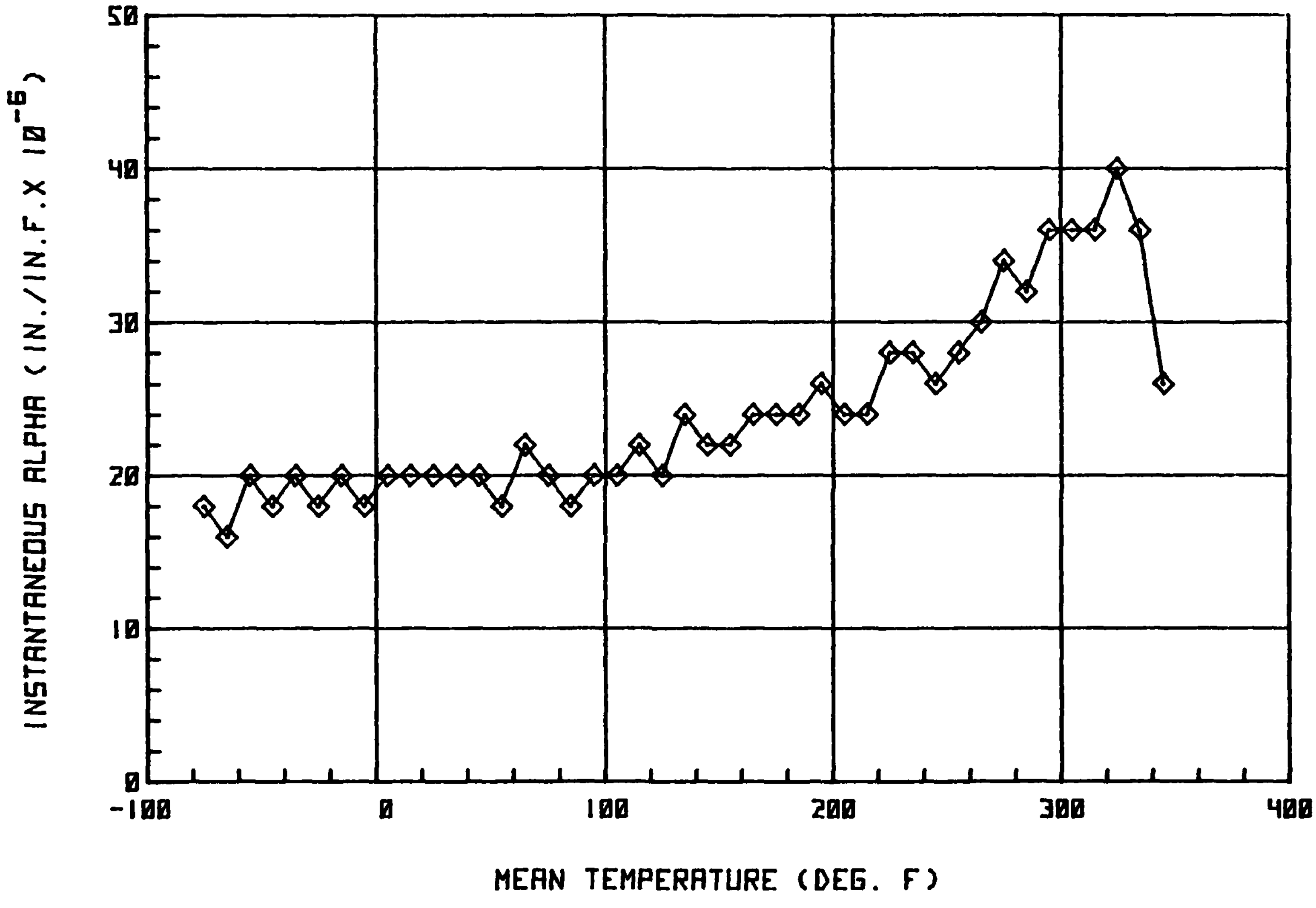

Figure A24 Thermal Expansion Coefficient of Dry RB-398 Adhesive

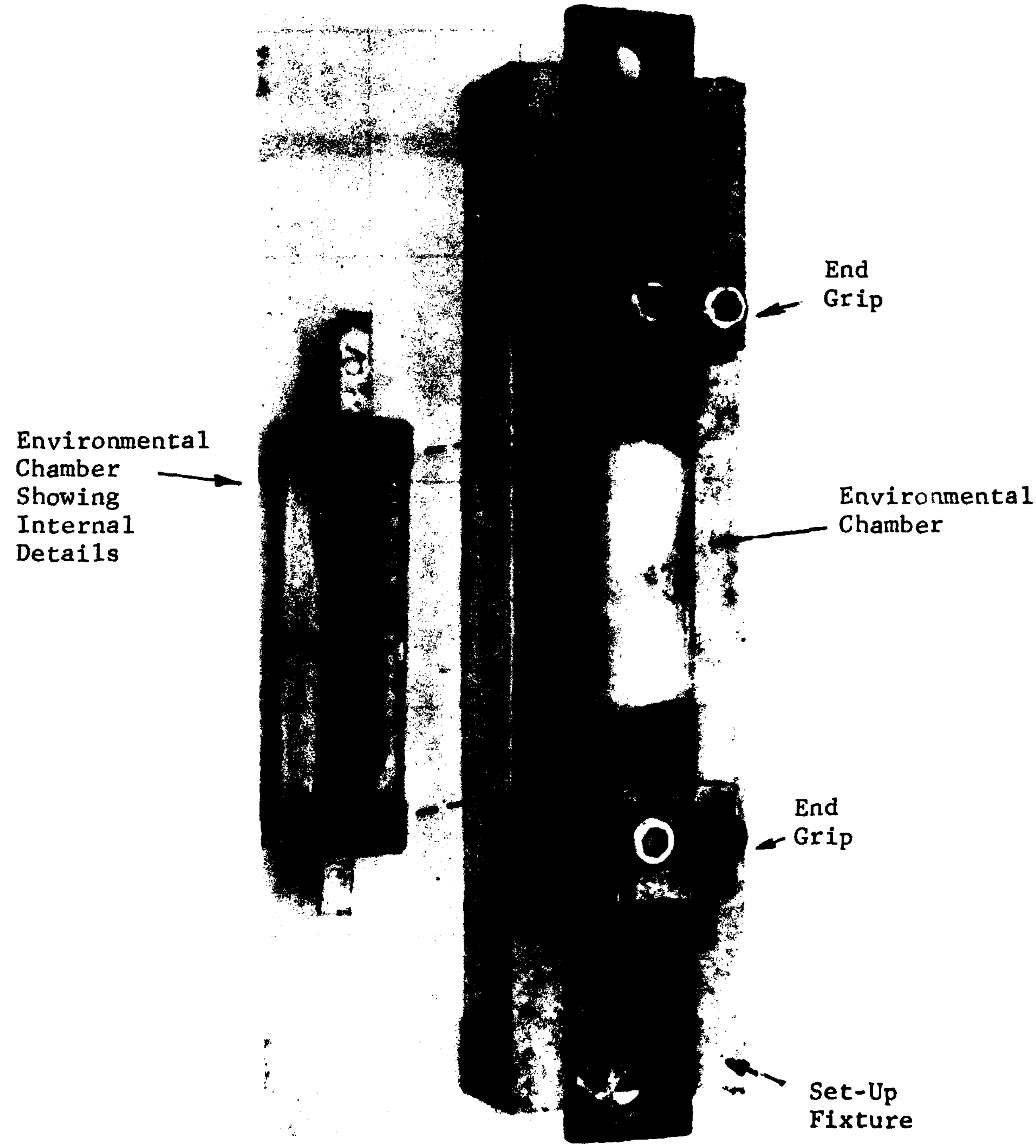

Figure A25 Environmental Chamber With Moisture-Conditioned Coupon for Smith Plot Measurements

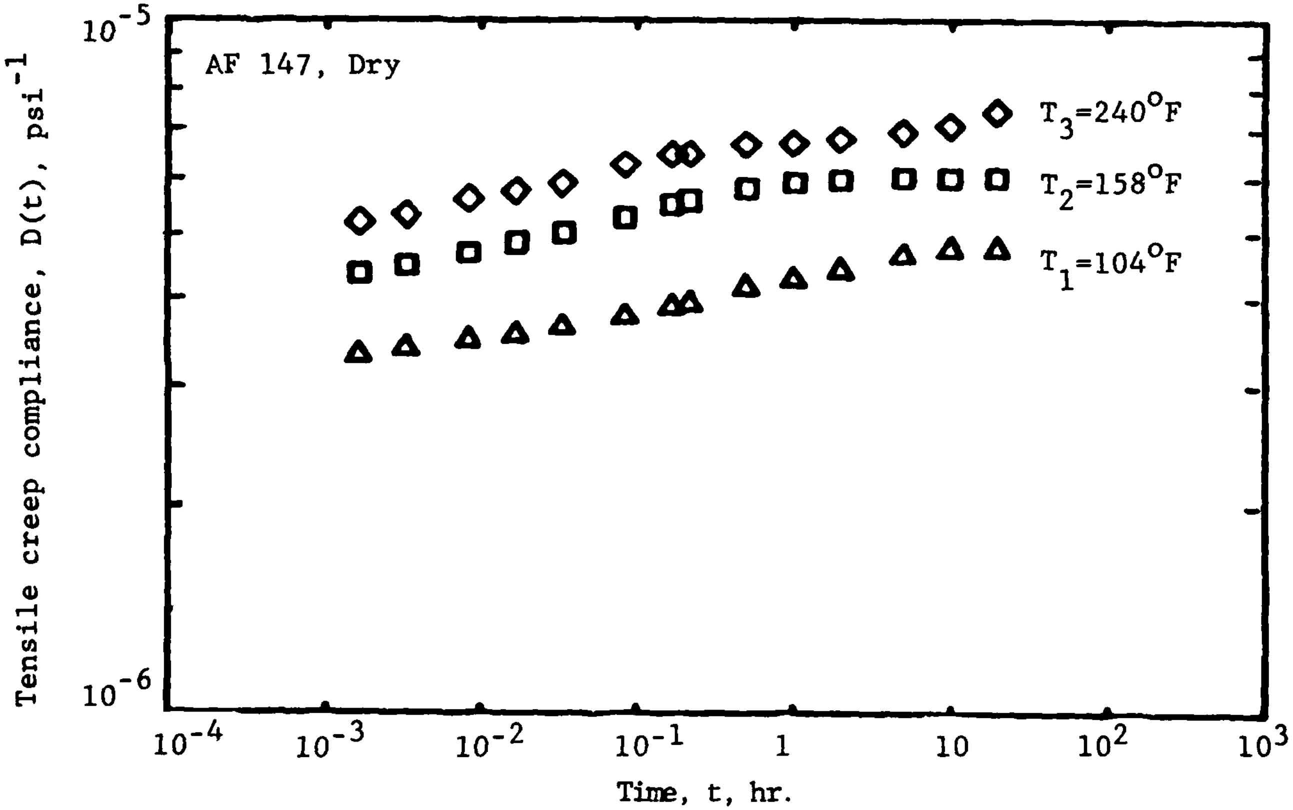

Figure A26 Tensile Creep Compliance – AF-147, Dry

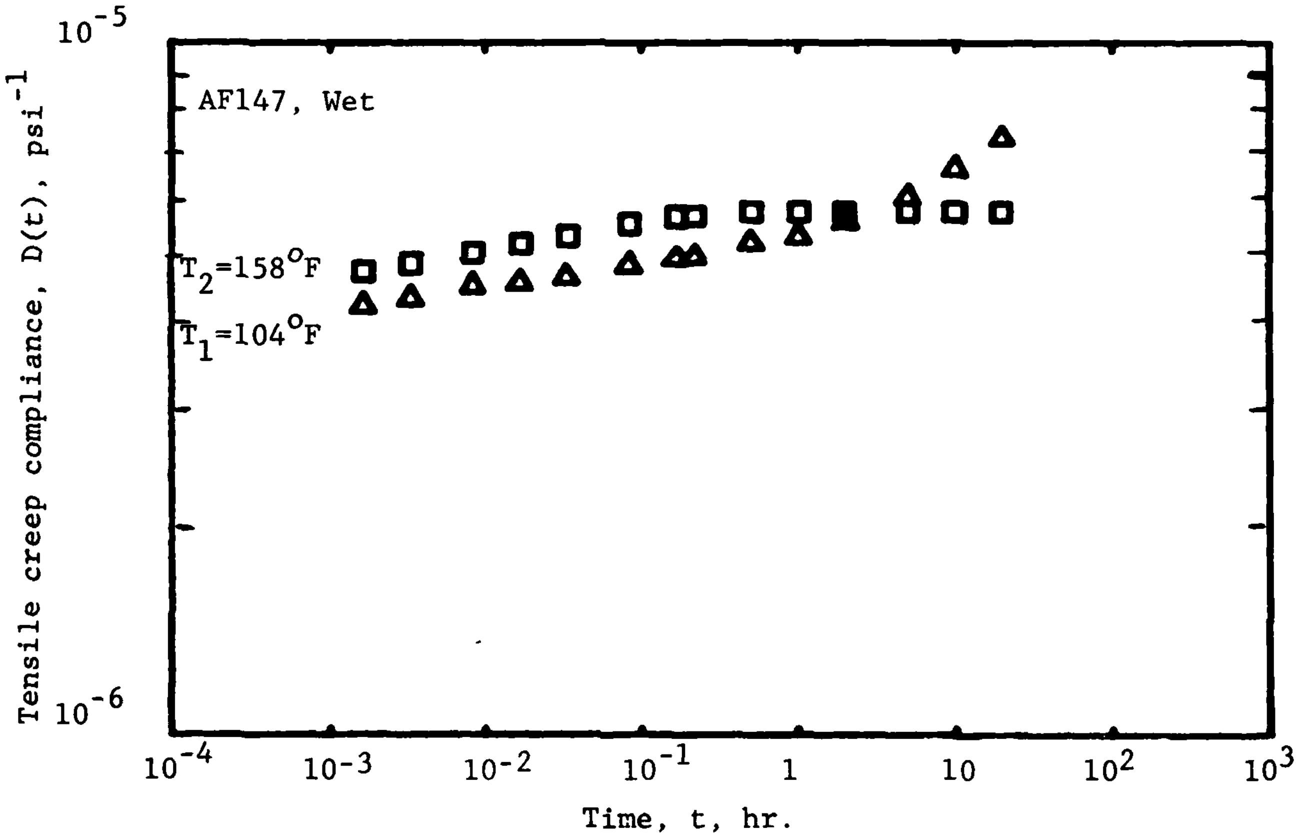

Figure A27 Tensile Creep Compliance of Wet AF-147

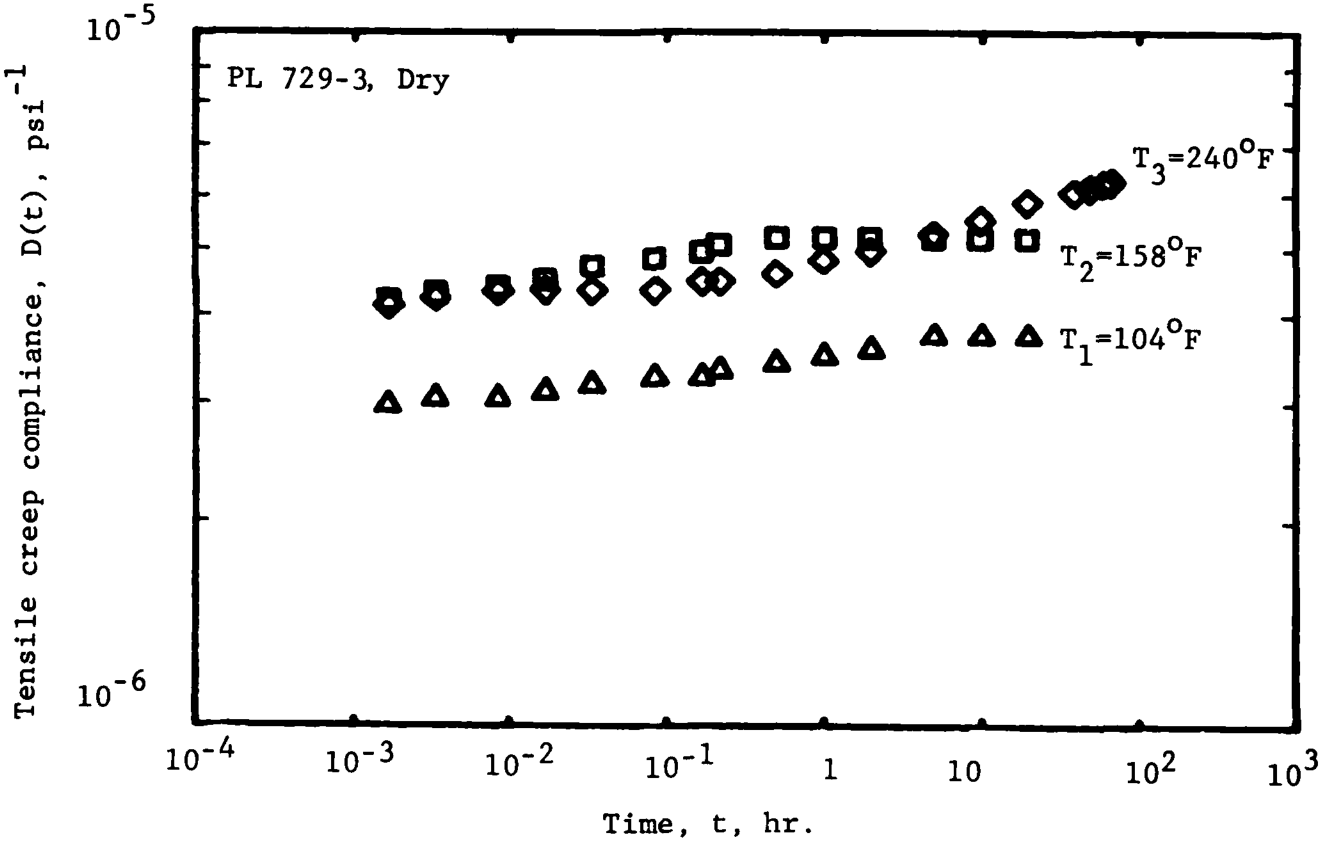

Figure A28 Tensile Creep Compliance of Dry PL 729-3

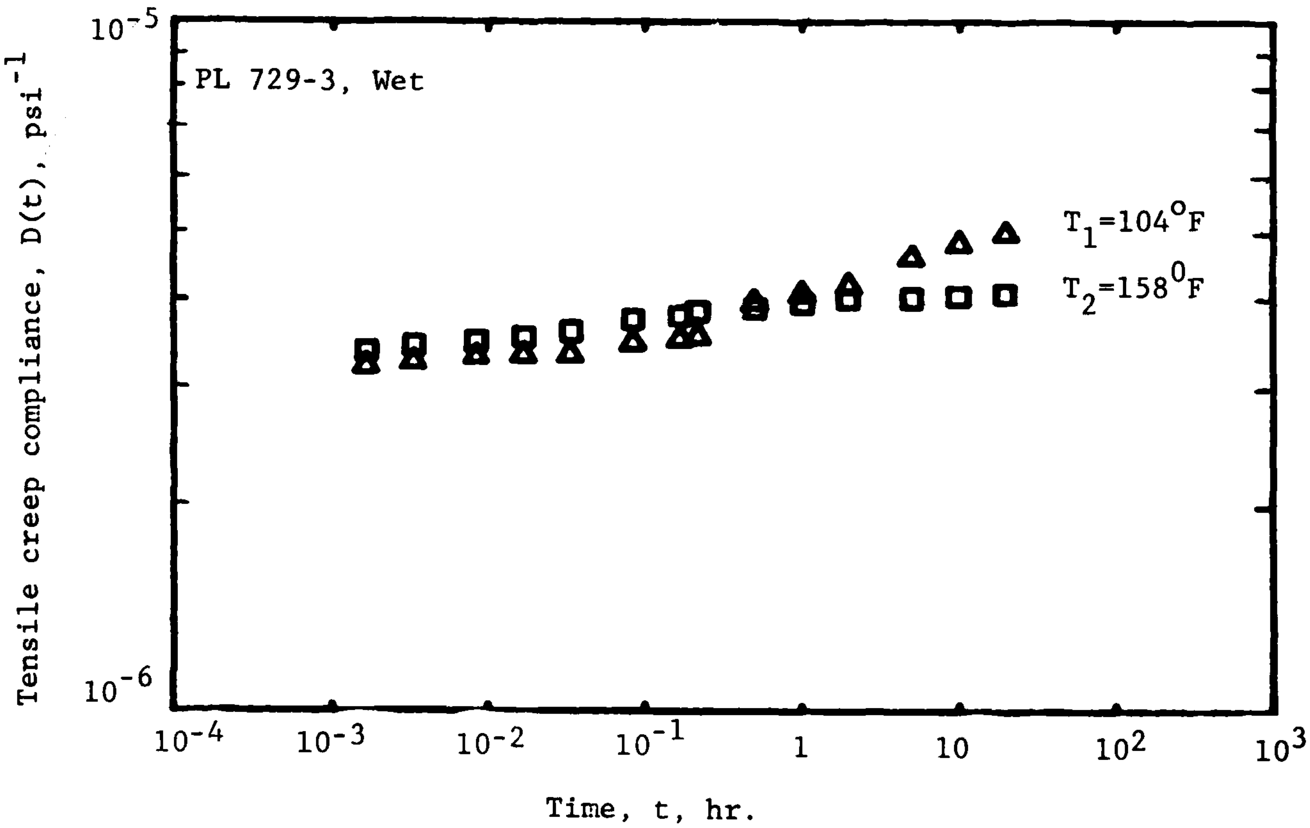

Figure A29 Tensile Creep Compliance of Wet PL 729-3

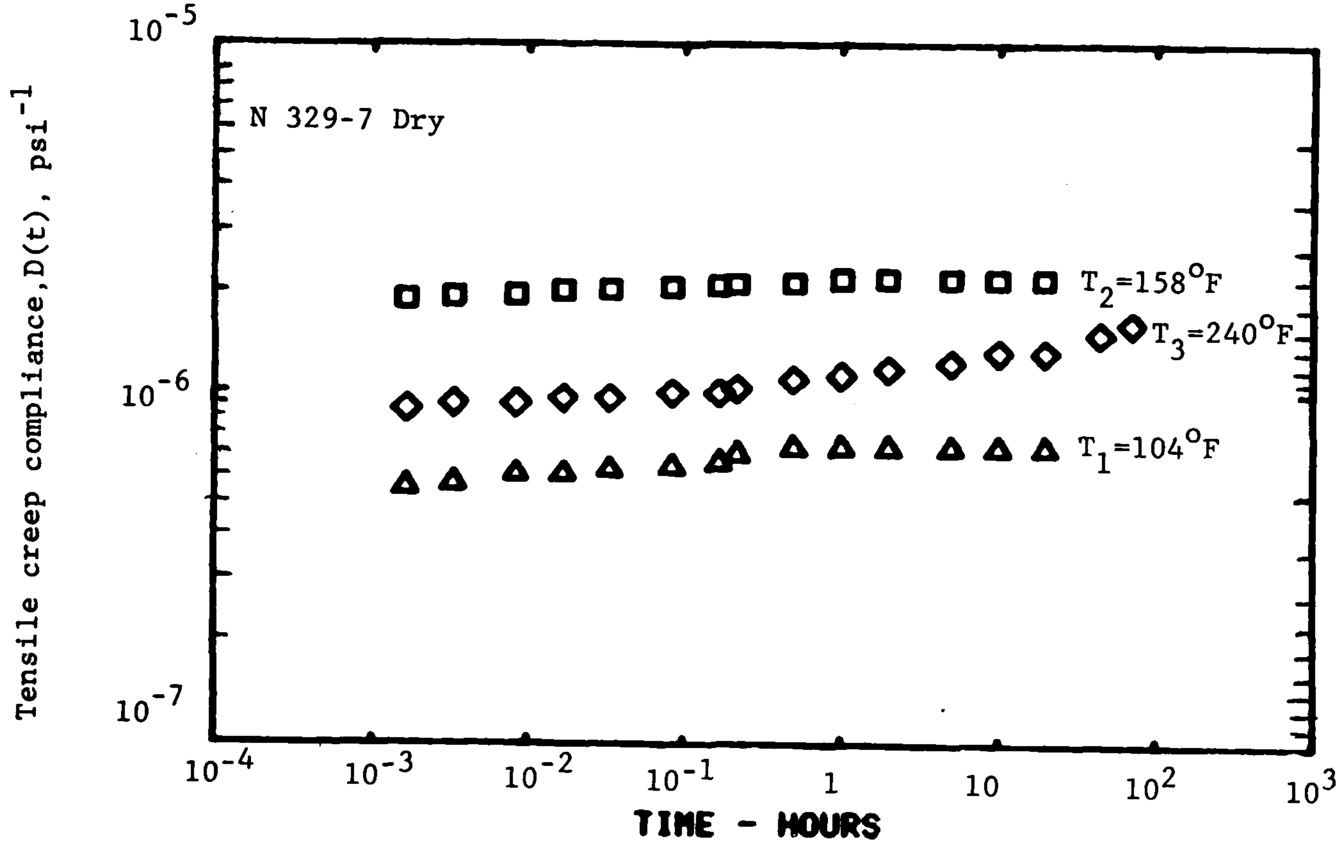

Figure A30 Tensile Creep Compliance of Dry N 329-7

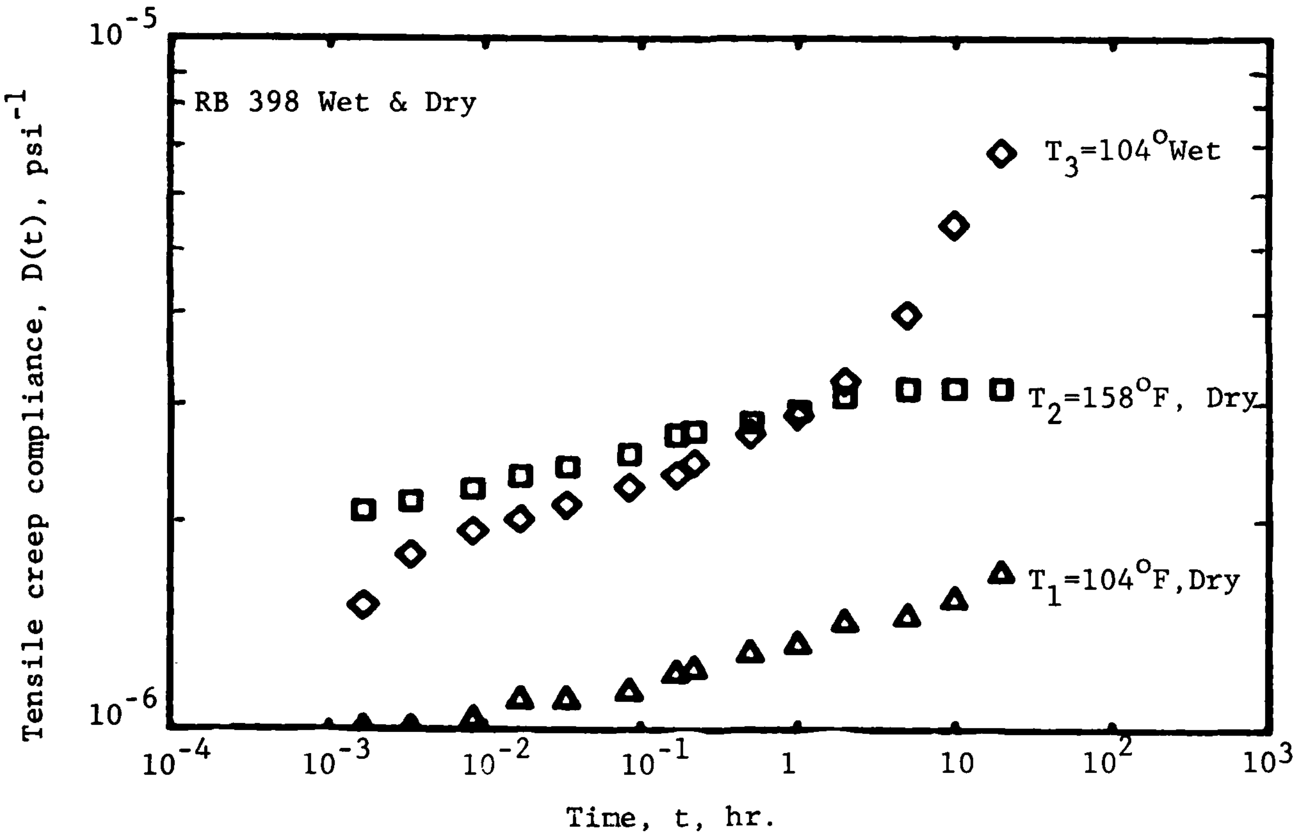

Figure A31 Tensile Creep Compliance of Dry and Wet RB 398

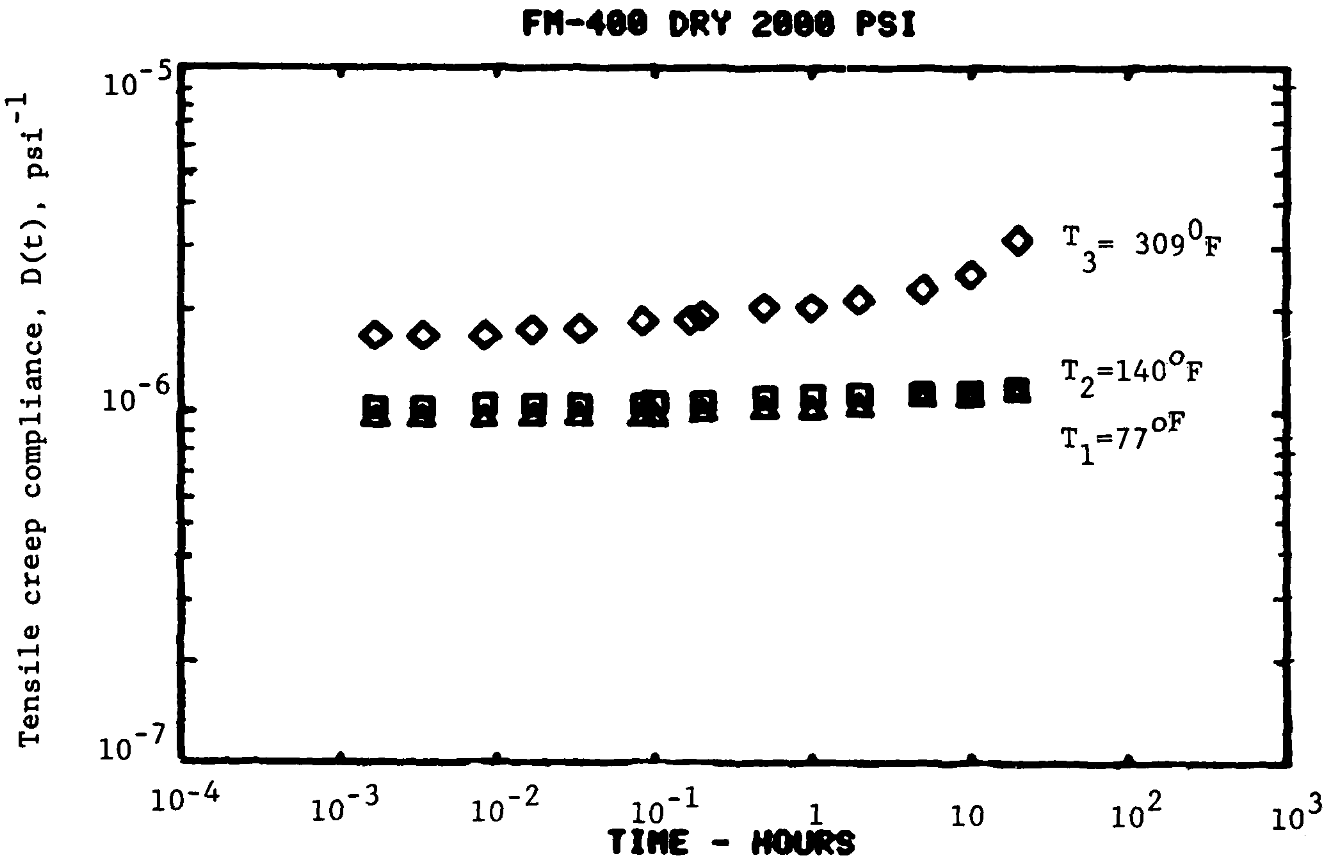

Figure A32 Tensile Creep Compliance of Dry FM-400

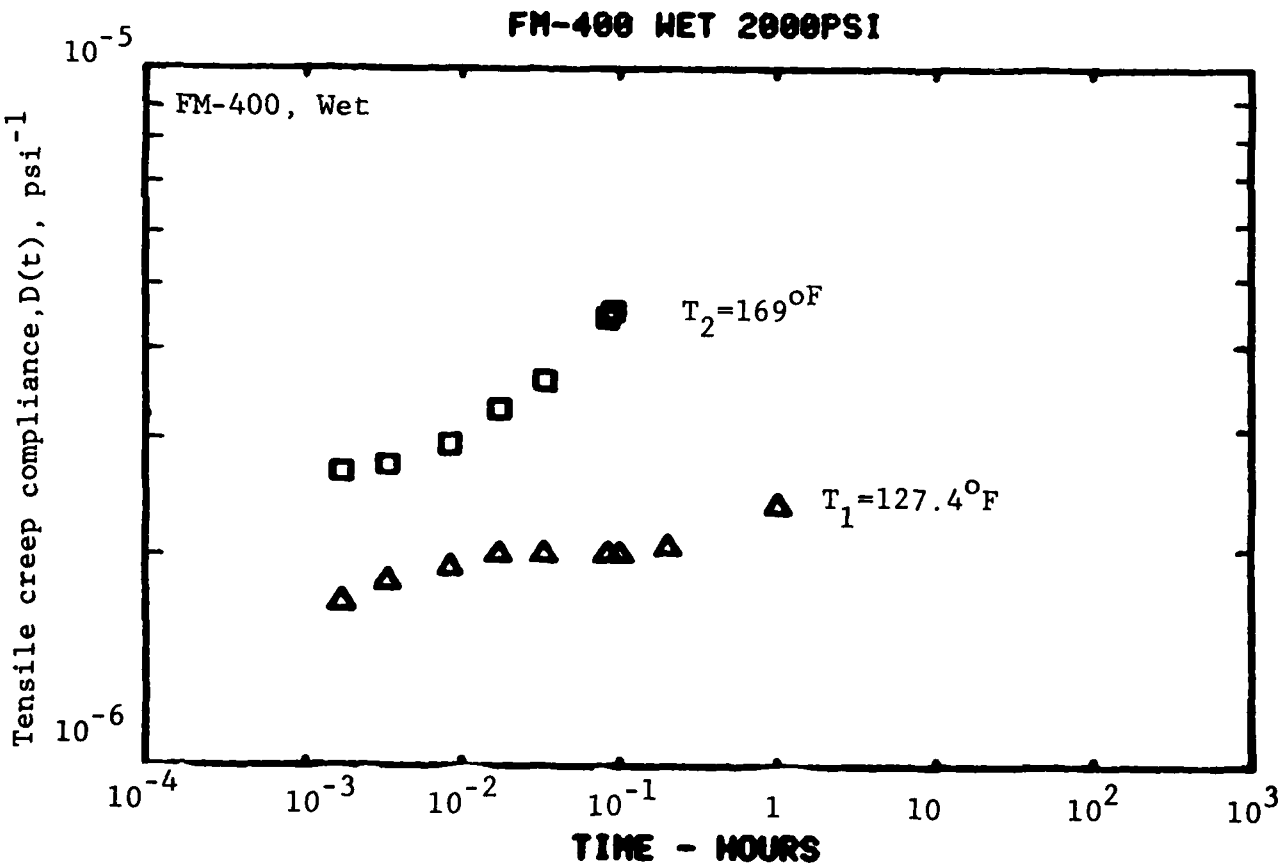

Figure A33 Tensile Creep Compliance of Wet FM-400

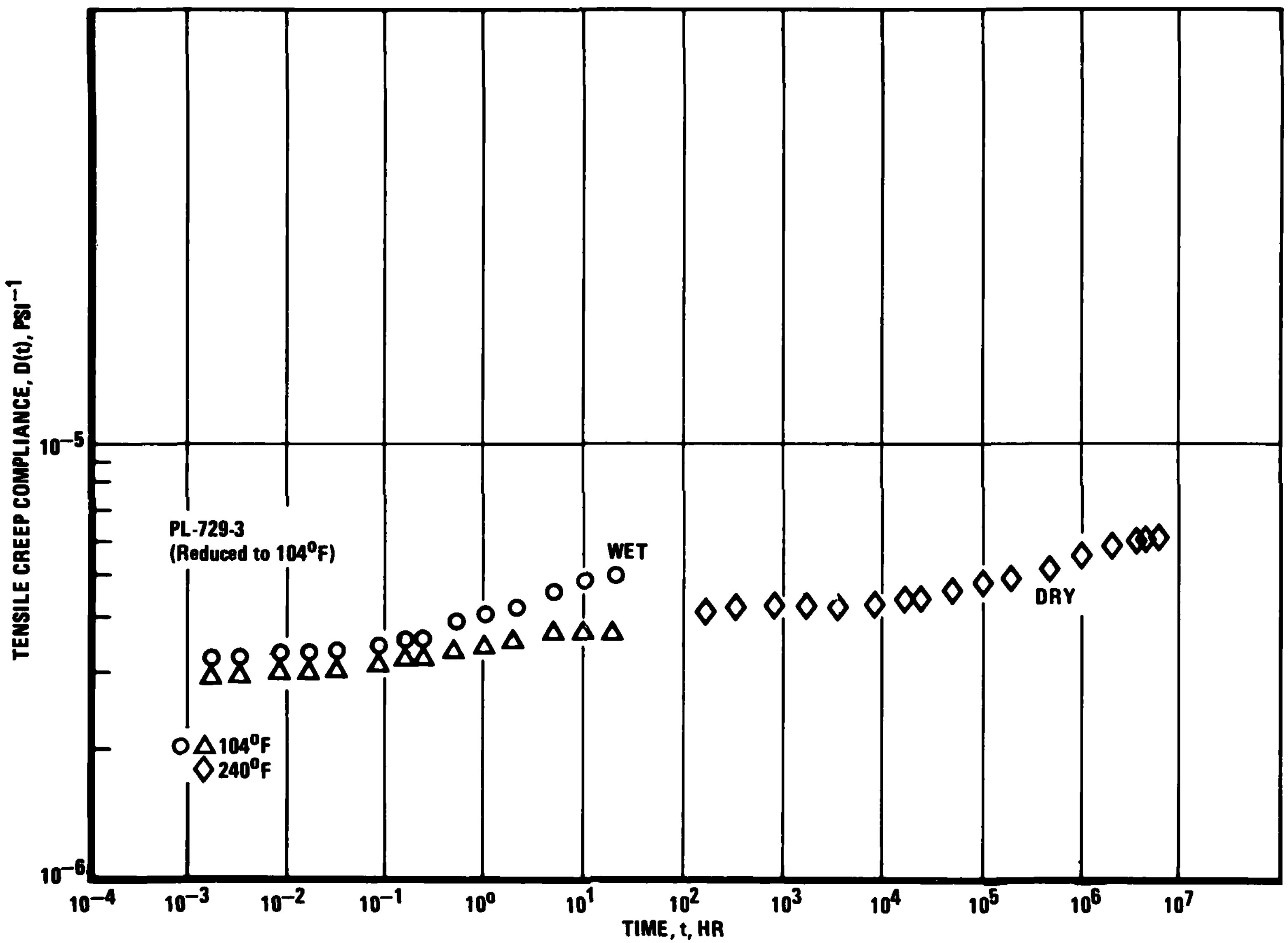

Figure A34 Tensile Creep Compliance of PL 729-3, Dry and Wet, (Reduced to 104°F)

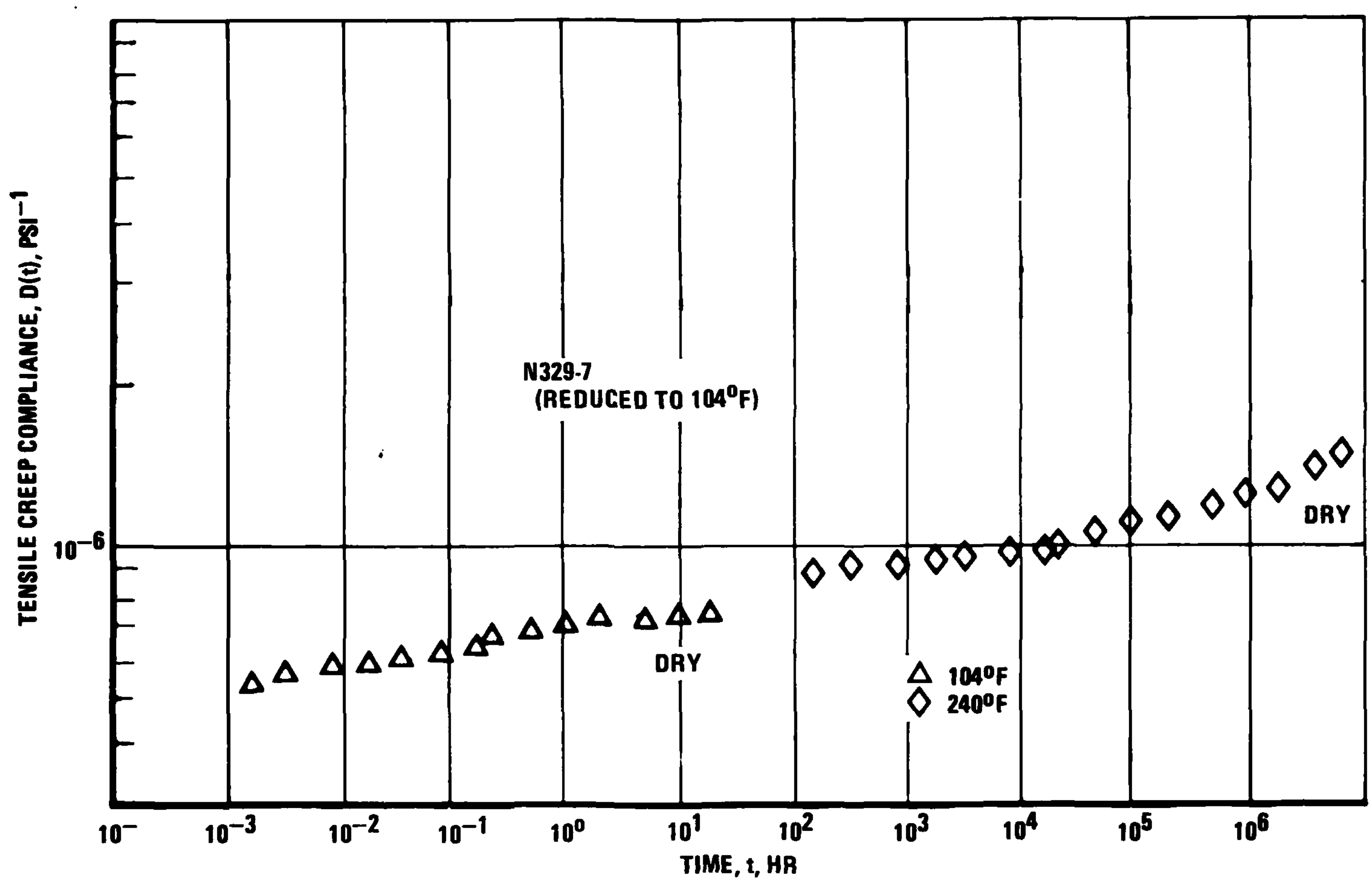

Figure A35 Tensile Creep Compliance of Dry N 329-7 (Reduced to 104°F)

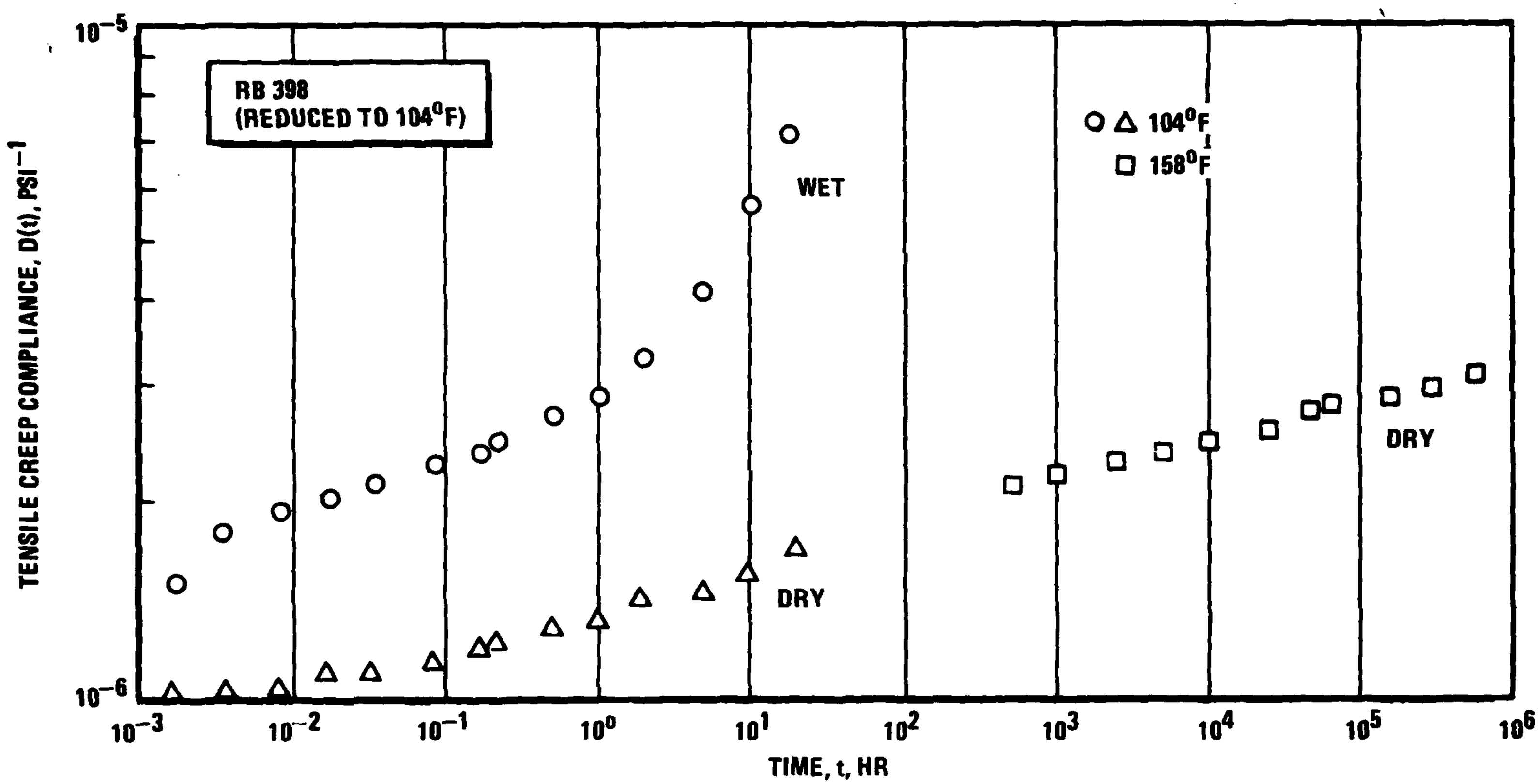

Figure A36 Tensile Creep Compliance of RB-398, Dry and Wet, (Reduced to 104°F)

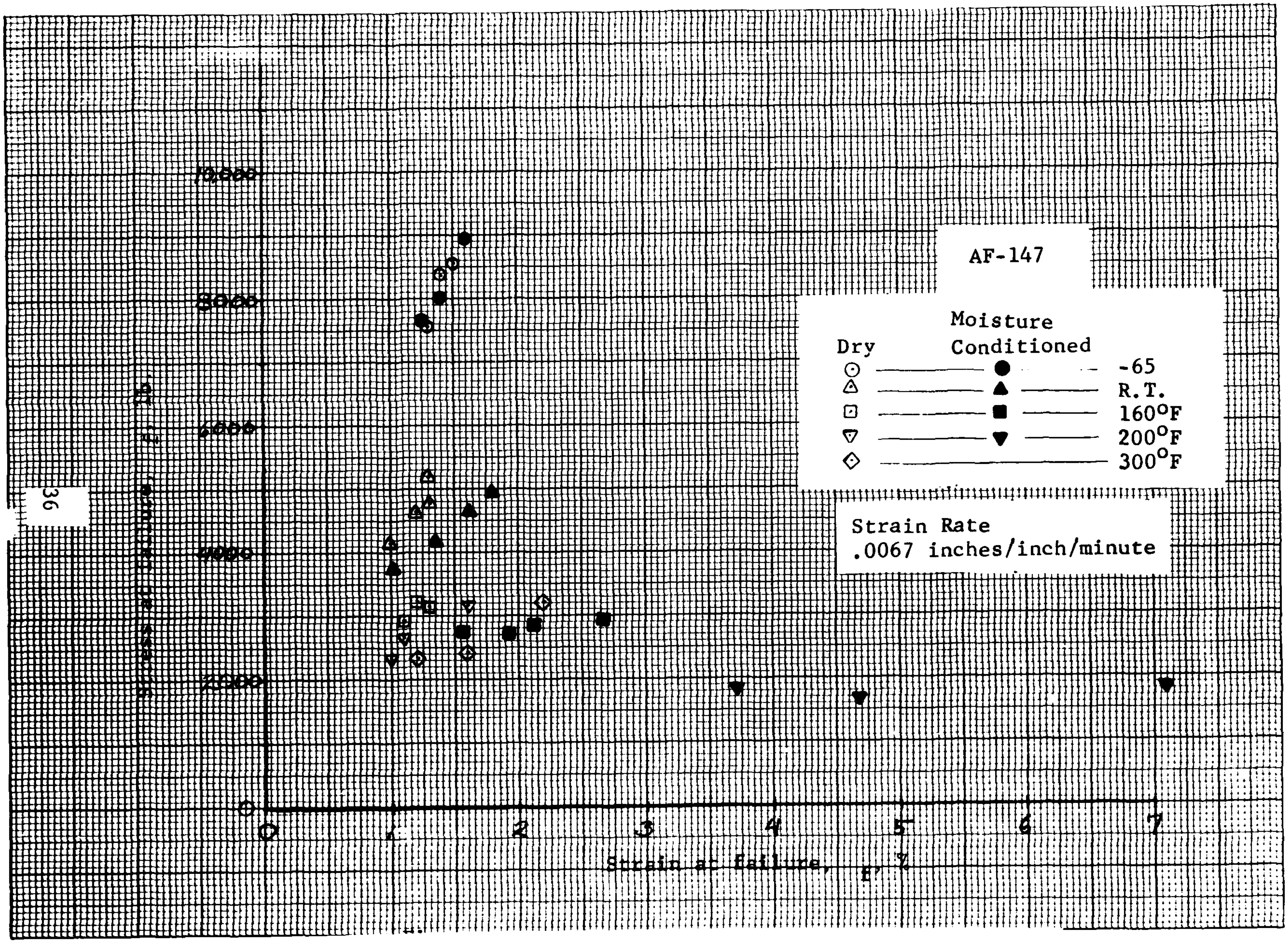

Figure A37 Smith Plots for AF-147 Adhesive

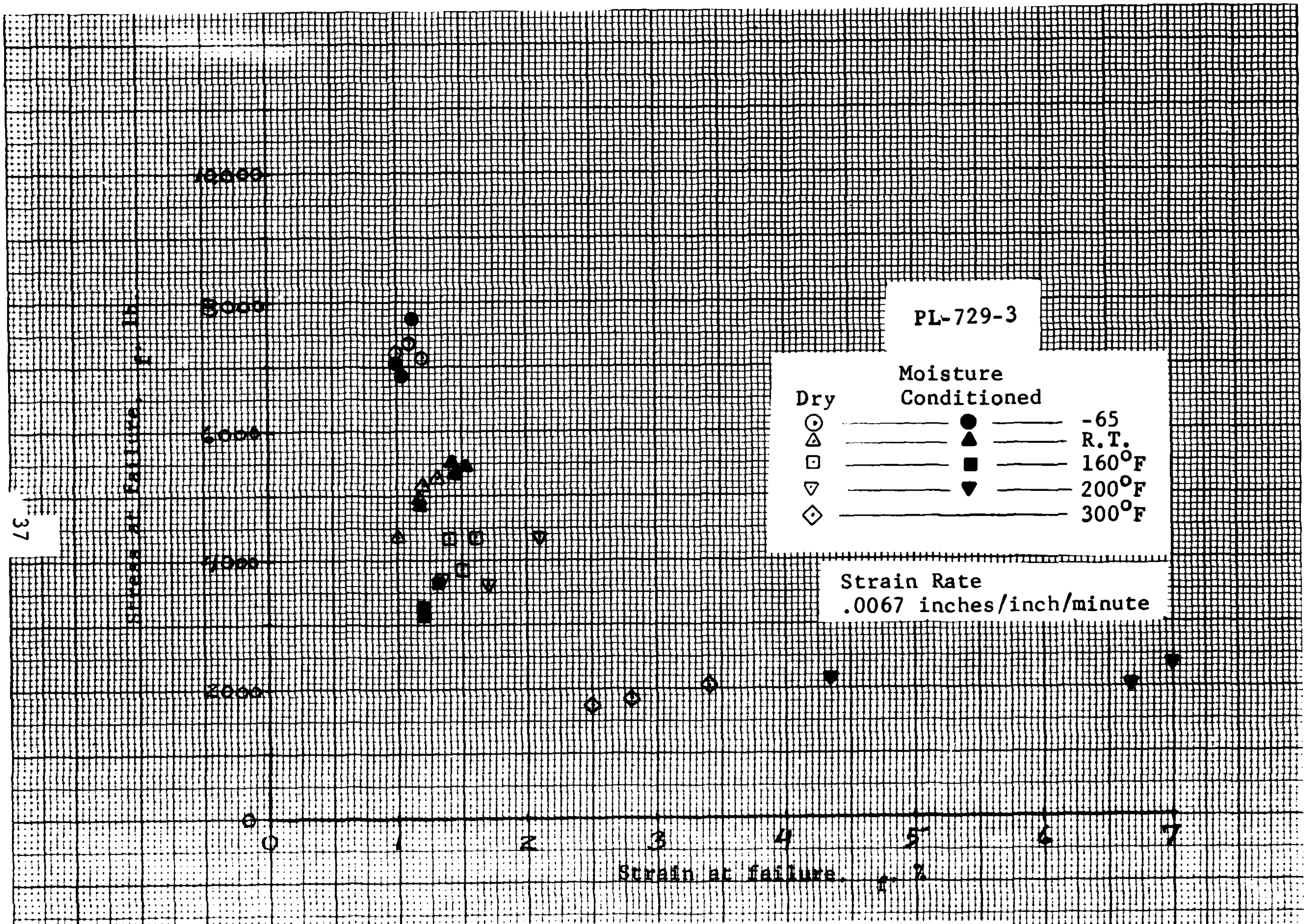

Figure A38 Smith Plots for PL-729-3 Adhesive

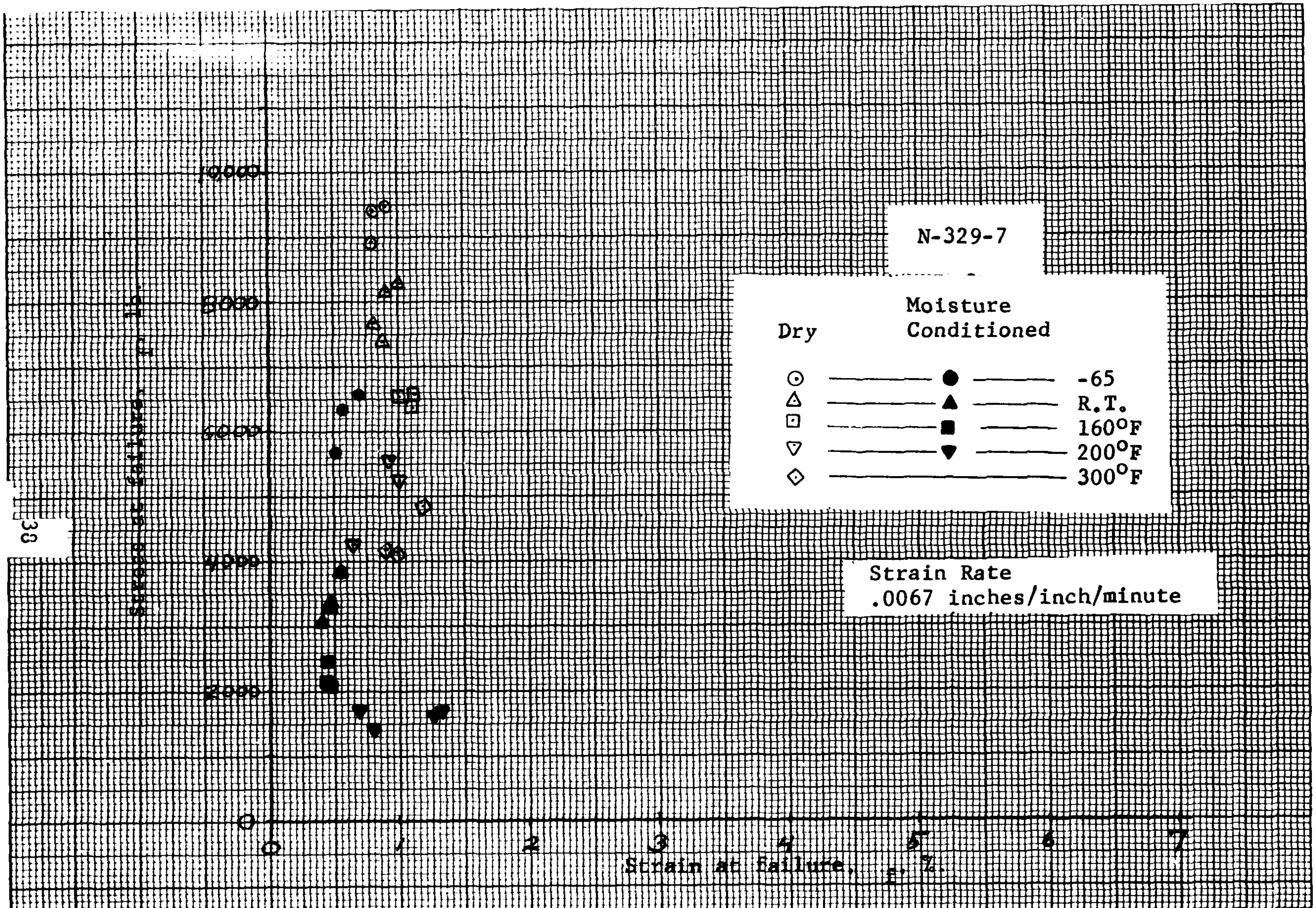

Figure A39 Smith Plots for N-329-7 Adhesive

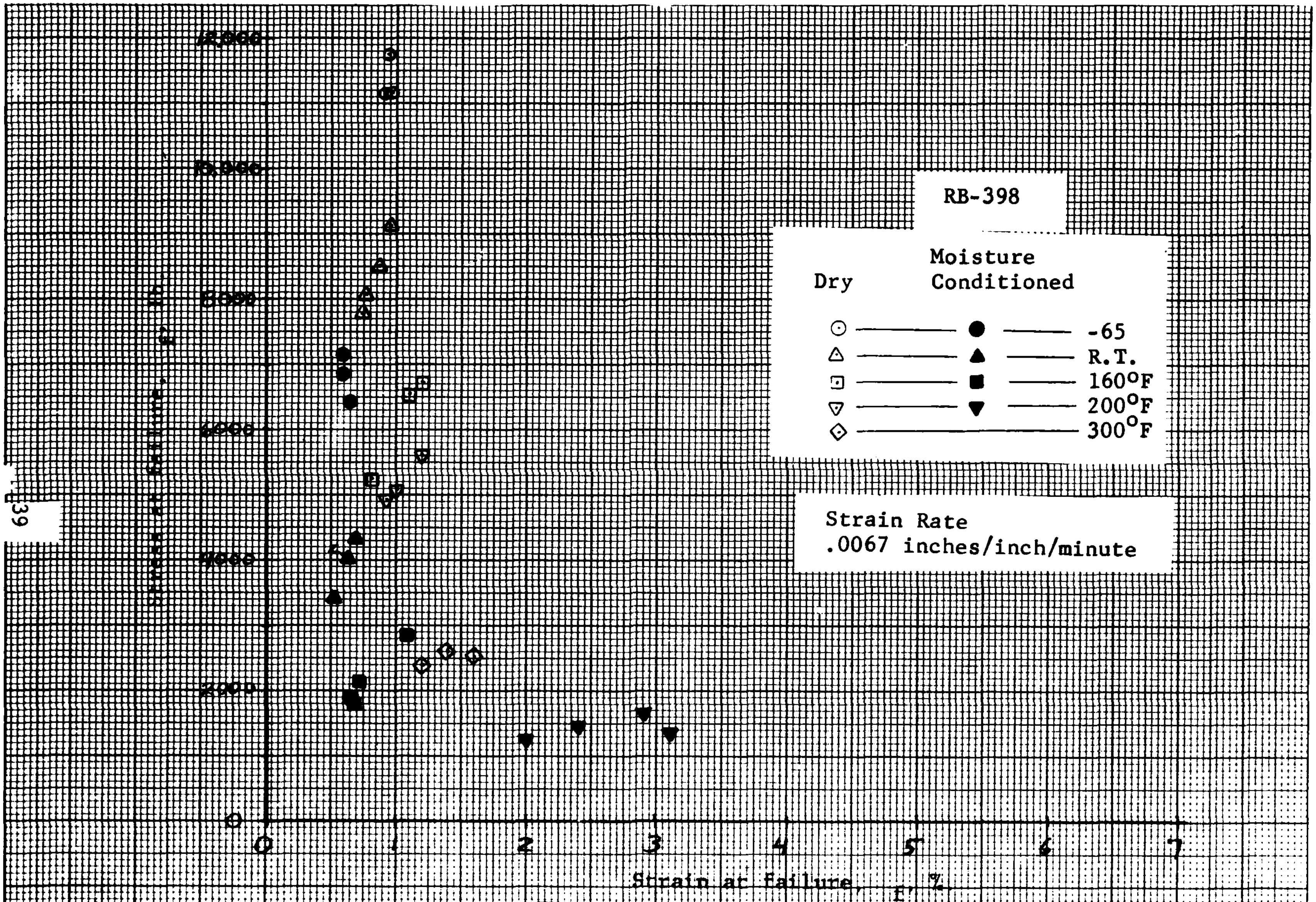

Figure A40 Smith Plots for RB-398 Adhesive

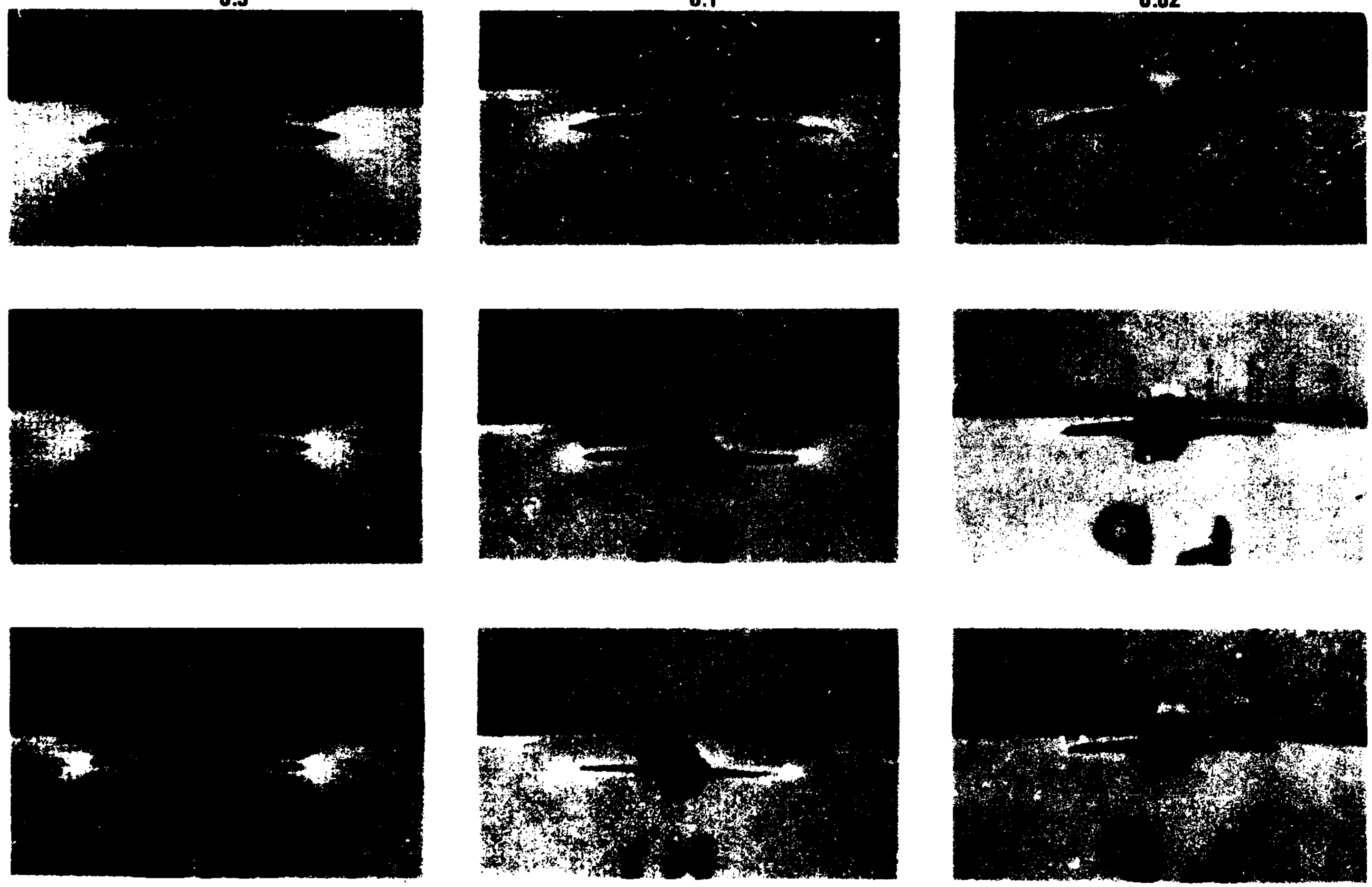

Figure A41 Crack Shape at Selected Crack Lengths of Fracture Mechanics FM-73M Neat Adhesive Specimens Tested Dry at 140°F

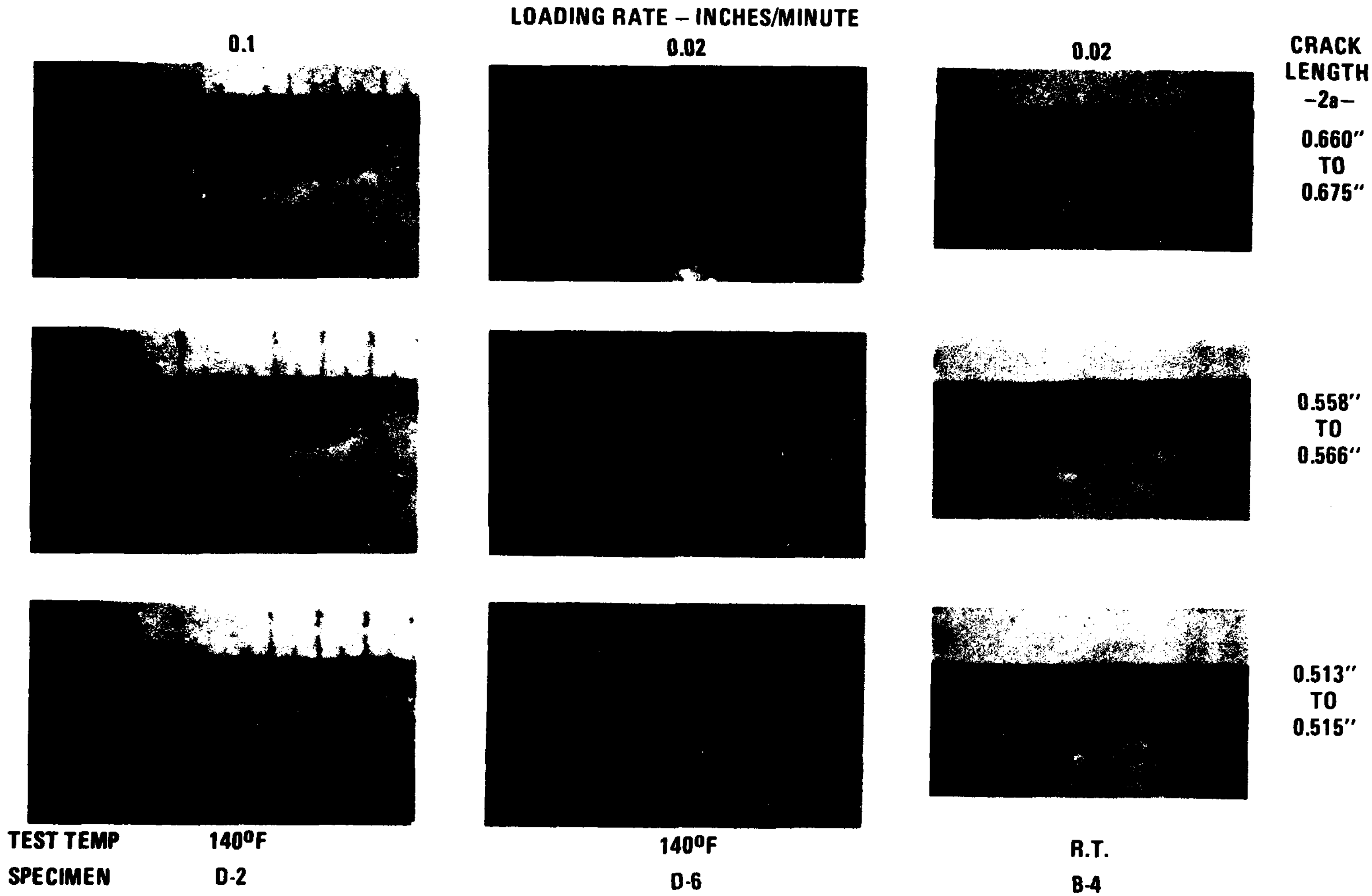

Figure A42 Crack Shapes at Selected Crack Lengths of Moisture Conditioned FM-73M Neat Adhesive Specimens Tested at Room Temperature and 140°F

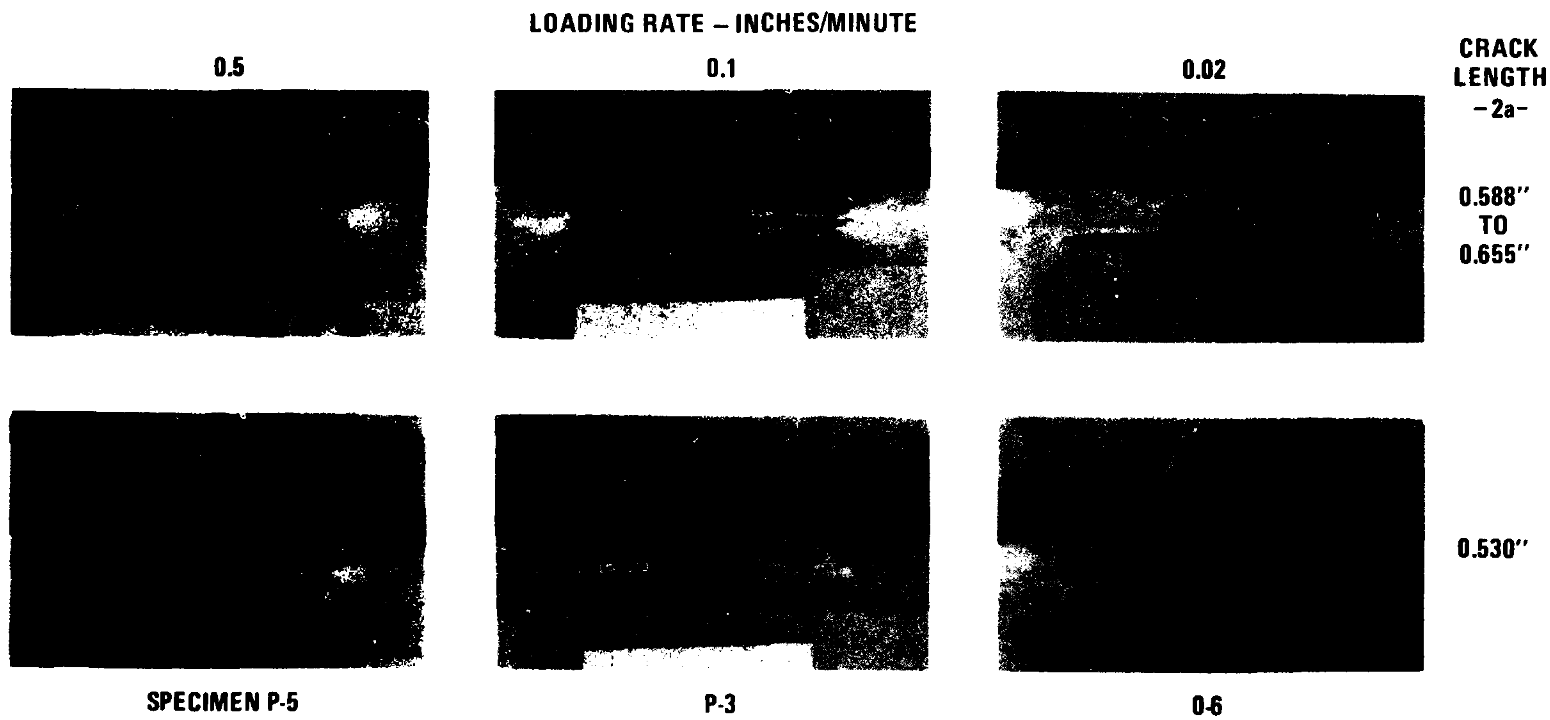

Figure A43 Crack Shape at Selected Crack Lengths of Fracture Mechanics FM-73M Neat Adhesives Specimens Tested Dry at Room Temperature

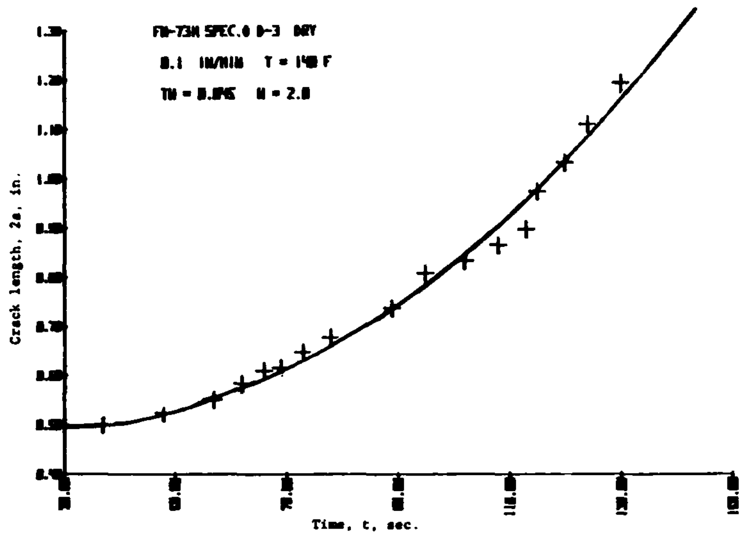

Figure A44 Crack Growth in Wet FM-73M at 140°F

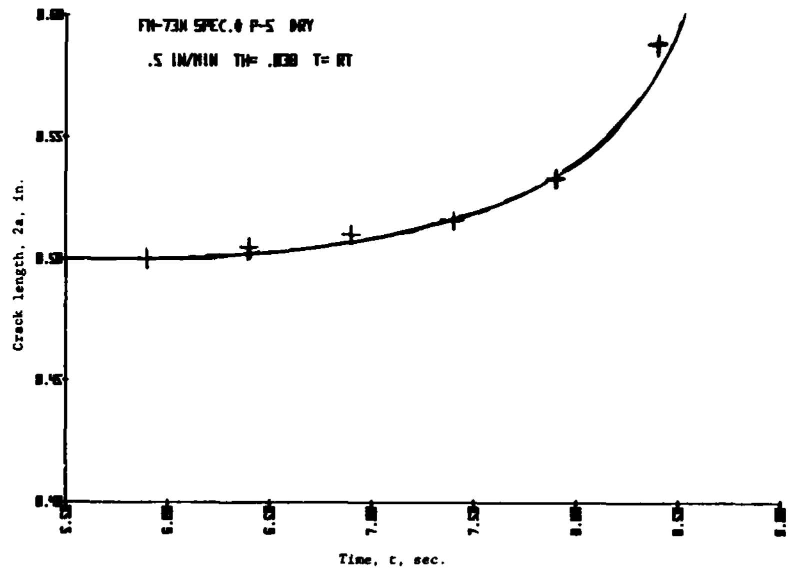

Figure A45 Crack Growth in Dry FM-73M at 75°F

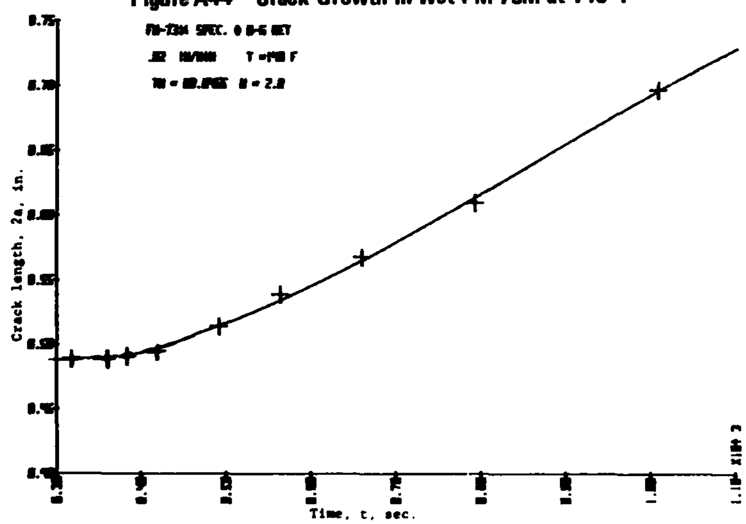

Figure A46 Crack Growth in Wet FM-73M at 140°F (2)

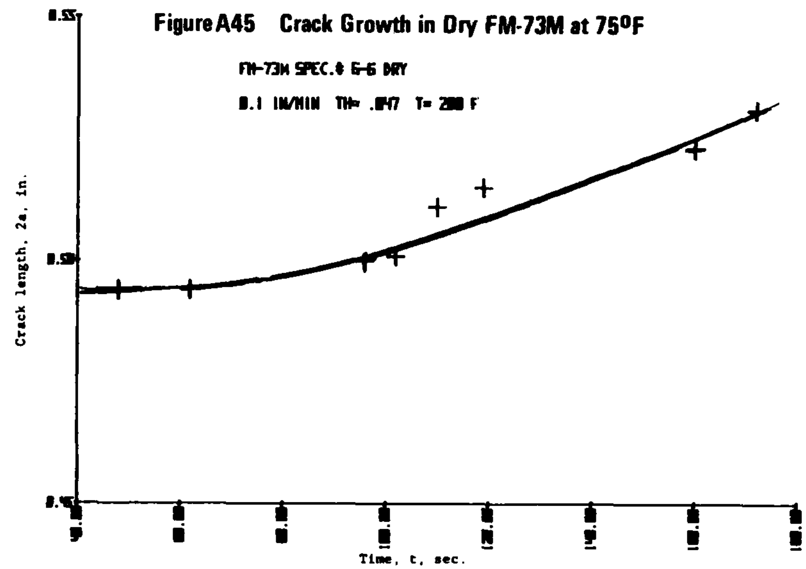

Figure A47 Crack Growth in Dry FM-73M at 200°F

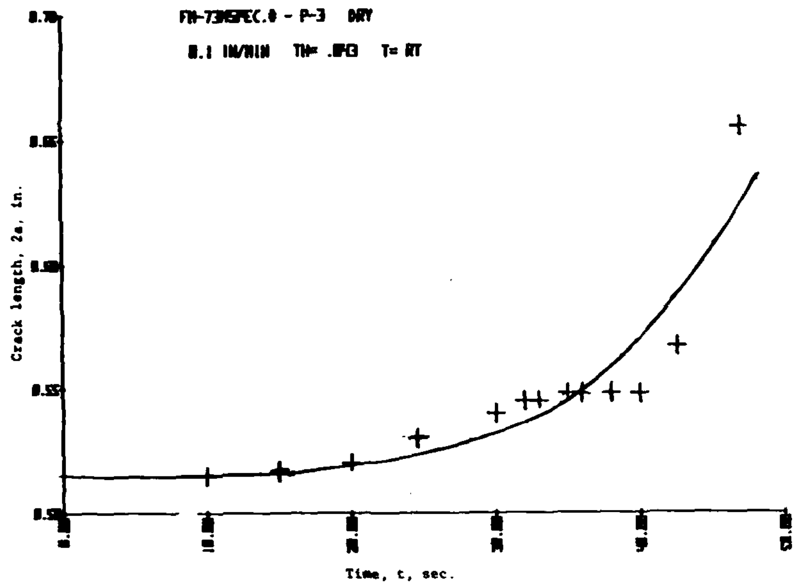

Figure A48 Crack Growth in Dry FM-73M at 75°F (2)

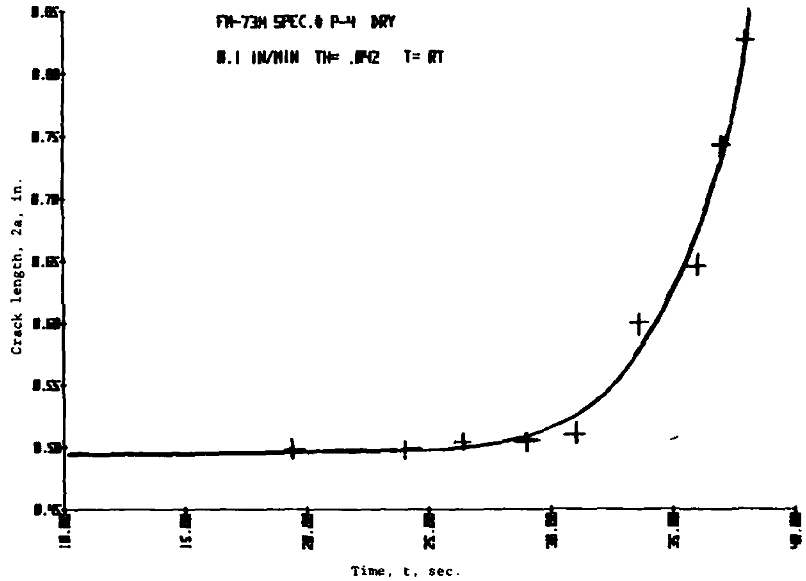

Figure A49 Crack Growth in Dry FM-73M at 75°F (3)

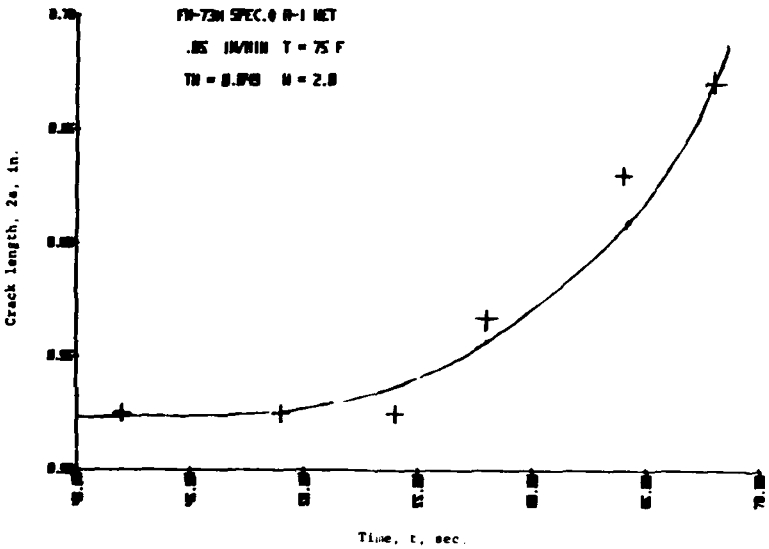

Figure A50 Crack Growth in Wet FM-73M at 75°F

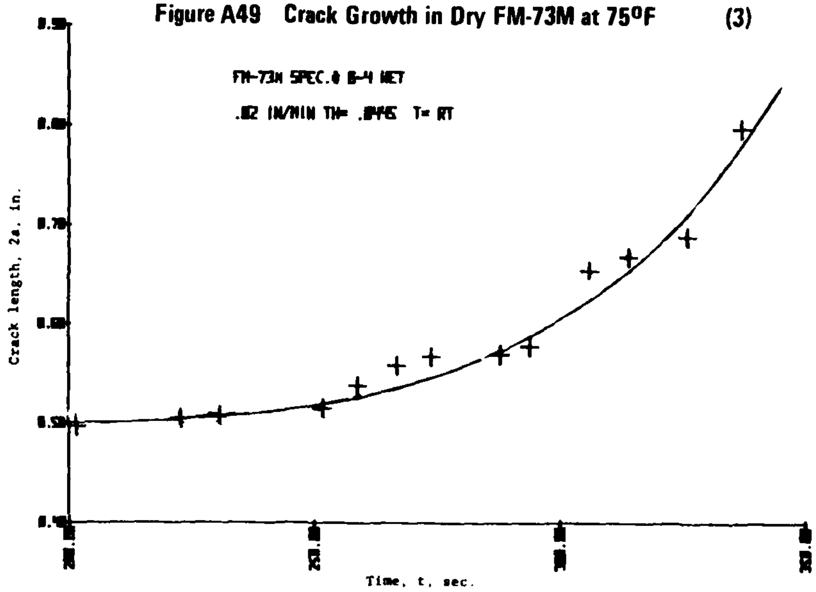

Figure A51 Crack Growth in Wet FM-73M at 75°F (2)

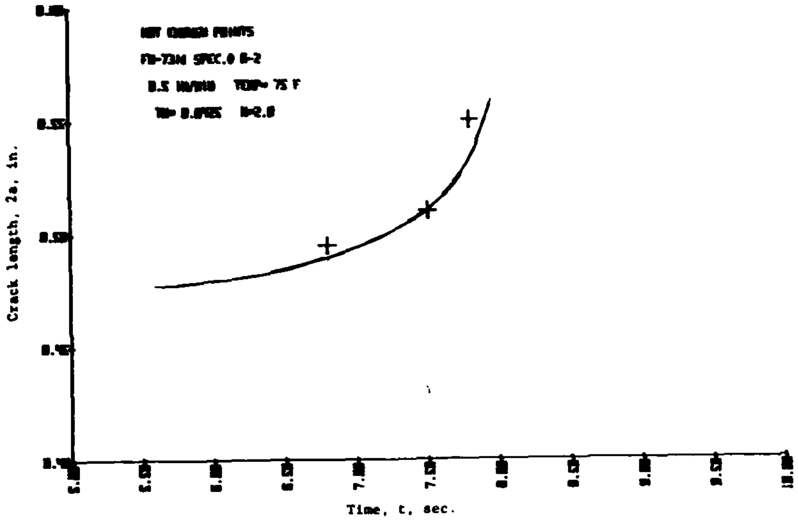

Figure A52 Crack Growth in Dry FM-73M at 75^{0}F (4)

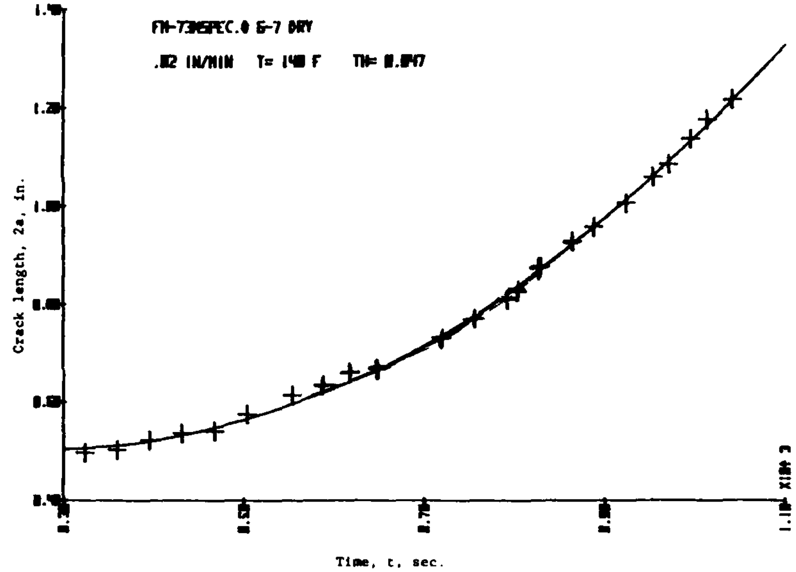

Figure A53 Crack Growth in Dry FM-73M at 140^{0}F

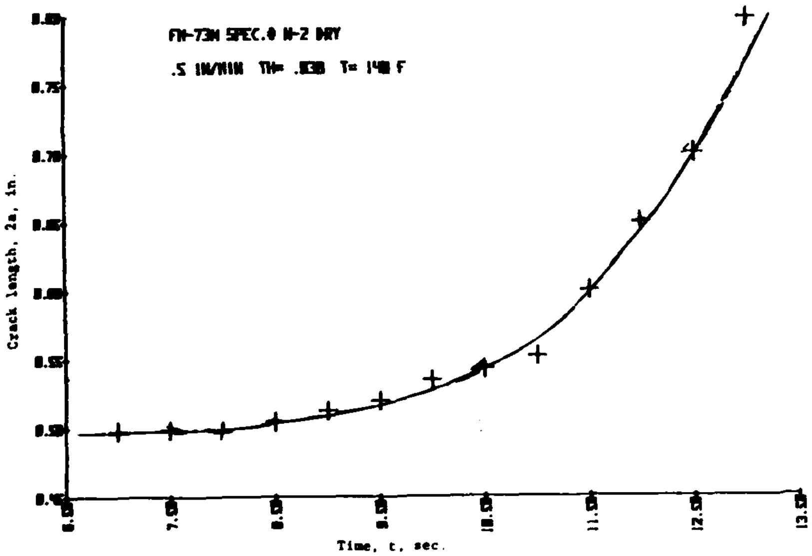

Figure A54 Crack Growth in Dry FM-73M at 140^{0}F (2)

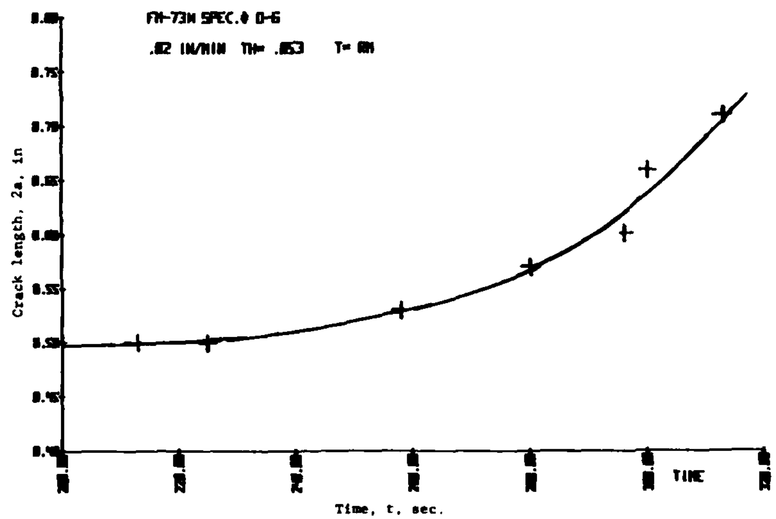

Figure A55 Crack Growth in Dry FM-73M at 75^{0}F (5)

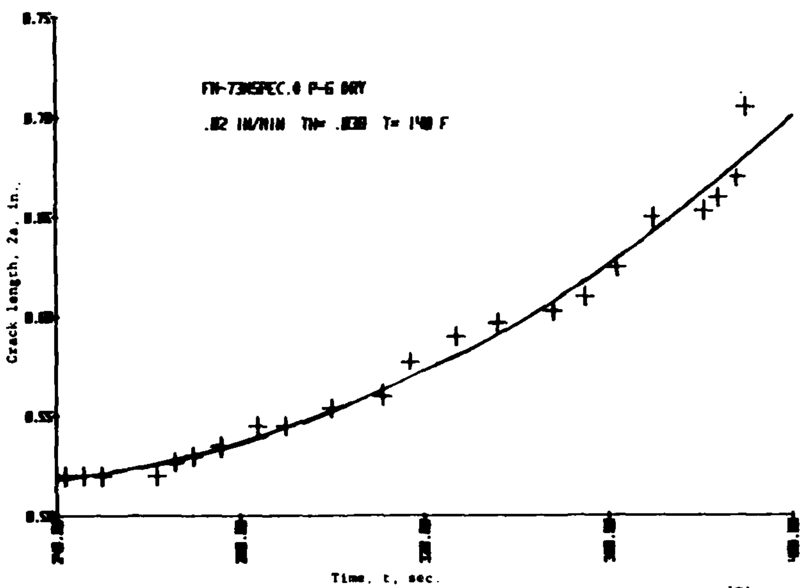

Figure A56 Crack Growth in Dry FM-73M at 140°F (2)

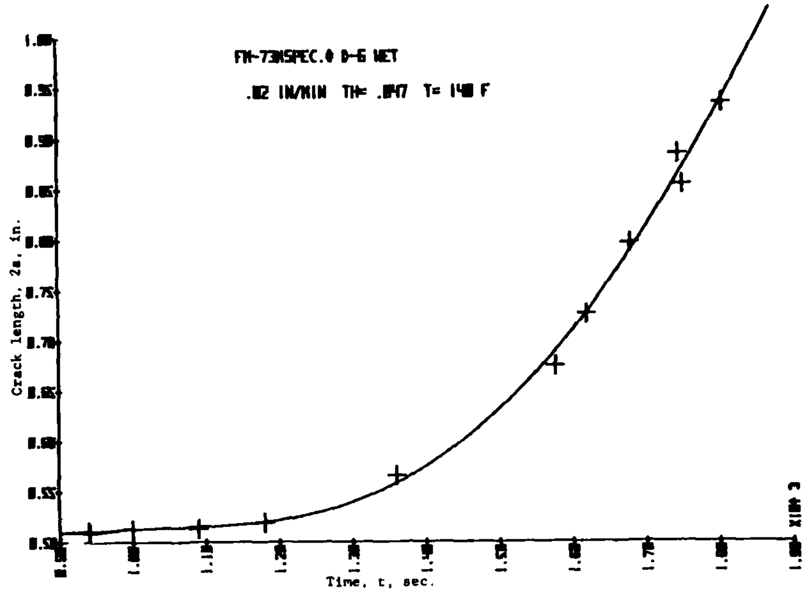

Figure A57 Crack Growth in Wet FM-73M at 140°F (3)

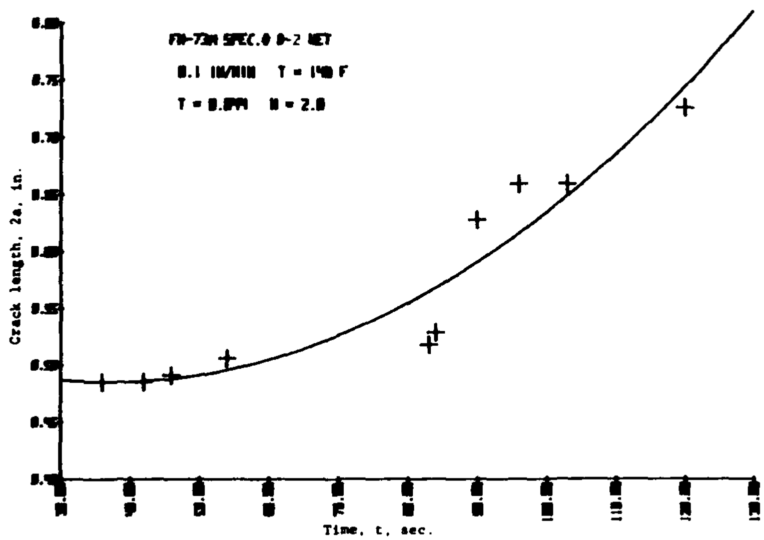

Figure A58 Crack Growth in Wet FM-73M at 140°F (4)

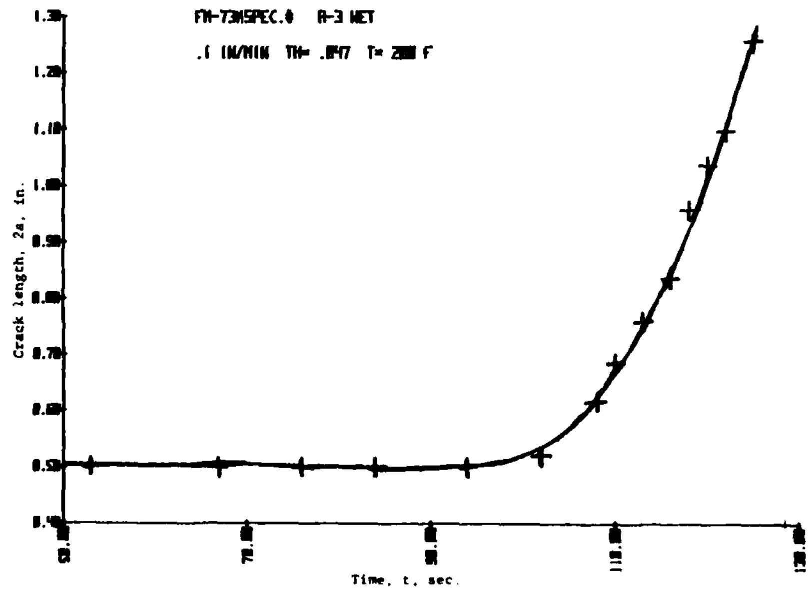

Figure A59 Crack Growth in Wet FM-73M at 200°F

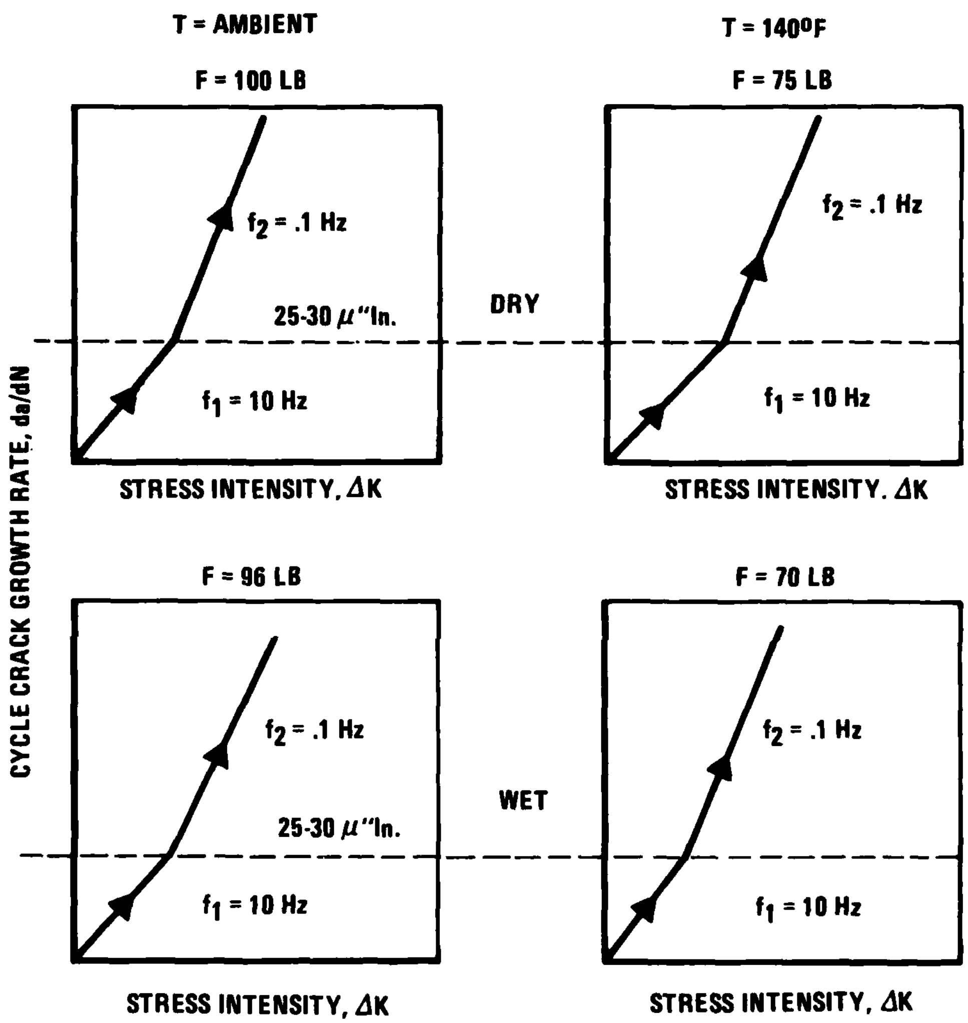

Figure A60 Cyclic Crack Growth Rate vs Stress Intensity Test Plan

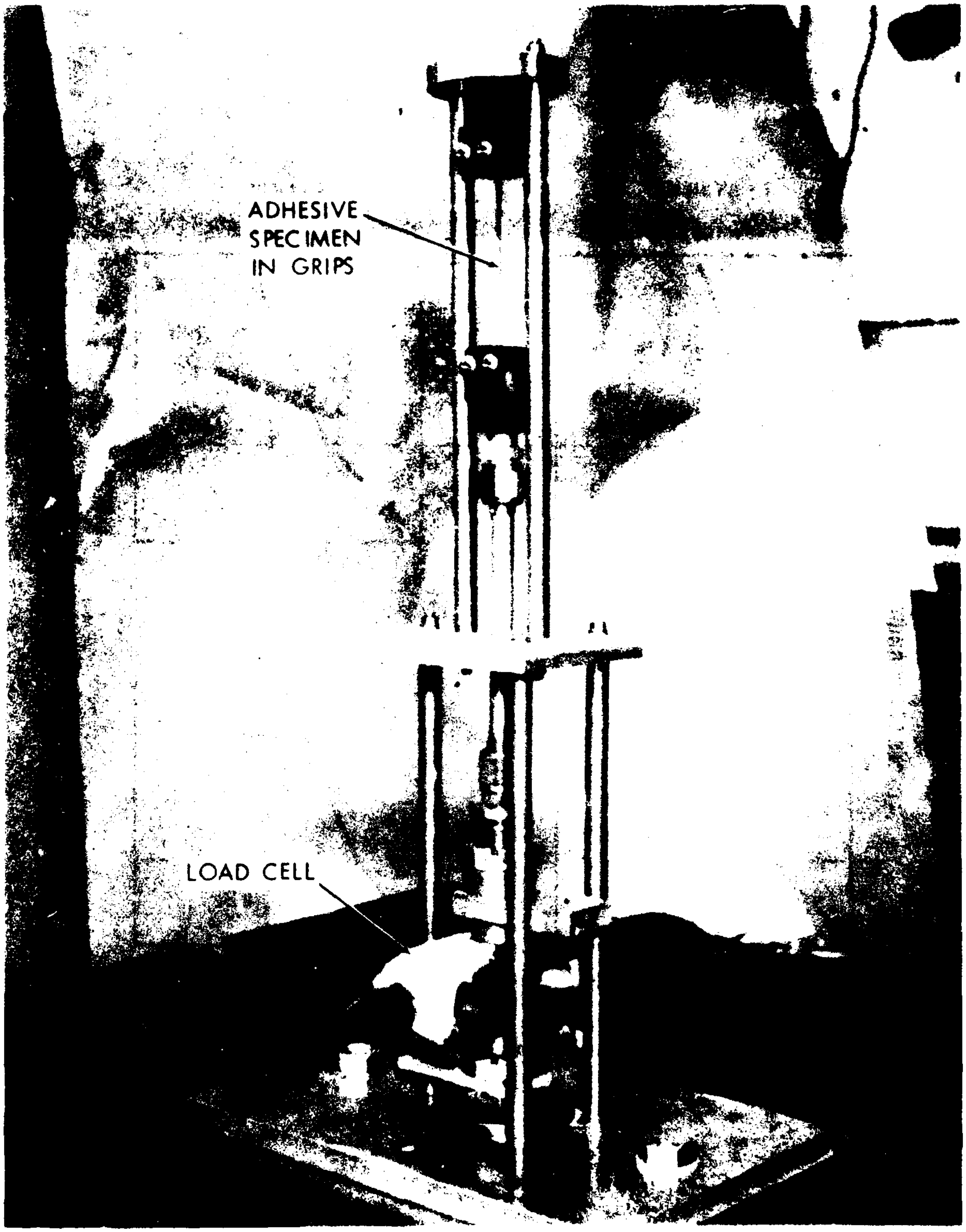

Figure A61 Loading Fixture for Fatigue Testing of Environmentally Conditioned Adhesive Materials

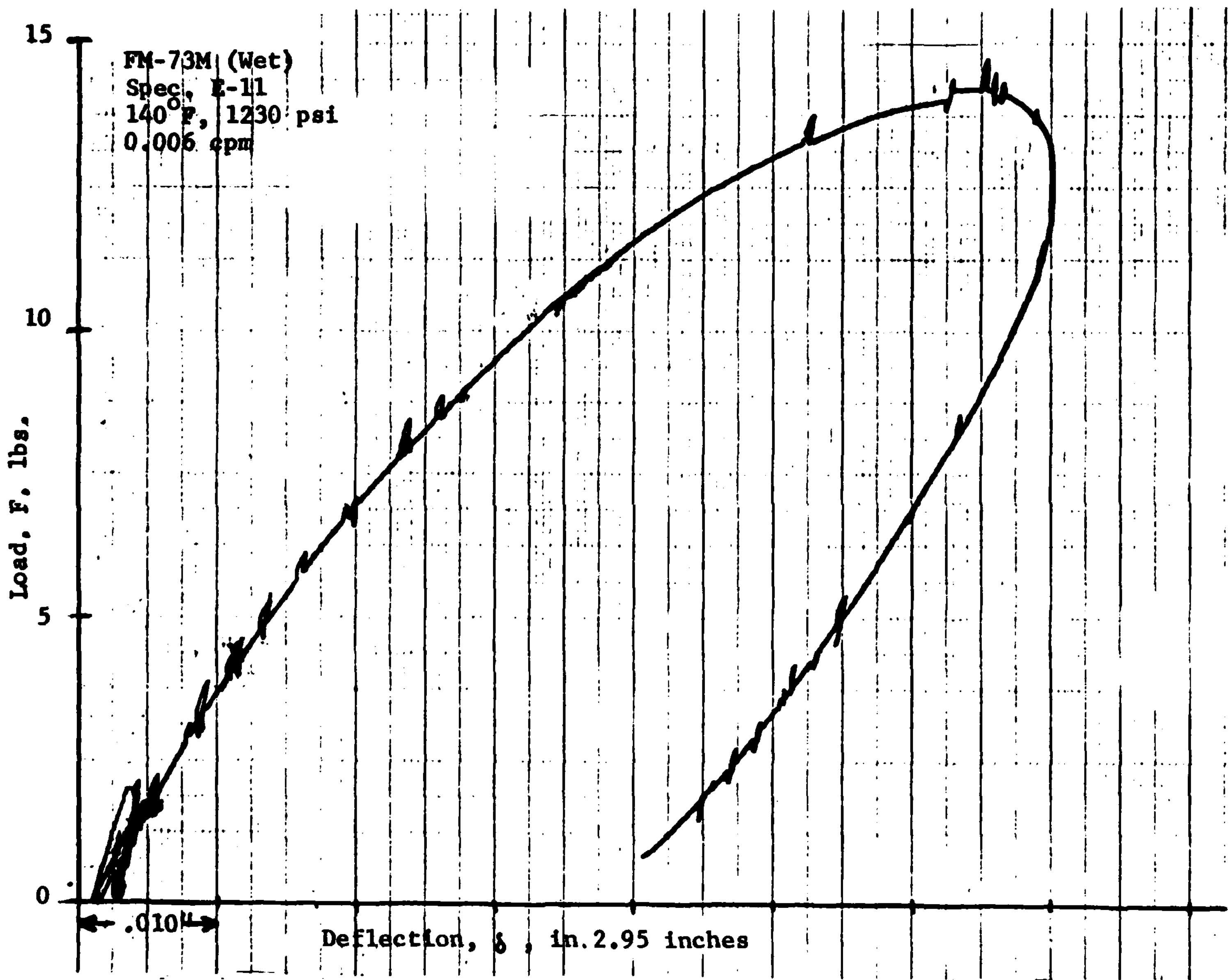

Figure A62 Load-Deflection History of Wet FM-73M Coupon, First Cycle of Loading and Unloading; Low Frequency

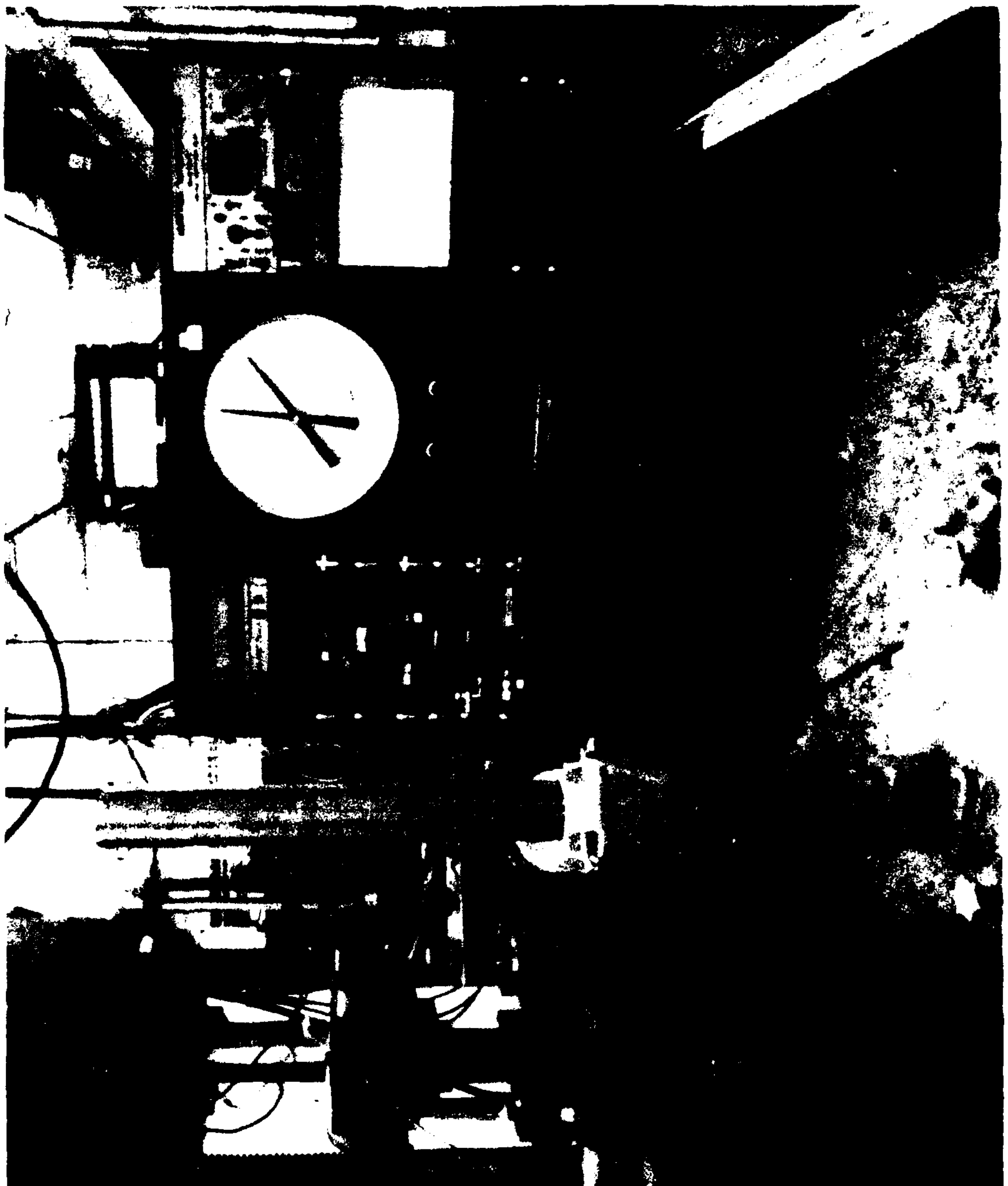

Figure A63 Fatigue Testing Equipment for Model Lap Shear Joints

Figure A64 FM-73M Adhesive Interlayer of Model Joint 12C11 After Adherend Etching, 10K Cycles

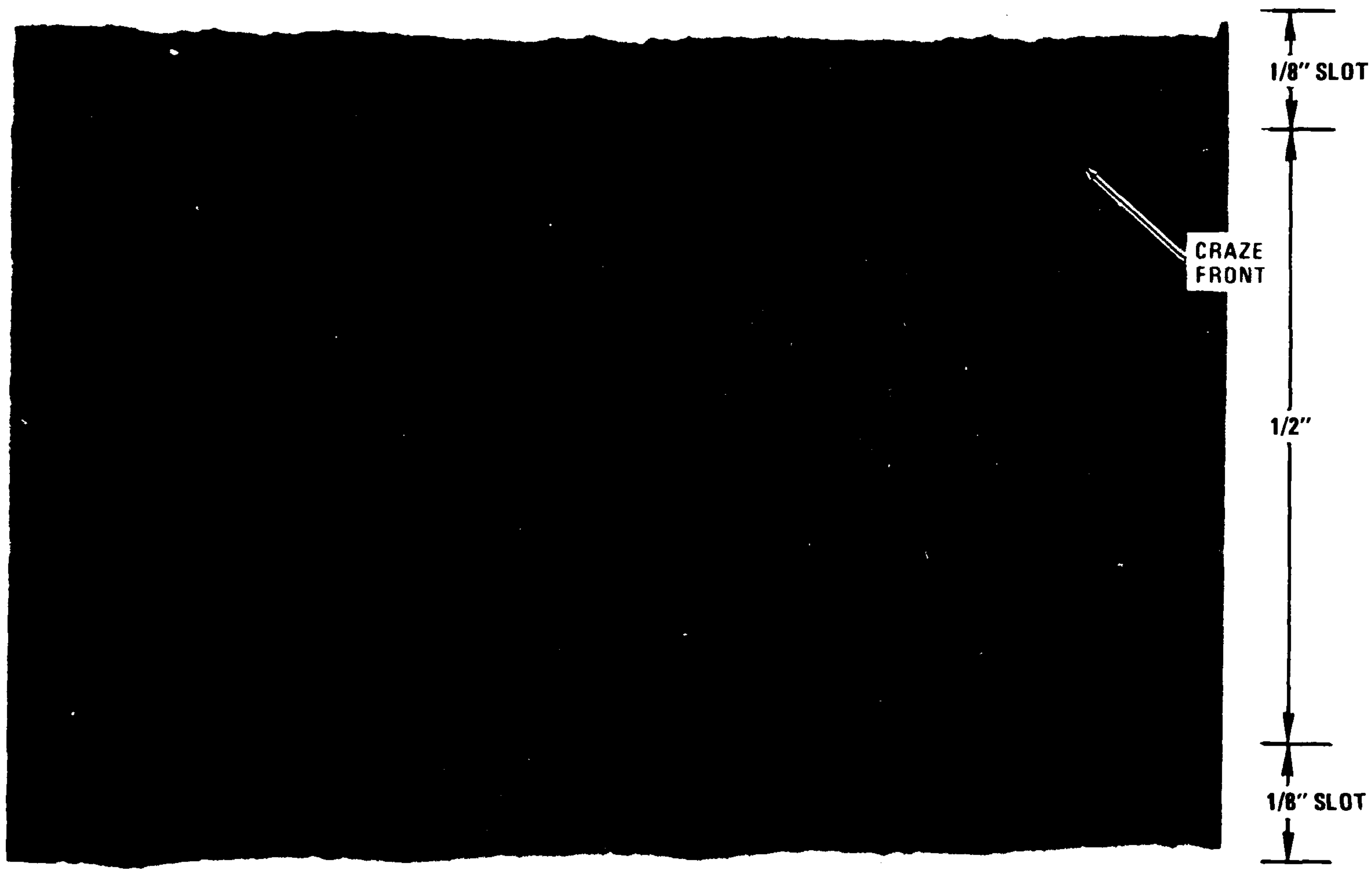

Figure A65 FM-73M Adhesive Interlayer of Model Joint 10C12 After Adherend Etching, 15K Cycles

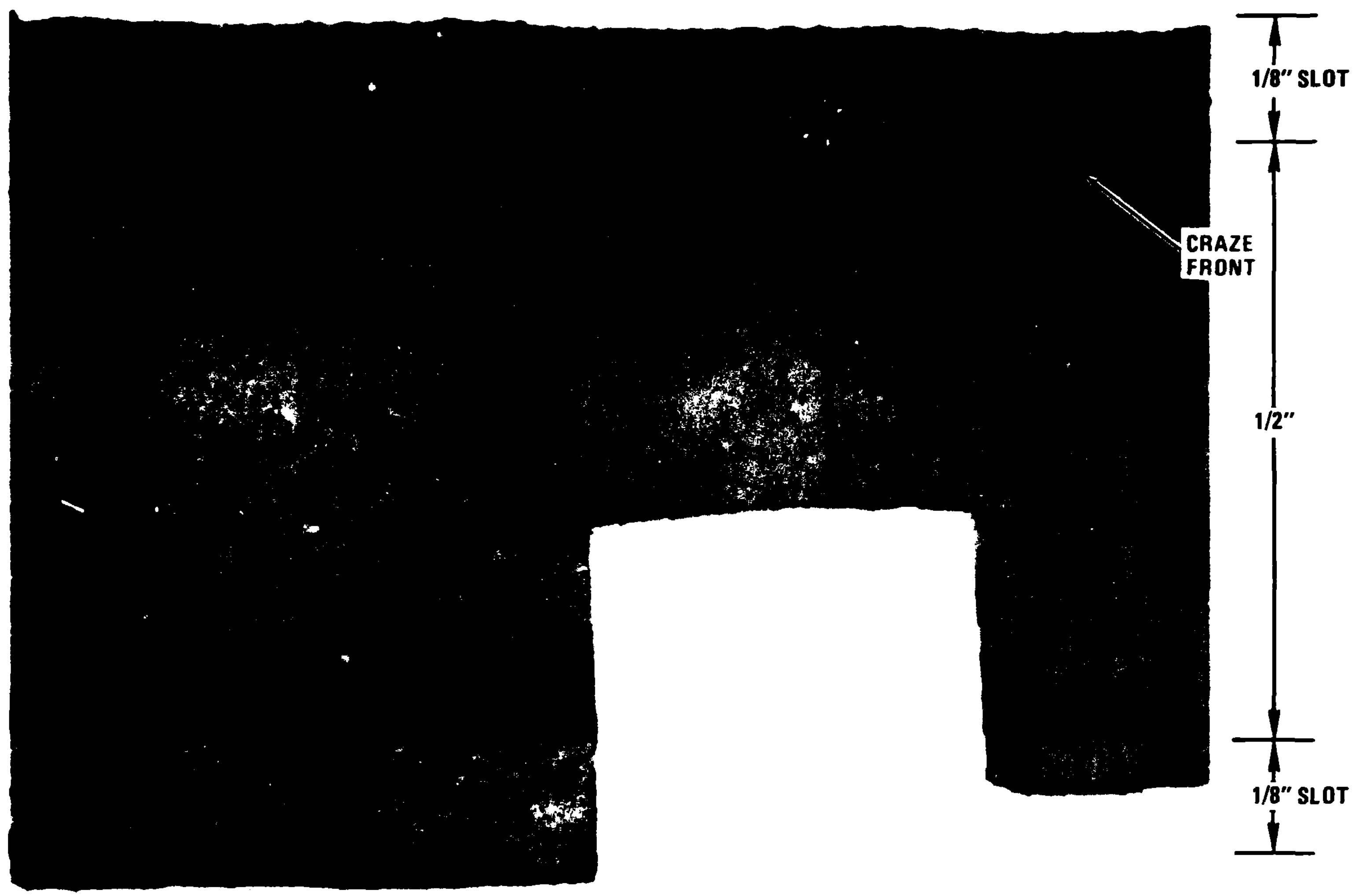

Figure A66 FM-73M Adhesive Interlayer of Model Joint 12C12 After Adherend Etching, 20K Cycles

Figure A67 FM-73M Adhesive Interlayer of Failed Model Joint 3C10 After Adherend Etching, 27K Cycles

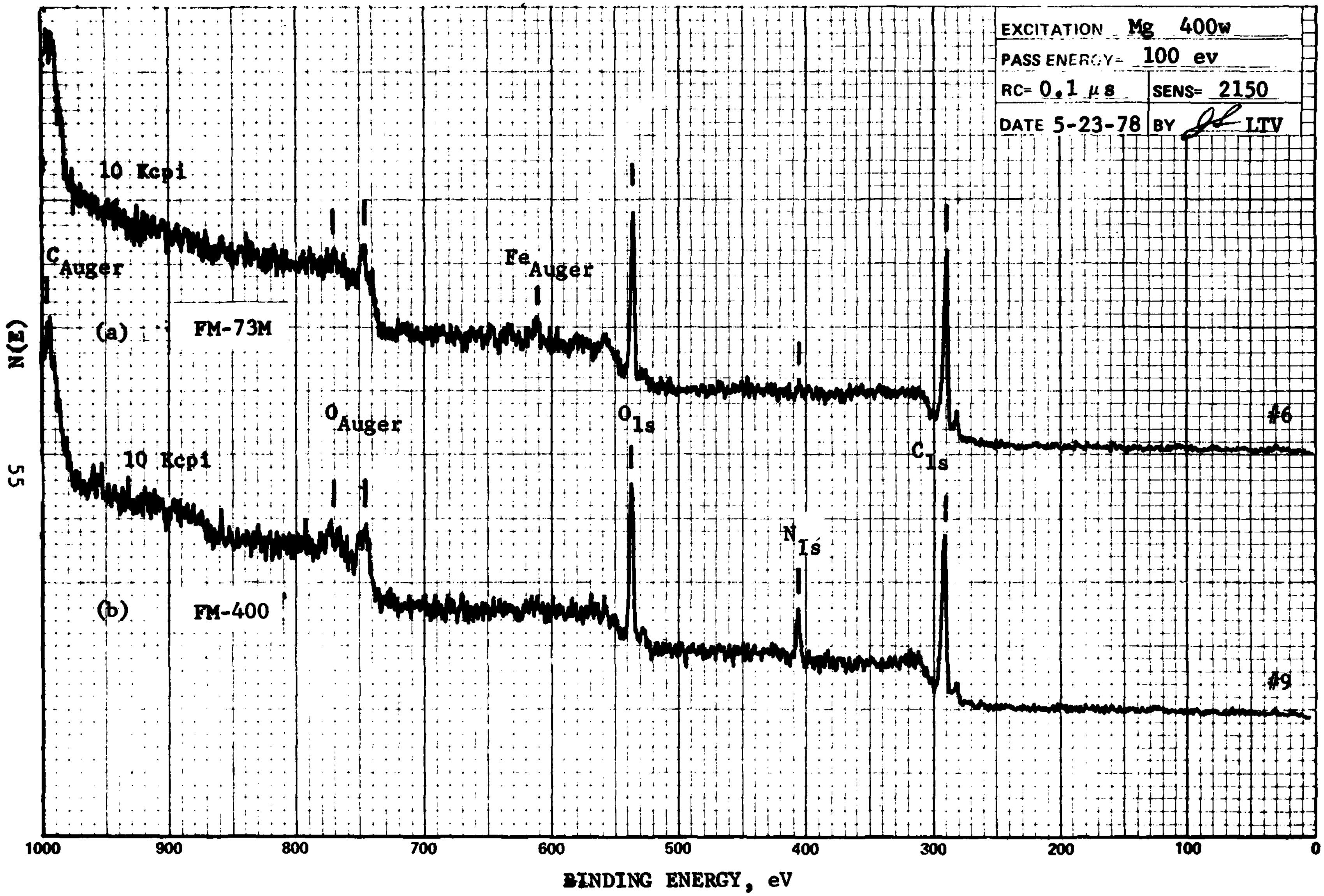

Figure A68 XPS Spectra of Dry FM-73M and FM-400 Model Joints

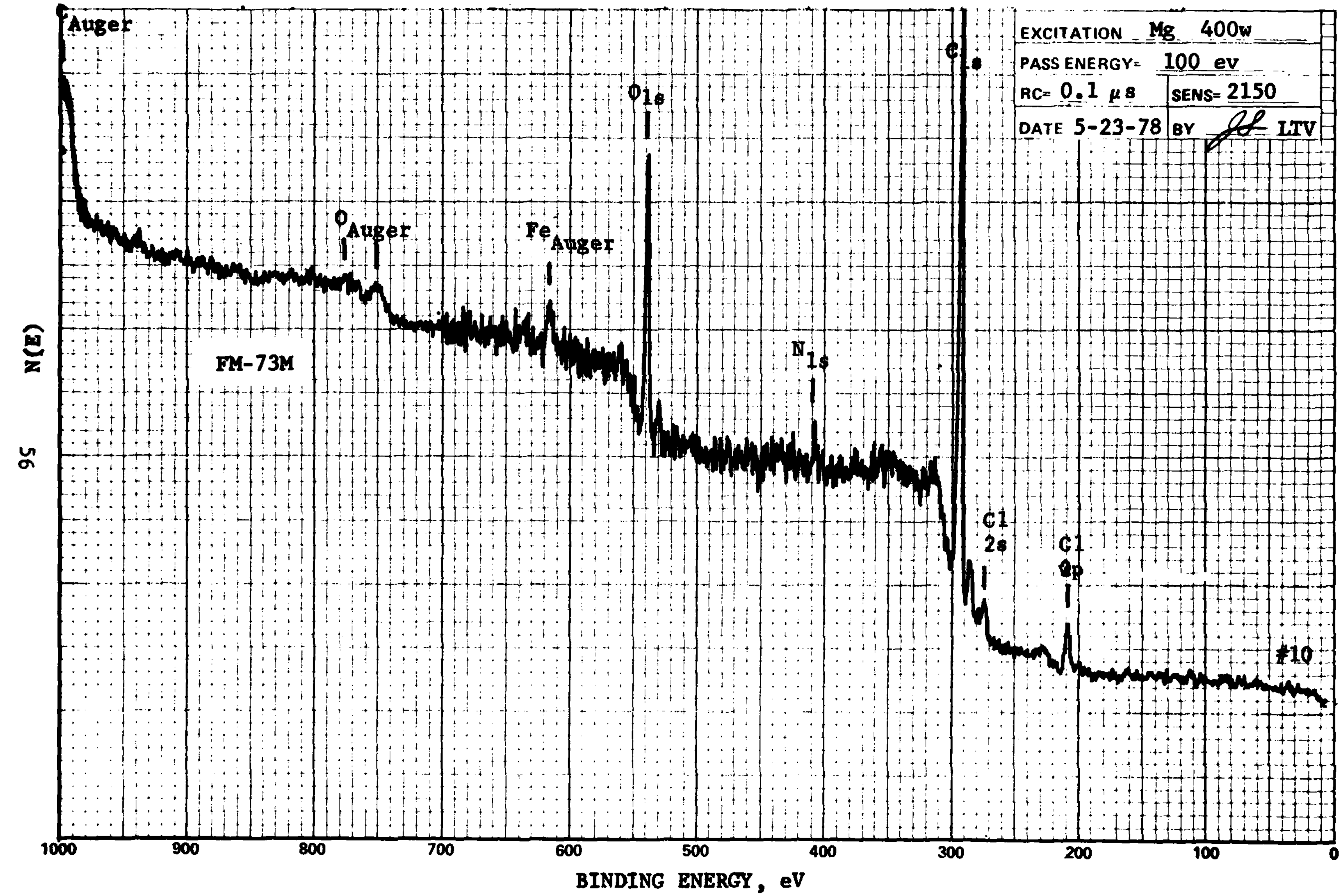

Figure A69 XPS Spectrum of Dry FM-73M Adhesive Interlayer

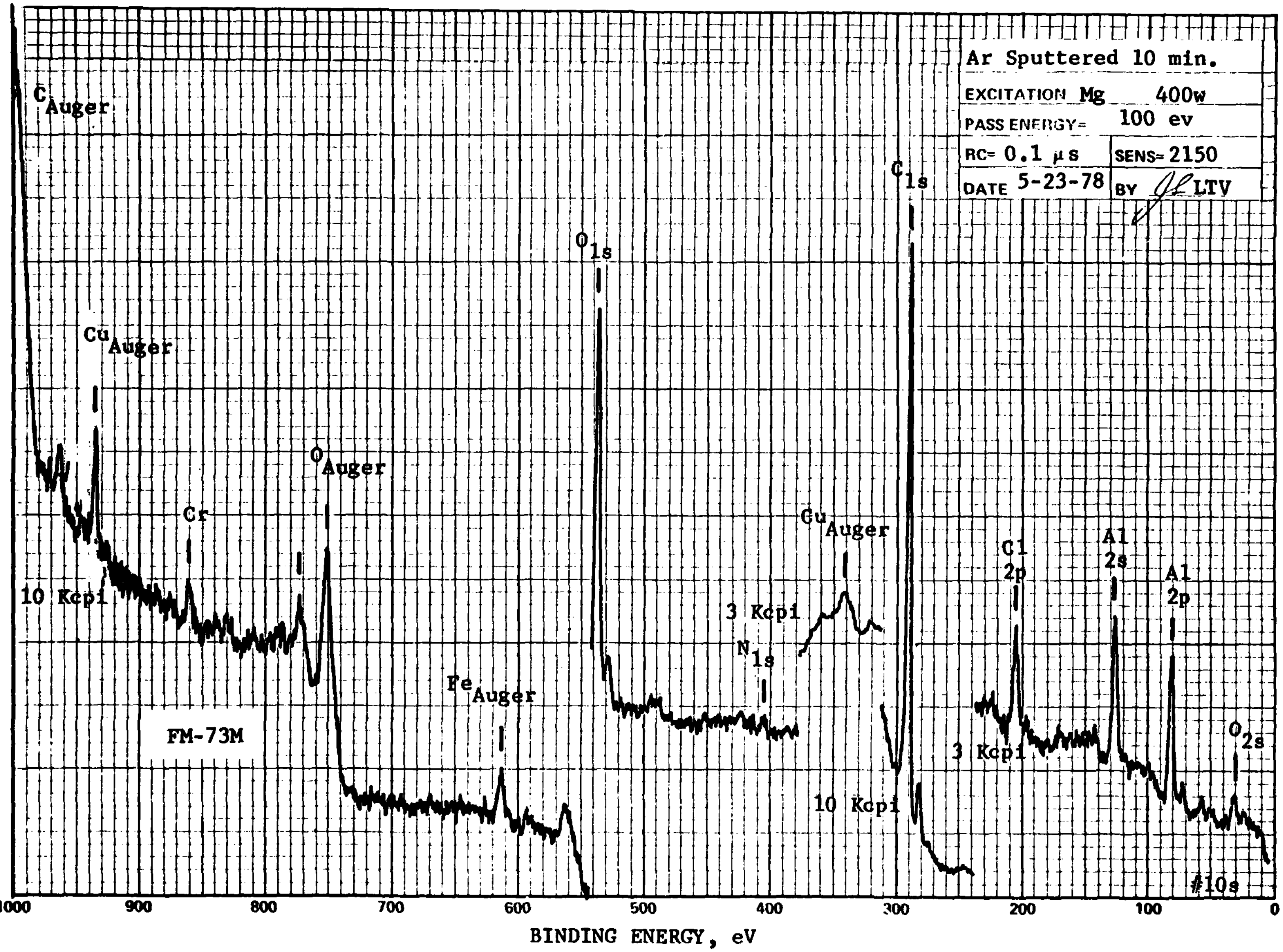

Figure A70 XPS Spectrum of Sputtered FM-73M Adhesive Interlayer

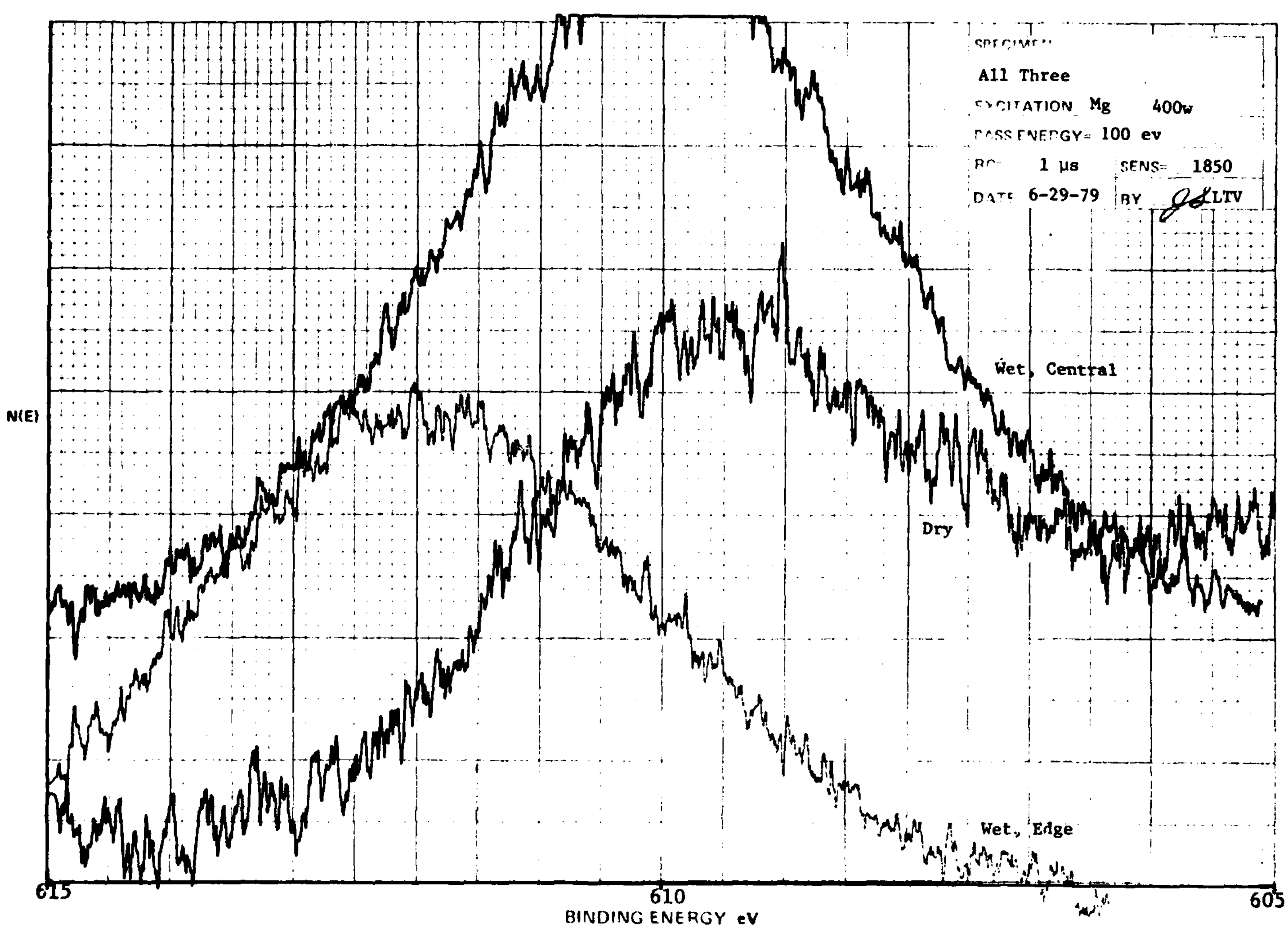

Figure A71 High Resolution XPS Spectra: C_{1s} Peak for Different FM-73M Adhesive Conditions

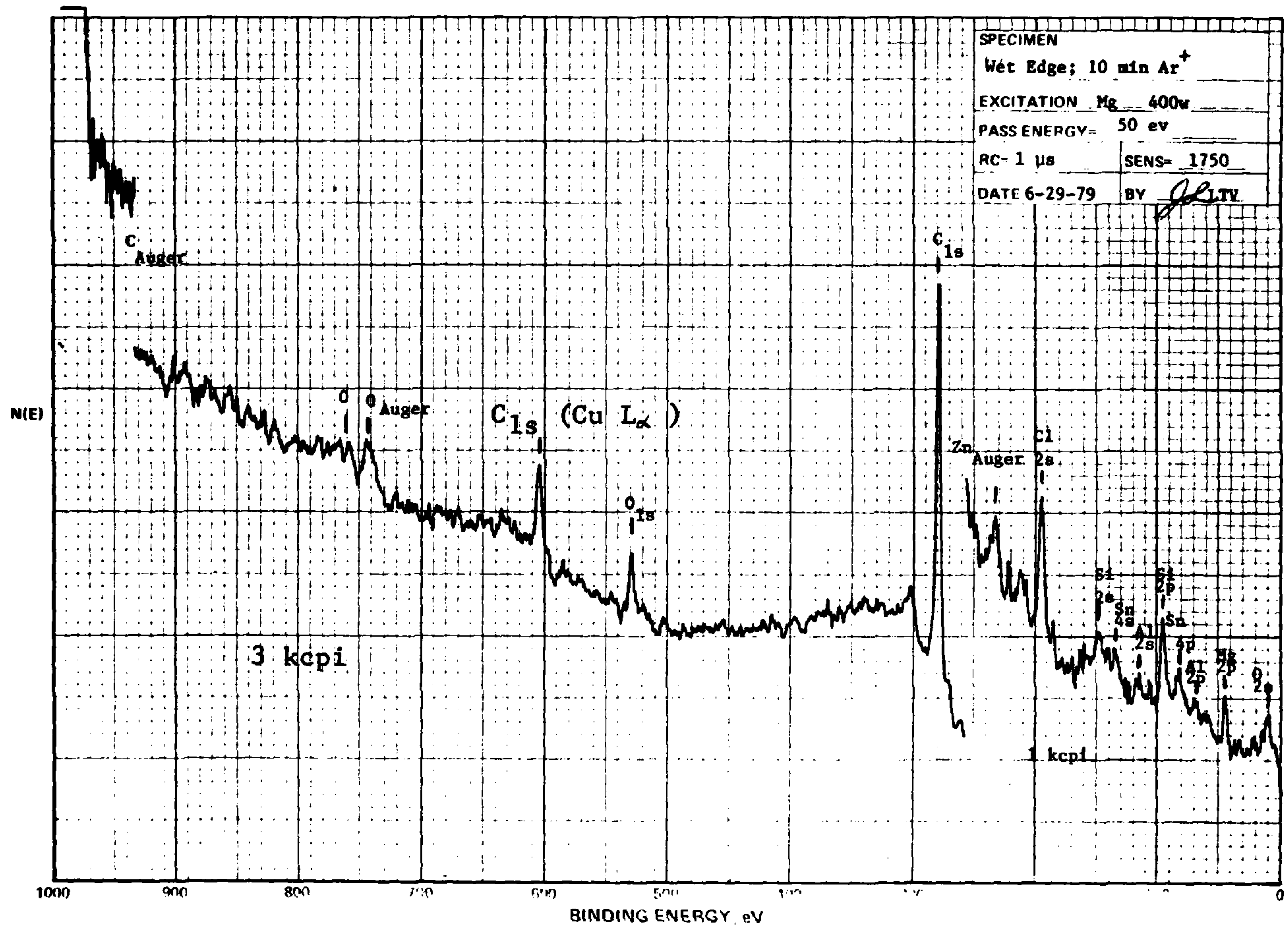

Figure A72 XPS Spectrum of 800 A-Sputtered Wet FM-73M Interlayer Edge

Appendix A

ON THE STRESS DISTRIBUTION IN THE ADHESIVE INTERLAYER OF A MODEL JOINT WITH RIGID ADHERENDS

We assume that Poisson's ratio, ν , is a constant and that only Young's modulus, E , is a (viscoelastic) time-dependent function, $E(t)$.

The formulation of the two-dimensional boundary value problem starts with listing the field equations. We consider all field functions to depend on the spatial coordinates x , y , and time. Laplace transformation (indicated by a bar over the field quantity) introduces the Laplace parameter p .

$$\overline{\tau_{ij,j}} = 0 \qquad \text{equilibrium equation} \qquad (1)$$

$$\begin{aligned} \overline{\sigma_x} &= \overline{\phi}_{,yy} \\ \overline{\sigma_y} &= \overline{\phi}_{,xx} \\ \overline{\tau_{xy}} &= -\overline{\phi}_{,xy} \end{aligned} \qquad \phi = \text{Airy stress function} \qquad (2)$$

$$\nabla^4 \overline{\phi} = 0 \qquad \text{compatibility equation(s)} \qquad (3)$$

$$\bar{\epsilon}_x = \frac{1-\nu^2}{p\bar{E}}\left(\bar{\sigma}_x - \frac{\nu}{1+\nu}\bar{\sigma}_y\right)$$
$$\bar{\epsilon}_y = \frac{1-\nu^2}{p\bar{E}}\left(\bar{\sigma}_y - \frac{\nu}{1+\nu}\bar{\sigma}_x\right)$$
$$\bar{\epsilon}_{xy} = \frac{1+\nu}{p\bar{E}}\,\bar{\tau}_{xy}$$

stress-strain relations (plane stress) (4)

$$\bar{\epsilon}_x = \frac{\partial \bar{u}}{\partial x}$$
$$\bar{\epsilon}_y = \frac{\partial \bar{v}}{\partial y}$$
$$2\bar{\epsilon}_{xy} = \frac{\partial \bar{u}}{\partial y} + \frac{\partial \bar{v}}{\partial x}$$

strain-displacement relations (5)

Besides satisfying these field equations the stresses and displacements must satisfy the boundary conditions.

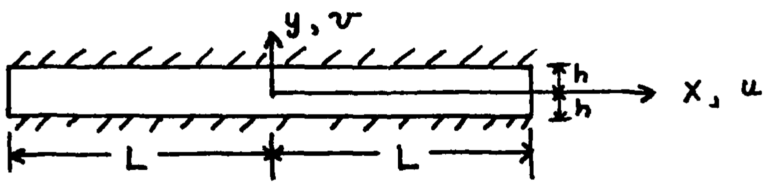

We assume rigid adherends

on $y = +h$ $\quad u = u_0(t)\,;\ v = 0$ $\quad$ or $\quad \bar{u} = \bar{u}_0\,;\ \bar{v} = 0$ (6a)

$\quad y = -h$ $\quad u = -u_0(t)\,;\ v = 0$ $\quad$ or $\quad \bar{u} = -\bar{u}_0\,;\ \bar{v} = 0$

on $x = L$ $\quad \sigma_x = \tau_{xy} = 0$ $\quad$ or $\quad \bar{\sigma}_x = \bar{\tau}_{xy} = 0$ (6b)

$\quad x = -L$ $\quad \sigma_x = \tau_{xy} = 0$ $\quad$ or $\quad \bar{\sigma}_x = \bar{\tau}_{xy} = 0$

Because Equation (3) is independent of material properties, we find $\overline{\phi}$ independent of $\overline{E}$. We find the stresses $\overline{\sigma}_x$, $\overline{\sigma}_y$, $\overline{\tau}_{xy}$ from Equation (2) in terms of $\overline{\phi}$, and these are independent of $\overline{E}$. Define $\nu' = \frac{\nu}{1+\nu}$, $E'(t) = \frac{E(t)}{1-\nu^2}$, or $\overline{E}' = \frac{\overline{E}}{1-\nu^2}$.

Then we find from Equations (4) and (5) that

$$p\overline{E}' \frac{\partial \overline{u}}{\partial x} = \overline{\sigma}_x - \nu' \overline{\sigma}_y \tag{7}$$

$$p\overline{E}' \frac{\partial \overline{v}}{\partial y} = \overline{\sigma}_y - \nu' \overline{\sigma}_x$$

In order to be able to apply the boundary conditions of Equation (6a), we integrate Equation (7) to find

$$p\overline{E}'\overline{u} = \overline{F}(x, y, p, \nu) = \int(\overline{\sigma}_x - \nu'\overline{\sigma}_y)\,dx + \overline{f}(y, p) \tag{8a}$$

$$p\overline{E}'\overline{v} = \overline{G}(x, y, p, \nu) = \int(\overline{\sigma}_y - \nu'\overline{\sigma}_x)\,dy + \overline{g}(x, p) \tag{8b}$$

The $\overline{F}$ and $\overline{G}$ denote functions of the coordinates x, y, of the constant Poisson's ratio, ν, and the Laplace parameter p. The latter dependence enters through the dependence of the stresses on p, not directly through the material property

E or $\bar{E}$. The functions $\bar{f}(y, p)$ and $\bar{g}(x, p)$ are determined by substituting Equations (8a) and (8b) into:

$$\frac{\partial \bar{u}}{\partial y} + \frac{\partial \bar{v}}{\partial x} = \frac{2(1+\nu)}{p\bar{E}} = \frac{1}{p\bar{E}'} \frac{2\bar{\tau}_{xy}}{1-\nu} \tag{9}$$

In this latter substitution operation, the modulus $\bar{E}'$ will drop out. So far then, the stresses are not functions of $\bar{E}'$. $\bar{E}'$ enters through the boundary condition given by Equation (6a). From Equation (8) we have

$$\begin{aligned} \bar{u} &= \frac{1}{p\bar{E}'} \bar{F}(x, y, p, \nu) \\ \bar{v} &= \frac{1}{p\bar{E}'} \bar{G}(x, y, p, \nu) \end{aligned} \tag{10}$$

Boundary condition of Equation (6a) requires

$$v(x, \pm h, t) = 0$$

and therefore $\bar{G}(x, \pm h, p, \nu) = 0$ and does not introduce E' or $\bar{E}'$. The conditions

$$\bar{u}_0 = \frac{1}{p\bar{E}'} \bar{F}(x, +h, p, \nu) \quad \Rightarrow \quad p\bar{E}' u_0 = \bar{F}(x, +h, p, \nu) \tag{11a}$$

$$-\bar{u}_0 = \frac{1}{p\bar{E}'} \bar{F}(x, -h, p, \nu) \quad \Rightarrow \quad p\bar{E}' u_0 = -\bar{F}(x, -h, p, \nu) \tag{11b}$$

say that $\overline{F}$ is an odd function in y. Let $\overline{F}_*$ be that odd function so that Equation (11b) is satisfied if Equation (11a) is satisfied. But $\overline{F}_*$ depends on $\overline{E}^*$, but only in a product form with $\overline{u}_0$. Thus the function $\overline{F}_*$ is proportional to the product $\overline{E}^*\overline{u}_0$. But this makes the whole solution proportional to the product $\overline{E}^*\overline{u}_0$. $u_0(t)$ or $\overline{u}_0$ is, of course, the only forcing function and thus all stresses and displacements are proportional to it. If $\overline{F}_*$ is proportional to $\overline{E}^*\overline{u}_0$ then from Equation (10) it follows that $\overline{u}$ is proportional to $\overline{u}_0$, but not to $\overline{E}^*$, nor to $\frac{1}{\overline{E}^*}$. Furthermore, the stresses are also proportional to E' or $\overline{E}'$, and E' (or $\overline{E}'$) is factored out of the functions for the stresses.

We now turn the problem around in the sense of prescribing the loading on the rigid adherends and ask for the resulting creep displacement.

Choose the displacement function $u_0(t)$ such that

$$u_0(t) = u_0 D'(t) \qquad \overline{u}_0 = u_* \overline{D}'(t)$$

then $D'(t) = (1-\nu^2)\, D(t)$ (creep compliance in tension)

and $p^2 \overline{D}' \overline{E}' = 1$

then $\overline{u}_0 \overline{E}' = u_* \quad \Rightarrow \quad \overline{u}_0 = \dfrac{u_*}{\overline{E}'}$

Since the stresses were proportional to $\bar{E}'\bar{u}_0$, this choice of $u_0(t)$ now makes the stresses independent of $\bar{E}'$. In fact, the stresses will be time-independent and the displacements will increase with time as the creep compliance.

Integrate τ_{xy} over x along $y = \pm h$. That total load is also time independent. We have now essentially the bond problem. A constant load is accompanied by a time-independent stress distribution and by time dependent creep displacements.

This was possible only because we assumed Poisson's ratio, ν = constant, and because we could prescribe, a priori, the displacements at $y = \pm h$ on rigid boundaries.

Appendix B

PUBLICATIONS

The following presentations, technical reports, and publications cover work carried out under this contract. They were either prepared or appeared publicly during the reporting period:

ASM Metals Handbook, Chapters on "Inspection by Optical and Ultrasonic Holography", Vol. 11, Nondestructive Inspection and Control, Eighth Edition, 1976, pp. 198-233.

"Fatigue Behavior of Adhesively Bonded Joints", 1st PABST Industry Review, Long Beach CA, 5-7 October 1976.

"Environmental Effects in Adhesively Bonded Joints", General Dynamics' Fort Worth Division Report ERR-FW-1768, 16 December 1976.

"Fatigue Behavior of Adhesively Bonded Joints:, 2nd PABST Industry Review, Long Beach, CA, 14-16 September 1977.

"Fatigue Behavior of Adhesively Bonded Joints", 1st AFOSR-AFML "Workshop on Significance of Time-Dependent Behavior of Structural Adhesives", Grand Prairie, TX, 4-5 December 1977.

"Joint Failure Model - Environmental Effects", General Dynamics' Fort Worth Division Report ERR-FW-1850, 16 December 1977.

"AES/ESCA analyses of Surfaces of Adhesively Bonded Joints", 2nd Southwest Electron Spectroscopy Users' Conference, Texas A & M University, College Station, TX, 2 June 1978.

"Fatigue Behavior of Adhesively Bonded Joints", 3rd PABST Industry Review, Long Beach, CA, 27 September 1978.

"Environmental Serviceability of Bonded Joints", General Dynamics' Fort Worth Division Report ERR-FW-1963, 22 December 1978.

"Behavior of Adhesively Bonded Joints Under Cyclic Loading", Seminar to AFFDL, W-P, OH 10 January 1979.

"Fatigue Behavior of Adhesively Bonded Joints", Meeting of the Adhesion Society, Savannah, GA, 12-14 February 1979.

"Fatigue Behavior of Adhesively Bonded Joints", and Session Chairman, Workshop on Mechanics of Adhesively Bonded Joints", AFML/MBC, W-P AFB, OH, 6 March 1979.

Lecture 4, "Behavior of Adhesively Bonded Joints Under Cyclic Loading", AGARD-NATO Lecture Series No. 102 on "Adhesive Bonding and Preparation for Bonding", Oslo, Norway, 2-3 April 1979; The Hague, The Netherlands, 5-6 April 1979; and W-P AFB, OH, 16-17 October 1979; also AGARD publ. AGARD-LS-102 March 1979.

"On the Time-Dependence of Poisson's Ratio of a Commercial Adhesive", with W. G. Knauss, J. Adhesion, 1979.

"Fatigue Mechanisms in Adhesively Bonded Joints", AFOSR Seminar at Texas A & M University, Mechanics and Materials Research Center, March 27, 1980.

"Fatigue Behavior of Adhesively Bonded Joints", 25th National SAMPE Symposium & Exhibition, San Diego, CA, May 6-8, 1980.

"Fatigue Mechanisms in Adhesive Joints", Developments in Adhesives - 2, edited by A. J. Kinloch, Applied Science Publishers, 1980.

☆U.S.Government Printing Office: 1980 — 657-084/754

g